

PRIMAL FINITE ELEMENT SCHEME OF THE HODGE-LAPLACE PROBLEM

WENYU DONG AND SHUO ZHANG*

ABSTRACT. In this paper, we construct nonconforming finite element spaces $\mathbf{V}_h^{\mathbf{d}\cap\delta}\Lambda^k$ for the approximation of $H\Lambda^k \cap H_0^*\Lambda^k$ on simplicial meshes, for $n \geq 2$ and $1 \leq k \leq n-1$, by enforcing adjoint continuity against piecewise Whitney spaces rather than trace matching. It holds, with \mathbf{d}_h^k and $\delta_{k,h}$ denoting respectively the piecewise action of differential and codifferential operators, and $\mathfrak{H}_h\Lambda^k$ being the discrete harmonic forms in the FEEC sense, that

$$\mathfrak{H}_h\Lambda^k = \{\boldsymbol{\mu}_h \in \mathbf{V}_h^{\mathbf{d}\cap\delta}\Lambda^k : \mathbf{d}_h^k\boldsymbol{\mu}_h = 0, \delta_{k,h}\boldsymbol{\mu}_h = 0\},$$

which mirrors the continuous Hodge–Laplace kernel on domains with nontrivial topology. The space is not a classical Ciarlet-type finite element space; though, a uniform discrete Poincaré inequality and locally supported basis functions (supported on at most two cells) are guaranteed. The resulting primal scheme yields an $\mathcal{O}(h)$ error bound for smooth data and $\mathcal{O}(h^s)$ on s -regular domains ($0 < s \leq 1$), nontrivial topology admitted. Two- and three-dimensional eigenvalue tests agree with the mixed method on perforated domains, which are given to verify the validity of the scheme.

CONTENTS

1. Introduction	2
2. Preliminaries	6
2.1. Preliminary notations	6
2.2. Finite element spaces for $H\Lambda^k$ by Whitney forms	7
2.3. A pair of adjoint operators associated with the Hodge-Laplacian	9
3. The main results of this paper	11
3.1. Shape function spaces on a single simplex	11
3.2. Finite element space for $H\Lambda^k \cap H_0^*\Lambda^k$	13
3.3. A primal finite element scheme for the Hodge-Laplace problem	15
4. Proofs of Theorems 3.6 and 3.7	15
4.1. Some technical preparation	15

2020 *Mathematics Subject Classification.* Primary 65N30; Secondary 65N12, 65N15, 65N22.

Key words and phrases. Hodge–Laplace problem, finite element exterior calculus, primal formulation, nonconforming finite element, discrete harmonic forms, discrete Poincaré inequality, mixed finite element method.

*Corresponding author.

The research is partially supported by NSFC (12271512, 11871465).

4.2. Proof of Theorem 3.6	17
4.3. Proof of Theorem 3.7	18
5. Proof of Theorem 3.9	21
5.1. Auxiliary mixed formulations and their connections	21
5.2. Proof of Theorem 3.9	24
6. Numerical experiments	25
6.1. Overview	25
6.2. Two-dimensional tests	26
6.3. Three-dimensional tests	28
7. Concluding remarks	33
References	34
Guide to the appendices	35
Appendix A. Eigenvalue results obtained by the vector Lagrange element	35
A.1. Two-dimensional vector Lagrange discretization and results	36
A.2. Three-dimensional vector Lagrange discretization and results	36
A.3. Summary of the vector Lagrange element	38
Appendix B. Eigenvalue results obtained by the vector Crouzeix–Raviart element	38
B.1. Two-dimensional vector Crouzeix–Raviart discretizations and results	38
B.2. Three-dimensional vector Crouzeix–Raviart discretizations and results	41
B.3. Summary of the vector Crouzeix–Raviart element	43
Appendix C. Illustration of basis functions of $\mathbf{W}_h^{*,nc} \Lambda^k$ in two and three dimensions	43
C.1. $\mathbf{W}_h^{*,nc} \Lambda^1$ in 2D revisited	43
C.2. $\mathbf{W}_h^{*,nc} \Lambda^2$ in 3D revisited	44
Appendix D. Basis functions of the two-dimensional nonconforming space (3.12) for $H(\text{rot}, \Omega) \cap H_0(\text{div}, \Omega)$	45
Appendix E. Basis functions of the three-dimensional nonconforming space (3.13) for $H(\text{div}, \Omega) \cap H_0(\text{curl}, \Omega)$	47
Appendix F. Numerical results for boundary-value problems	53
F.1. Two-dimensional boundary-value problem	54
F.2. Three-dimensional boundary-value problem	54

1. INTRODUCTION

Let $\Omega \subset \mathbb{R}^n$ be a bounded Lipschitz domain. The Hodge-Laplace problem in its primal weak formulation reads: find $\omega \in H\Lambda^k(\Omega) \cap H_0^* \Lambda^k(\Omega)$, orthogonal to the harmonic forms $\mathfrak{H}\Lambda^k$, such that

$$(1.1) \quad \langle \mathbf{d}^k \omega, \mathbf{d}^k \mu \rangle_{L^2 \Lambda^{k+1}} + \langle \delta_k \omega, \delta_k \mu \rangle_{L^2 \Lambda^{k-1}} = \langle \mathbf{f} - \mathbf{P}_{\mathfrak{H}} \mathbf{f}, \mu \rangle_{L^2 \Lambda^k},$$

for all $\boldsymbol{\mu} \in H\Lambda^k(\Omega) \cap H_0^*\Lambda^k(\Omega)$, where $\mathbf{P}_{\mathfrak{H}}$ denotes the $L^2\Lambda^k$ projection onto $\mathfrak{H}\Lambda^k$. The model problem (1.1) corresponds to the strong form that

$$(1.2) \quad \mathbf{d}^k\boldsymbol{\omega} \in H_0^*\Lambda^{k+1}(\Omega), \quad \delta_k\boldsymbol{\omega} \in H\Lambda^{k-1}(\Omega),$$

and

$$(1.3) \quad \boldsymbol{\omega} \perp \mathfrak{H}\Lambda^k(\Omega), \quad \text{and} \quad \delta_{k+1}\mathbf{d}^k\boldsymbol{\omega} + \mathbf{d}^{k-1}\delta_k\boldsymbol{\omega} = \mathbf{f} - \mathbf{P}_{\mathfrak{H}}\mathbf{f}.$$

The Hodge-Laplace problem arises in many applied sciences, including electromagnetics [16, 19], fluid-structure interaction [7, 8, 15], and others.

The standard remedy for the Hodge-Laplace problem in the FEEC literature is to adopt a mixed method. Particularly, the numerical solution of the Hodge-Laplace problem is a central subject of the theory of finite element exterior calculus (FEEC), and we refer to [1, 3, 4] for a thorough introduction to FEEC. This is due to the well known difficulty that a *conforming* discretization of (1.1) requires finite element subspaces of $H\Lambda^k \cap H_0^*\Lambda^k$ and a piecewise polynomial subspace of this intersection is necessarily contained in $H^1\Lambda^k \cap H_0^*\Lambda^k$, which is a nontrivial closed subspace. — Consequently, when the exact solution possesses a singular component (as occurs on non-convex domains or domains with non-trivial topology), the conforming finite element solution may converge to a wrong limit. The mixed approach decomposes the second-order problem into first-order equations, discretizes each with conforming Whitney forms, and relies on the de Rham complex structure to guarantee stability. A key ingredient is that spaces of discrete harmonic forms $\mathfrak{H}_h\Lambda^k$ are established isomorphic to the space of continuous harmonic forms $\mathfrak{H}\Lambda^k$, which is essential for problems on domains with non-trivial topology.

The primal formulation involves only a single unknown field, and for problems coupled with other physics that also admit primal variational formulations, a primal discretization of the Hodge-Laplace operator can be integrated more naturally. Meanwhile, the mixed approach introduces *nonlocal* discretization of the codifferentials [17]. These considerations have motivated continuing efforts to discretize the primal formulation directly. So far, several methods have been proposed for the two-dimensional $H(\text{curl}) \cap H(\text{div})$ problem: interior penalty methods [11], quadratic non-conforming elements [10], nonconforming elements with inter-element penalties [9], and more recent constructions [5, 6, 18]. Virtual element methods have also been designed for the three-dimensional vector potential formulation [14], though the analysis there is restricted to domains without re-entrant corners, where harmonic forms vanish and the solution is smooth.

A crucial limitation by all existing primal discretizations is that they have not reconstructed the fundamental identity

$$(1.4) \quad \mathfrak{H}\Lambda^k = \left\{ \boldsymbol{\mu} \in H\Lambda^k \cap H_0^*\Lambda^k : \mathbf{d}^k\boldsymbol{\mu} = 0, \delta_k\boldsymbol{\mu} = 0 \right\}$$

at the discrete level. Namely the joint kernel of the discrete exterior derivative and codifferential cannot be characterized as a space of discrete harmonic forms. Without this property, the method cannot correctly capture the topology of the domain.

The construction of nonconforming finite element spaces in this paper is inspired by a reinterpretation ([21]) of the classical Crouzeix-Raviart (CR) nonconforming element ([13]). Let V_h^{CR} be the space of piecewise linear polynomials with continuity at edge midpoints, and let $\underline{V}_{h0}^{\text{RT}}$ be the lowest-degree Raviart-Thomas space with vanishing normal traces on the boundary. On a triangulation \mathcal{G}_h , it is well known that these spaces satisfy the integration-by-parts identity

$$(1.5) \quad \sum_{T \in \mathcal{G}_h} \int_T \nabla v_h \cdot \underline{\tau}_h \, dx = - \sum_{T \in \mathcal{G}_h} \int_T v_h \operatorname{div} \underline{\tau}_h \, dx, \quad v_h \in V_h^{\text{CR}}, \underline{\tau}_h \in \underline{V}_{h0}^{\text{RT}}.$$

The standard perspective treats (1.5) as a **consequence** of the definitions of V_h^{CR} and $\underline{V}_{h0}^{\text{RT}}$. A crucial observation, however, is that the identity also serves as a **sufficient** condition, namely, *a piecewise linear function v_h belongs to V_h^{CR} if and only if (1.5) holds for every $\underline{\tau}_h \in \underline{V}_{h0}^{\text{RT}}$* ([21]). In other words, the nonconforming space V_h^{CR} is completely characterized by its adjoint relationship with a conforming space $\underline{V}_{h0}^{\text{RT}}$. — Simultaneously, $\underline{V}_{h0}^{\text{RT}}$ is also characterized by V_h^{CR} . Namely, the pairing of V_h^{CR} and $\underline{V}_{h0}^{\text{RT}}$ inherits the adjoint relation between $(\nabla, H^1(\Omega))$ and $(\operatorname{div}, H_0(\operatorname{div}, \Omega))$. This perspective shifts the problem of constructing a nonconforming finite element space from *imposing trace continuity conditions* (which may be difficult or impossible to formulate for the target function space) to *enforcing an adjoint identity against an already-available conforming space*. Following this idea, a unified family of nonconforming finite element spaces $\mathbf{W}_h^{\text{nc}} \Lambda^k$ ($\mathbf{W}_h^{*,\text{nc}} \Lambda^k$ simultaneously) by piecewise Whitney forms has been established in [21] for $H\Lambda^k$ ($H^* \Lambda^k$, respectively); the Poincaré-Hodge decomposition for $L^2 \Lambda^k$ and the Poincaré-Lefschetz dualities as equalities were established at the discrete level for the first time therein.

For the primal Hodge–Laplace problem, in this paper, we construct a nonconforming trial space for the intersection $H\Lambda^k \cap H_0^* \Lambda^k$. The space of piecewise polynomials is $\mathbf{P}_{\mathbf{d} \cap \delta} \Lambda^k(\mathcal{G}_h)$, precisely given later, built from a local enrichment of the minimal trimmed space $\mathcal{P}_0 \Lambda^k + \kappa(\mathcal{P}_0 \Lambda^{k+1}) + \star \kappa \star (\mathcal{P}_0 \Lambda^{k-1})$; global membership is imposed through simultaneous adjoint continuity against the two spaces $\mathbf{W}_{h0}^{*,\text{nc}} \Lambda^{k+1}$ established in [21] for $H_0^* \Lambda^{k+1}$ and $\mathbf{W}_h \Lambda^{k-1}$ the standard conforming finite element space by piecewise Whitney forms for $H\Lambda^{k-1}$:

$$(1.6) \quad \mathbf{V}_h^{\mathbf{d} \cap \delta} \Lambda^k := \left\{ \boldsymbol{\mu}_h \in \mathbf{P}_{\mathbf{d} \cap \delta} \Lambda^k(\mathcal{G}_h) : \langle \mathbf{d}_h^k \boldsymbol{\mu}_h, \boldsymbol{\eta}_h \rangle - \langle \boldsymbol{\mu}_h, \boldsymbol{\delta}_{k+1,h} \boldsymbol{\eta}_h \rangle = 0, \forall \boldsymbol{\eta}_h \in \mathbf{W}_{h0}^{*,\text{nc}} \Lambda^{k+1}, \right. \\ \left. \text{and } \langle \boldsymbol{\delta}_{k,h} \boldsymbol{\mu}_h, \boldsymbol{\tau}_h \rangle - \langle \boldsymbol{\mu}_h, \mathbf{d}^{k-1} \boldsymbol{\tau}_h \rangle = 0, \forall \boldsymbol{\tau}_h \in \mathbf{W}_h \Lambda^{k-1} \right\}.$$

It is this pairing of adjoint partners—one nonconforming for the codifferential side and one conforming Whitney for the differential side—that transfers the topology-sensitive discrete Hodge structure of [21] to the primal setting and makes nontrivial topology tractable. Particularly, it can be proved that

$$(1.7) \quad \mathfrak{H}_h \Lambda^k = \left\{ \boldsymbol{\mu}_h \in \mathbf{V}_h^{\mathbf{d}\cap\delta} \Lambda^k : \mathbf{d}_h^k \boldsymbol{\mu}_h = 0, \delta_{k,h} \boldsymbol{\mu}_h = 0 \right\},$$

which mirrors the continuous identity (1.4). Here $\mathfrak{H}_h \Lambda^k$ denotes the space of discrete harmonic forms in the standard FEEC theory, and \mathbf{d}_h^k and $\delta_{k,h}$ denote the piecewise action of the differential and codifferential operators, respectively. Crucial for correct approximation on domains with nontrivial topology, the identity (1.7) is not automatic for a primal discretization; it follows just from taking $\mathbf{W}_{h0}^{*,\text{nc}} \Lambda^{k+1}$ and $\mathbf{W}_h \Lambda^{k-1}$ as the adjoint partners in (1.6), so that the trial space is aligned with the discrete cohomology already built into these spaces.

The conditions in (1.6) are precisely the adjoint relations that the function in $H\Lambda^k \cap H_0^* \Lambda^k$ satisfies when tested against functions in the corresponding partner spaces. In this sense, intercell continuity is imposed through adjoint relationships rather than through pointwise or tracewise matching on the mesh skeleton; we refer to this strategy as “adjoint continuity.” Moreover, at the continuous level, the primal formulation (1.1) and mixed Hodge–Laplace formulations are equivalent, and a legitimate primal discretization should preserve this link at the discrete level at least approximately, which is necessary for the convergence of the scheme. The construction above is designed so that the primal solution is closed to the solution of a classical mixed discretization based on conforming Whitney forms. This makes it possible—similarly to [2]—to establish the convergence of the primal finite element scheme by the aid of the classical mixed finite element scheme. In particular, Section 5 shows that the discrete primal and mixed solutions agree up to $\mathcal{O}(h\|f\|_{L^2})$ (Proposition 5.7). Theorem 3.9, proved in Section 5, records the resulting error bounds, including $\mathcal{O}(h)$ convergence in the $L^2 \Lambda^k$ and broken $H\Lambda^k$, and $H^* \Lambda^k$ norms for smooth data and $\mathcal{O}(h^s)$ on s -regular domains ($0 < s \leq 1$), independently of the topology; on the perforated domains emphasized below, the rate is regularity-limited by s .

The space $\mathbf{V}_h^{\mathbf{d}\cap\delta} \Lambda^k$ does not correspond to a classical finite element space of Ciarlet’s type [12], because the adjoint continuity conditions (1.6) couple degrees of freedom across neighboring cells in a manner that cannot be reduced to matching nodal values on the mesh skeleton. Nevertheless, uniform discrete Poincaré inequalities can be proved for $\mathbf{V}_h^{\mathbf{d}\cap\delta} \Lambda^k$, therefore the well-posedness of the discretization follows. Implementably, we can construct a set of globally defined, locally supported basis functions; each is supported on a vertex patch spanning at most two cells, not necessarily adjacent. The existence of these basis functions is rigorously guaranteed, and once computed, they can be used in a standard cell-by-cell assembly routine. The construction is presented

in a unified manner for all n and k , and is illustrated concretely for the two- and three-dimensional $H(\text{curl}) \cap H(\text{div})$ cases in the numerical section.

The remaining of the paper is organized as follows. Section 2 collects preliminaries and notation. Section 3 presents the construction of the finite element spaces and schemes and states the main theorems of the paper. Section 4 proves the discrete Poincaré inequality and the existence of locally supported basis functions, and Section 5 establishes error estimates by the aid of several mixed FEEC schemes. Section 6 reports numerical experiments to verify the validity of the schemes by eigenvalue tests, especially on domains with nontrivial topology. Additional numerical and implementation material is collected in the appendices: manufactured-solution boundary-value tests (Appendix F), explicit basis functions (Appendices D and E), and eigenvalue counterexamples with vector Lagrange and vector Crouzeix–Raviart elements (Appendices A and B). Section 7 concludes with remarks and prospects.

2. PRELIMINARIES

2.1. Preliminary notations. Throughout the paper, we use \mathcal{N} and \mathcal{R} to denote the null space and the range of certain operators. For example, $\mathcal{N}(\mathbf{T}, \mathbf{D})$ denotes $\{\mathbf{v} \in \mathbf{D} : \mathbf{T}\mathbf{v} = 0\}$, and $\mathcal{R}(\mathbf{T}, \mathbf{D})$ denotes $\{\mathbf{T}\mathbf{v} : \mathbf{v} \in \mathbf{D}\}$. For a Hilbert space \mathbf{H} , we use $\oplus_{\mathbf{H}}^{\perp}$ and $\ominus_{\mathbf{H}}^{\perp}$ to denote orthogonal summation and orthogonal difference; namely, for two spaces \mathbf{A} and \mathbf{B} in \mathbf{H} , the notation $\mathbf{A} \oplus_{\mathbf{H}}^{\perp} \mathbf{B}$ means that \mathbf{A} and \mathbf{B} are orthogonal in \mathbf{H} and their sum is direct; for $\mathbf{A} \subset \mathbf{B} \subset \mathbf{H}$, $\mathbf{B} \ominus_{\mathbf{H}}^{\perp} \mathbf{A}$ denotes the orthogonal complement of \mathbf{A} in \mathbf{B} . The subscript \mathbf{H} may occasionally be dropped.

We use \mathbf{d}^k and δ_k for the exterior *differential* and *codifferential* operators on k -forms Λ^k ; $\delta_k = (-1)^{kn} \star \mathbf{d}^{n-k} \star$, with \star the Hodge star operator. We use κ for the Koszul operator defined by

$$\kappa(\mathbf{d}x^{\alpha_1} \wedge \cdots \wedge \mathbf{d}x^{\alpha_k}) := \sum_{j=1}^k (-1)^{j+1} x^{\alpha_j} \mathbf{d}x^{\alpha_1} \wedge \cdots \wedge \mathbf{d}x^{\alpha_{j-1}} \wedge \mathbf{d}x^{\alpha_{j+1}} \wedge \cdots \wedge \mathbf{d}x^{\alpha_k}, \text{ for } \alpha \in \mathbb{I}\mathbb{X}_{k,n},$$

where $\mathbb{I}\mathbb{X}_{k,n} := \{\alpha = (\alpha_1, \dots, \alpha_k) \in \mathbb{Z}^k : 1 \leq \alpha_1 < \alpha_2 < \cdots < \alpha_k \leq n\}$ is the set of k -indices, $k \leq n$. Then for $\alpha \in \mathbb{I}\mathbb{X}_{k+1,n}$, $\mathbf{d}^k(\kappa(\mathbf{d}x^{\alpha_1} \wedge \cdots \wedge \mathbf{d}x^{\alpha_{k+1}})) = (k+1)\mathbf{d}x^{\alpha_1} \wedge \cdots \wedge \mathbf{d}x^{\alpha_{k+1}}$, and for $\alpha \in \mathbb{I}\mathbb{X}_{k-1,n}$, $\delta_k(\star \kappa \star (\mathbf{d}x^{\alpha_1} \wedge \cdots \wedge \mathbf{d}x^{\alpha_{k-1}})) = (-1)^{kn-n-1}(n-k+1)(\mathbf{d}x^{\alpha_1} \wedge \cdots \wedge \mathbf{d}x^{\alpha_{k-1}})$. The homotopy formula $(\mathbf{d}^{k-1} \kappa + \kappa \mathbf{d}^k)\mu = (k+r)\mu$ holds for $\mu \in \mathcal{H}_r \Lambda^k$, where $\mathcal{H}_r \Lambda^k$ denotes the space of k -forms with homogeneous polynomial coefficients of degree r . In the sequel, denote $\kappa^\delta := \star \circ \kappa \circ \star$ for short.

Denote, on a domain Ξ ,

$$H\Lambda^k(\Xi) := \{\omega \in L^2\Lambda^k(\Xi) : \mathbf{d}^k\omega \in L^2\Lambda^{k+1}(\Xi)\}, \quad 0 \leq k \leq n-1,$$

and by $H_0\Lambda^k(\Xi)$ the closure of $C_0^\infty\Lambda^k(\Xi)$ in $H\Lambda^k(\Xi)$. Denote

$$H^*\Lambda^k(\Xi) := \left\{ \boldsymbol{\mu} \in L^2\Lambda^k(\Xi) : \delta_k\boldsymbol{\mu} \in L^2\Lambda^{k-1}(\Xi) \right\}, \quad 1 \leq k \leq n,$$

and $H_0^*\Lambda^k(\Xi)$ the closure of $C_0^\infty\Lambda^k(\Xi)$ in $H^*\Lambda^k(\Xi)$. Ξ can occasionally be dropped. $H^*\Lambda^k = \star H\Lambda^{n-k}$ and $H_0^*\Lambda^k = \star H_0\Lambda^{n-k}$. The spaces of harmonic forms are $\mathfrak{H}\Lambda^k := \mathcal{N}(\mathbf{d}^k, H\Lambda^k) \ominus^\perp \mathcal{R}(\mathbf{d}^{k-1}, H\Lambda^{k-1})$, $\mathfrak{H}_0\Lambda^k := \mathcal{N}(\mathbf{d}^k, H_0\Lambda^k) \ominus^\perp \mathcal{R}(\mathbf{d}^{k-1}, H_0\Lambda^{k-1})$, $\mathfrak{H}^*\Lambda^k := \mathcal{N}(\delta_k, H^*\Lambda^k) \ominus^\perp \mathcal{R}(\delta_{k+1}, H^*\Lambda^{k+1})$, and $\mathfrak{H}_0^*\Lambda^k := \mathcal{N}(\delta_k, H_0^*\Lambda^k) \ominus^\perp \mathcal{R}(\delta_{k+1}, H_0^*\Lambda^{k+1})$. As the Helmholtz decompositions hold that

$$\mathcal{N}(\mathbf{d}^k, H\Lambda^k) \oplus^\perp \mathcal{R}(\delta_{k+1}, H_0^*\Lambda^{k+1}) = L^2\Lambda^k = \mathcal{R}(\mathbf{d}^{k-1}, H\Lambda^{k-1}) \oplus^\perp \mathcal{N}(\delta_k, H_0^*\Lambda^k),$$

it follows that $\mathfrak{H}\Lambda^k = \mathfrak{H}_0^*\Lambda^k$ and $\mathfrak{H}_0\Lambda^k = \mathfrak{H}^*\Lambda^k$. This is the Poincaré-Lefschetz duality (cf. [1, Section 4.5.5]), which links the two dual complexes connected respectively by \mathbf{d}^k and δ_k .

For Ω a domain and Ξ a subdomain of Ω , we denote by E_Ξ^Ω the extension-by-zero operator from $L_{\text{loc}}^1(\Xi)$ to $L_{\text{loc}}^1(\Omega)$. Namely,

$$E_\Xi^\Omega : L_{\text{loc}}^1(\Xi) \rightarrow L_{\text{loc}}^1(\Omega), \quad E_\Xi^\Omega v = \begin{cases} v, & \text{on } \Xi, \\ 0, & \text{else,} \end{cases} \quad \text{for } v \in L_{\text{loc}}^1(\Xi).$$

For $V_T \subset L^1(T)$, we write $E_T^\Omega V_T$ to denote $\mathcal{R}(E_T^\Omega, V_T)$. We use the same notation L_{loc}^1 for scalar and non-scalar locally integrable functions, and E_Ξ^Ω for the extension of both.

Let $\mathcal{F}^\mathcal{G}$ be a set of shape regular simplicial subdivisions of Ω . On a subdivision $\mathcal{G}_h \in \mathcal{F}^\mathcal{G}$, define formally the product of a set of function spaces $\{\Upsilon(T)\}_{T \in \mathcal{G}_h}$ defined cell by cell such that $E_T^\Omega \Upsilon(T)$ for all $T \in \mathcal{G}_h$ are compatible, $\prod_{T \in \mathcal{G}_h} \Upsilon(T) := \sum_{T \in \mathcal{G}_h} E_T^\Omega \Upsilon(T)$. The summation is direct.

2.2. Finite element spaces for $H\Lambda^k$ by Whitney forms. Following [1, 3, 4], the space of Whitney forms is denoted by $\mathcal{P}_1^-\Lambda^k = \mathcal{P}_0\Lambda^k + \boldsymbol{\kappa}(\mathcal{P}_0\Lambda^{k+1})$. The operator \mathbf{d}^k maps $\boldsymbol{\kappa}(\mathcal{P}_0\Lambda^{k+1})$ bijectively onto $\mathcal{P}_0\Lambda^{k+1}$. Note that $\mathcal{P}_1^-\Lambda^0 = \mathcal{P}_1\Lambda^0$ and $\mathcal{P}_1^-\Lambda^n = \mathcal{P}_0\Lambda^n$. The Whitney forms associated with the operator δ_k are denoted by $\mathcal{P}_1^{*, -}\Lambda^k := \star(\mathcal{P}_1^-\Lambda^{n-k}) = \mathcal{P}_0\Lambda^k + \boldsymbol{\kappa}^\delta(\mathcal{P}_0\Lambda^{k-1})$. The operator δ_k maps $\boldsymbol{\kappa}^\delta(\mathcal{P}_0\Lambda^{k-1})$ bijectively onto $\mathcal{P}_0\Lambda^{k-1}$. Note that

$$(2.1) \quad \mathcal{N}(\mathbf{d}^k, \mathcal{P}_1^-\Lambda^k) = \mathcal{R}(\mathbf{d}^{k-1}, \mathcal{P}_1^-\Lambda^{k-1}) = \mathcal{P}_0\Lambda^k = \mathcal{R}(\delta_{k+1}, \mathcal{P}_1^{*, -}\Lambda^{k+1}) = \mathcal{N}(\delta_k, \mathcal{P}_1^{*, -}\Lambda^k).$$

Denote, on a simplicial subdivision \mathcal{G}_h of Ω , for $0 \leq k \leq n$,

$$(2.2) \quad \mathcal{P}_1^-\Lambda^k(\mathcal{G}_h) := \prod_{T \in \mathcal{G}_h} \mathcal{P}_1^-\Lambda^k(T), \quad \mathcal{P}_1^{*, -}\Lambda^k(\mathcal{G}_h) := \prod_{T \in \mathcal{G}_h} \mathcal{P}_1^{*, -}\Lambda^k(T).$$

Here and in the sequel, the subscript \cdot_h denotes mesh dependence. In particular, an operator bearing the subscript \cdot_h is understood to act cell by cell. Particularly, throughout, \mathbf{d}_h^k and $\delta_{k,h}$ denote the cell-by-cell exterior differential and codifferential.

The conforming finite element spaces with Whitney forms are denoted by

$$\begin{aligned} \mathbf{W}_h \Lambda^k &:= \mathcal{P}_1^- \Lambda^k(\mathcal{G}_h) \cap H \Lambda^k, & \mathbf{W}_{h_0} \Lambda^k &:= \mathcal{P}_1^- \Lambda^k(\mathcal{G}_h) \cap H_0 \Lambda^k, \\ \mathbf{W}_h^* \Lambda^k &:= \mathcal{P}_1^{*,-} \Lambda^k(\mathcal{G}_h) \cap H^* \Lambda^k, & \mathbf{W}_{h_0}^* \Lambda^k &:= \mathcal{P}_1^{*,-} \Lambda^k(\mathcal{G}_h) \cap H_0^* \Lambda^k. \end{aligned}$$

Then $\mathbf{W}_h^* \Lambda^k = \star \mathbf{W}_h \Lambda^{n-k}$ and $\mathbf{W}_{h_0}^* \Lambda^k = \star \mathbf{W}_{h_0} \Lambda^{n-k}$. These spaces coincide with the finite element spaces of piecewise Whitney forms defined by continuity of the nodal parameters [1]. Denote the spaces of discrete harmonic forms by, orthogonally in $L^2 \Lambda^k$,

$$\begin{aligned} \mathfrak{H}_h \Lambda^k &:= \mathcal{N}(\mathbf{d}^k, \mathbf{W}_h \Lambda^k) \ominus^\perp \mathcal{R}(\mathbf{d}^{k-1}, \mathbf{W}_h \Lambda^{k-1}), \\ \mathfrak{H}_{h_0} \Lambda^k &:= \mathcal{N}(\mathbf{d}^k, \mathbf{W}_{h_0} \Lambda^k) \ominus^\perp \mathcal{R}(\mathbf{d}^{k-1}, \mathbf{W}_{h_0} \Lambda^{k-1}), \\ \mathfrak{H}_h^* \Lambda^k &:= \mathcal{N}(\delta_k, \mathbf{W}_h^* \Lambda^k) \ominus^\perp \mathcal{R}(\delta_{k+1}, \mathbf{W}_h^* \Lambda^{k+1}), \\ \mathfrak{H}_{h_0}^* \Lambda^k &:= \mathcal{N}(\delta_k, \mathbf{W}_{h_0}^* \Lambda^k) \ominus^\perp \mathcal{R}(\delta_{k+1}, \mathbf{W}_{h_0}^* \Lambda^{k+1}). \end{aligned}$$

Then $\mathfrak{H}_h \Lambda^k = \star \mathfrak{H}_h^* \Lambda^{n-k}$ and $\mathfrak{H}_{h_0} \Lambda^k = \star \mathfrak{H}_{h_0}^* \Lambda^{n-k}$.

Lemma 2.1 ([1]). $\mathfrak{H}_h \Lambda^k$ and $\mathfrak{H}_{h_0} \Lambda^k$ are isomorphic to $\mathfrak{H} \Lambda^k$ and $\mathfrak{H}_0 \Lambda^k$, respectively.

Following [21], we denote the nonconforming finite element spaces for $H \Lambda^k$, $H_0 \Lambda^k$, $H^* \Lambda^k$, and $H_0^* \Lambda^k$, respectively, with piecewise Whitney forms by

$$\begin{aligned} \mathbf{W}_h^{\text{nc}} \Lambda^k &:= \left\{ \boldsymbol{\mu}_h \in \mathcal{P}_1^- \Lambda^k(\mathcal{G}_h) : \sum_{T \in \mathcal{G}_h} \langle \mathbf{d}^k \boldsymbol{\mu}_h, \boldsymbol{\eta}_h \rangle_{L^2 \Lambda^{k+1}(T)} = \sum_{T \in \mathcal{G}_h} \langle \boldsymbol{\mu}_h, \delta_{k+1} \boldsymbol{\eta}_h \rangle_{L^2 \Lambda^k(T)}, \forall \boldsymbol{\eta}_h \in \mathbf{W}_{h_0}^* \Lambda^{k+1} \right\}, \\ \mathbf{W}_{h_0}^{\text{nc}} \Lambda^k &:= \left\{ \boldsymbol{\mu}_h \in \mathcal{P}_1^- \Lambda^k(\mathcal{G}_h) : \sum_{T \in \mathcal{G}_h} \langle \mathbf{d}^k \boldsymbol{\mu}_h, \boldsymbol{\eta}_h \rangle_{L^2 \Lambda^{k+1}(T)} = \sum_{T \in \mathcal{G}_h} \langle \boldsymbol{\mu}_h, \delta_{k+1} \boldsymbol{\eta}_h \rangle_{L^2 \Lambda^k(T)}, \forall \boldsymbol{\eta}_h \in \mathbf{W}_h^* \Lambda^{k+1} \right\}, \\ \mathbf{W}_h^{*,\text{nc}} \Lambda^k &:= \left\{ \boldsymbol{\mu}_h \in \mathcal{P}_1^{*,-} \Lambda^k(\mathcal{G}_h) : \sum_{T \in \mathcal{G}_h} \langle \delta_k \boldsymbol{\mu}_h, \boldsymbol{\tau}_h \rangle_{L^2 \Lambda^{k-1}(T)} = \sum_{T \in \mathcal{G}_h} \langle \boldsymbol{\mu}_h, \mathbf{d}^{k-1} \boldsymbol{\tau}_h \rangle_{L^2 \Lambda^k(T)}, \forall \boldsymbol{\tau}_h \in \mathbf{W}_{h_0} \Lambda^{k-1} \right\}, \\ \mathbf{W}_{h_0}^{*,\text{nc}} \Lambda^k &:= \left\{ \boldsymbol{\mu}_h \in \mathcal{P}_1^{*,-} \Lambda^k(\mathcal{G}_h) : \sum_{T \in \mathcal{G}_h} \langle \delta_k \boldsymbol{\mu}_h, \boldsymbol{\tau}_h \rangle_{L^2 \Lambda^{k-1}(T)} = \sum_{T \in \mathcal{G}_h} \langle \boldsymbol{\mu}_h, \mathbf{d}^{k-1} \boldsymbol{\tau}_h \rangle_{L^2 \Lambda^k(T)}, \forall \boldsymbol{\tau}_h \in \mathbf{W}_h \Lambda^{k-1} \right\}. \end{aligned}$$

Note that $\mathbf{W}_{h(0)}^{\text{nc}} \Lambda^0$ and $\mathbf{W}_{h(0)}^{*,\text{nc}} \Lambda^n$ coincide with the classical lowest-degree Crouzeix-Raviart element spaces [13]. Moreover, the conforming spaces admit a dual characterization; i.e., for example,

$$\mathbf{W}_h \Lambda^k = \left\{ \boldsymbol{\mu}_h \in \mathcal{P}_1^- \Lambda^k(\mathcal{G}_h) : \sum_{T \in \mathcal{G}_h} \langle \mathbf{d}^k \boldsymbol{\mu}_h, \boldsymbol{\eta}_h \rangle_{L^2 \Lambda^{k+1}(T)} = \sum_{T \in \mathcal{G}_h} \langle \boldsymbol{\mu}_h, \delta_{k+1} \boldsymbol{\eta}_h \rangle_{L^2 \Lambda^k(T)}, \forall \boldsymbol{\eta}_h \in \mathbf{W}_{h_0}^{*,\text{nc}} \Lambda^{k+1} \right\}.$$

Hence, the adjoint relation between $H \Lambda^k$ and $H_0^* \Lambda^{k+1}$ is this way discretely inherited.

Theorem 2.2 ([21, Theorem 18]). *The spaces $\mathbf{W}_h^{\text{nc}}\Lambda^k$ and $\mathbf{W}_{h0}^{\text{nc}}\Lambda^k$ each admit a set of linearly independent basis functions that are each supported on at most two simplices.*

Theorem 2.3 (Discrete Helmholtz decomposition [21]). *The following decompositions are orthogonal in $L^2\Lambda^k(\Omega)$:*

$$\mathcal{P}_0\Lambda^k(\mathcal{G}_h) = \mathcal{R}(\mathbf{d}_h^{k-1}, \mathbf{W}_h^{\text{nc}}\Lambda^{k-1}) \oplus^\perp \mathcal{N}(\delta_{k,h}, \mathbf{W}_{h0}^*\Lambda^k) = \mathcal{R}(\mathbf{d}_h^{k-1}, \mathbf{W}_{h0}^{\text{nc}}\Lambda^{k-1}) \oplus^\perp \mathcal{N}(\delta_{k,h}, \mathbf{W}_h^*\Lambda^k),$$

$$\mathcal{P}_0\Lambda^k(\mathcal{G}_h) = \mathcal{N}(\mathbf{d}_h^k, \mathbf{W}_h^{\text{nc}}\Lambda^k) \oplus^\perp \mathcal{R}(\delta_{k+1,h}, \mathbf{W}_{h0}^*\Lambda^{k+1}) = \mathcal{N}(\mathbf{d}_h^k, \mathbf{W}_{h0}^{\text{nc}}\Lambda^k) \oplus^\perp \mathcal{R}(\delta_{k+1,h}, \mathbf{W}_h^*\Lambda^{k+1}),$$

where the first line holds for $1 \leq k \leq n$, and the second line holds for $0 \leq k \leq n-1$.

Denote

$$\mathfrak{S}_h^{\text{nc}}\Lambda^k := \mathcal{N}(\mathbf{d}_h^k, \mathbf{W}_h^{\text{nc}}\Lambda^k) \oplus^\perp \mathcal{R}(\mathbf{d}_h^{k-1}, \mathbf{W}_h^{\text{nc}}\Lambda^{k-1}),$$

$$\mathfrak{S}_{h0}^{\text{nc}}\Lambda^k := \mathcal{N}(\mathbf{d}_h^k, \mathbf{W}_{h0}^{\text{nc}}\Lambda^k) \oplus^\perp \mathcal{R}(\mathbf{d}_h^{k-1}, \mathbf{W}_{h0}^{\text{nc}}\Lambda^{k-1}),$$

$$\mathfrak{S}_h^{*,\text{nc}}\Lambda^k := \mathcal{N}(\delta_{k,h}, \mathbf{W}_h^{*,\text{nc}}\Lambda^k) \oplus^\perp \mathcal{R}(\delta_{k+1,h}, \mathbf{W}_h^{*,\text{nc}}\Lambda^{k+1}),$$

$$\mathfrak{S}_{h0}^{*,\text{nc}}\Lambda^k := \mathcal{N}(\delta_{k,h}, \mathbf{W}_{h0}^{*,\text{nc}}\Lambda^k) \oplus^\perp \mathcal{R}(\delta_{k+1,h}, \mathbf{W}_{h0}^{*,\text{nc}}\Lambda^{k+1}).$$

Then $\mathfrak{S}_h^{\text{nc}}\Lambda^k = \star\mathfrak{S}_h^{*,\text{nc}}\Lambda^{n-k}$, and $\mathfrak{S}_{h0}^{\text{nc}}\Lambda^k = \star\mathfrak{S}_{h0}^{*,\text{nc}}\Lambda^{n-k}$. Further, the discrete Poincaré-Lefschetz dualities and discrete Hodge decompositions hold.

Lemma 2.4. [21] $\mathfrak{S}_h\Lambda^k = \mathfrak{S}_{h0}^{*,\text{nc}}\Lambda^k$, $\mathfrak{S}_{h0}\Lambda^k = \mathfrak{S}_h^{*,\text{nc}}\Lambda^k$, $\mathfrak{S}_h^*\Lambda^k = \mathfrak{S}_{h0}^{\text{nc}}\Lambda^k$ and $\mathfrak{S}_{h0}^*\Lambda^k = \mathfrak{S}_h^{\text{nc}}\Lambda^k$.

Lemma 2.5. [21] *The Hodge decompositions hold: with $1 \leq k \leq n-1$,*

$$\begin{aligned} \mathcal{P}_0\Lambda^k(\mathcal{G}_h) &= \mathcal{R}(\mathbf{d}^{k-1}, \mathbf{W}_h\Lambda^{k-1}) \oplus^\perp \mathfrak{S}_h\Lambda^k \oplus^\perp \mathcal{R}(\delta_{k+1,h}, \mathbf{W}_{h0}^{*,\text{nc}}\Lambda^{k+1}) \\ &= \mathcal{R}(\mathbf{d}^{k-1}, \mathbf{W}_{h0}\Lambda^{k-1}) \oplus^\perp \mathfrak{S}_{h0}\Lambda^k \oplus^\perp \mathcal{R}(\delta_{k+1,h}, \mathbf{W}_h^{*,\text{nc}}\Lambda^{k+1}). \end{aligned}$$

2.3. A pair of adjoint operators associated with the Hodge-Laplacian. Define

$$\mathbf{T}_k : \Lambda^k \rightarrow \Lambda^{k+1} \times \Lambda^{k-1}, \quad \text{by } \mathbf{T}_k\boldsymbol{\mu} := \begin{pmatrix} \mathbf{d}^k\boldsymbol{\mu} \\ \delta_k\boldsymbol{\mu} \end{pmatrix},$$

and

$$\mathbb{T}_k : \Lambda^{k+1} \times \Lambda^{k-1} \rightarrow \Lambda^k, \quad \text{by } \mathbb{T}_k \begin{pmatrix} \boldsymbol{\eta} \\ \boldsymbol{\tau} \end{pmatrix} := \delta_{k+1}\boldsymbol{\eta} + \mathbf{d}^{k-1}\boldsymbol{\tau}.$$

Formally, we have $\delta_{k+1}\mathbf{d}^k + \mathbf{d}^{k-1}\delta_k = \mathbb{T}_k \circ \mathbf{T}_k$.

Lemma 2.6. *The operator $(\mathbf{T}_k, H\Lambda^k \cap H_0^*\Lambda^k)$ is closed, and its range $\mathcal{R}(\mathbf{T}_k, H\Lambda^k \cap H_0^*\Lambda^k)$ is closed.*

Proof. We analyze the structure of $H\Lambda^k \cap H_0^*\Lambda^k$. First, decompose

$$H\Lambda^k = \mathcal{N}(\mathbf{d}^k, H\Lambda^k) \oplus^\perp (\mathcal{N}(\mathbf{d}^k, H\Lambda^k))^\perp = \mathcal{R}(\mathbf{d}^{k-1}, H\Lambda^{k-1}) \oplus^\perp \mathfrak{S}\Lambda^k \oplus^\perp (\mathcal{N}(\mathbf{d}^k, H\Lambda^k))^\perp.$$

By the Helmholtz decomposition, $(\mathcal{N}(\mathbf{d}^k, H\Lambda^k))^\perp \subset H\Lambda^k \cap \mathcal{N}(\delta_k, H_0^*\Lambda^k)$. Hence

$$\mathcal{R}(\mathbf{d}^k, (\mathcal{N}(\mathbf{d}^k, H\Lambda^k))^\perp) = \mathcal{R}(\mathbf{d}^k, H\Lambda^k), \text{ and } \mathcal{R}(\delta_k, (\mathcal{N}(\mathbf{d}^k, H\Lambda^k))^\perp) = \{0\}.$$

Similarly, decompose $H_0^*\Lambda^k = \mathcal{N}(\delta_k, H_0^*\Lambda^k) \oplus^\perp (\mathcal{N}(\delta_k, H_0^*\Lambda^k))^\perp$, giving

$$\mathcal{R}(\mathbf{d}^k, (\mathcal{N}(\delta_k, H_0^*\Lambda^k))^\perp) = \{0\}, \text{ and } \mathcal{R}(\delta_k, (\mathcal{N}(\delta_k, H_0^*\Lambda^k))^\perp) = \mathcal{R}(\delta_k, H_0^*\Lambda^k).$$

It follows that

$$\mathcal{R}(\mathbf{T}_k, H\Lambda^k \cap H_0^*\Lambda^k) = \mathcal{R}(\mathbf{d}^k, H\Lambda^k) \times \mathcal{R}(\delta_k, H_0^*\Lambda^k).$$

Simultaneously,

$$\begin{aligned} \mathcal{N}(\mathbf{T}_k, H\Lambda^k \cap H_0^*\Lambda^k) &= \mathcal{N}(\mathbf{d}^k, H\Lambda^k) \cap \mathcal{N}(\delta_k, H_0^*\Lambda^k) \\ &= [\mathcal{R}(\mathbf{d}^{k-1}, H\Lambda^{k-1}) \oplus^\perp \mathfrak{H}\Lambda^k] \cap [\mathcal{R}(\delta_{k+1}, H_0^*\Lambda^{k+1}) \oplus^\perp \mathfrak{H}^*\Lambda^k] = \mathfrak{H}\Lambda^k. \end{aligned}$$

Both \mathbf{d}^k and δ_k are closed operators on their respective domains; consequently \mathbf{T}_k is closed on $H\Lambda^k \cap H_0^*\Lambda^k$ equipped with the intersection graph norm, and the explicit description of its range shows that the range is closed as the product of two closed ranges. \square

Lemma 2.7. *The adjoint operator of $(\mathbf{T}_k, H\Lambda^k \cap H_0^*\Lambda^k)$ is $(\mathbb{T}_k, H_0^*\Lambda^{k+1} \times H\Lambda^{k-1})$.*

Proof. For any $\mu \in H\Lambda^k \cap H_0^*\Lambda^k$, $\eta \in H_0^*\Lambda^{k+1}$, and $\tau \in H\Lambda^{k-1}$, integration by parts gives

$$(2.3) \quad \langle \mathbf{d}^k \mu, \eta \rangle_{L^2\Lambda^{k+1}} + \langle \delta_k \mu, \tau \rangle_{L^2\Lambda^{k-1}} = \langle \mu, \delta_{k+1} \eta + \mathbf{d}^{k-1} \tau \rangle_{L^2\Lambda^k}.$$

Moreover,

$$\mathcal{R}(\mathbb{T}_k, H_0^*\Lambda^{k+1} \times H\Lambda^{k-1}) = \mathcal{R}(\delta_{k+1}, H_0^*\Lambda^{k+1}) \oplus^\perp \mathcal{R}(\mathbf{d}^{k-1}, H\Lambda^{k-1}),$$

where the orthogonality follows from $\langle \delta_{k+1} \eta, \mathbf{d}^{k-1} \tau \rangle_{L^2\Lambda^k} = \langle \eta, \mathbf{d}^k \mathbf{d}^{k-1} \tau \rangle_{L^2\Lambda^{k+1}} = 0$, and

$$\mathcal{N}(\mathbb{T}_k, H_0^*\Lambda^{k+1} \times H\Lambda^{k-1}) = \mathcal{N}(\delta_{k+1}, H_0^*\Lambda^{k+1}) \times \mathcal{N}(\mathbf{d}^{k-1}, H\Lambda^{k-1}).$$

Consequently,

$$\begin{aligned} L^2\Lambda^k &= \mathcal{N}(\mathbf{T}_k, H\Lambda^k \cap H_0^*\Lambda^k) \oplus^\perp \mathcal{R}(\mathbb{T}_k, H_0^*\Lambda^{k+1} \times H\Lambda^{k-1}), \\ L^2\Lambda^{k+1} \times L^2\Lambda^{k-1} &= \mathcal{R}(\mathbf{T}_k, H\Lambda^k \cap H_0^*\Lambda^k) \oplus^\perp \mathcal{N}(\mathbb{T}_k, H_0^*\Lambda^{k+1} \times H\Lambda^{k-1}). \end{aligned}$$

Thus $(\mathbb{T}_k, H_0^*\Lambda^{k+1} \times H\Lambda^{k-1})$ shares the same range and kernel as the adjoint of $(\mathbf{T}_k, H\Lambda^k \cap H_0^*\Lambda^k)$.

Together with (2.3), this establishes that it is indeed the adjoint operator. \square

Remark 2.8. *In the sequel we write \mathbf{T}_k^* for \mathbb{T}_k ; that is,*

$$\mathbf{T}_k^* \begin{pmatrix} \eta \\ \tau \end{pmatrix} = \delta_{k+1} \eta + \mathbf{d}^{k-1} \tau, \quad \text{for } \begin{pmatrix} \eta \\ \tau \end{pmatrix} \in \Lambda^{k+1} \times \Lambda^{k-1}.$$

In the discrete setting, $\mathbf{T}_{k,h}^$ denotes the piecewise application of \mathbf{T}_k^* .*

3. THE MAIN RESULTS OF THIS PAPER

In this section, we present the main results of this paper; the technical proofs are postponed to Sections 4 and 5. Basic polynomial shape function spaces are introduced in Subsection 3.1, followed by the global finite element spaces and primal discretization schemes.

3.1. Shape function spaces on a single simplex. Given a simplex T , let $\tilde{x}^j = x^j - c_j$ where the constants c_j are chosen so that $\int_T \tilde{x}^j = 0$. Replacing the coordinate functions in the definition of the standard Koszul operator by their centered counterparts yields the simplex-dependent Koszul operator κ_T defined by

$$\kappa_T(\mathrm{d}x^{\alpha_1} \wedge \cdots \wedge \mathrm{d}x^{\alpha_k}) := \sum_{j=1}^k (-1)^{j+1} \tilde{x}^{\alpha_j} \mathrm{d}x^{\alpha_1} \wedge \cdots \wedge \mathrm{d}x^{\alpha_{j-1}} \wedge \mathrm{d}x^{\alpha_{j+1}} \wedge \cdots \wedge \mathrm{d}x^{\alpha_k}, \text{ for } \alpha \in \mathbb{I}\mathbb{X}_{k,n}.$$

Then $\mathbf{d}^{k-1} \kappa_T(\mathrm{d}x^{\alpha_1} \wedge \cdots \wedge \mathrm{d}x^{\alpha_k}) = k \mathrm{d}x^{\alpha_1} \wedge \cdots \wedge \mathrm{d}x^{\alpha_k}$. With the aid of κ_T , the Whitney forms admit the orthogonal decomposition $\mathcal{P}_1^- \Lambda^k(T) = \mathcal{P}_0 \Lambda^k(T) \oplus^\perp \kappa_T(\mathcal{P}_0 \Lambda^{k+1}(T))$ in $L^2 \Lambda^k(T)$. We use κ_h to denote the cell-wise application of κ_T . Define $\kappa_T^\delta := \star \circ \kappa_T \circ \star$ and $\kappa_h^\delta := \star \circ \kappa_h \circ \star$.

From now on, we make the convention that, for $\alpha \in \mathbb{I}\mathbb{X}_{k,n}$, we use α^C for one in $\mathbb{I}\mathbb{X}_{n-k,n}$, such that α and α^C partition $\{1, 2, \dots, n\}$. For $\alpha \in \mathbb{I}\mathbb{X}_{k,n}$, denote

$$\tilde{\mu}_{\delta,T}^\alpha = \sum_{j=1}^k [(\tilde{x}^{\alpha_j})^2 - c^{\alpha_j}] \mathrm{d}x^{\alpha_1} \wedge \cdots \wedge \mathrm{d}x^{\alpha_k},$$

and

$$\tilde{\mu}_{\mathbf{d},T}^\alpha = \sum_{j=1}^{n-k} [(\tilde{x}^{\alpha_j^C})^2 - c^{\alpha_j^C}] \mathrm{d}x^{\alpha_1} \wedge \mathrm{d}x^{\alpha_2} \wedge \cdots \wedge \mathrm{d}x^{\alpha_k},$$

where c^{α_j} and $c^{\alpha_j^C}$ are constants such that $\int_T [(\tilde{x}^{\alpha_j})^2 - c^{\alpha_j}] = 0$ and $\int_T [(\tilde{x}^{\alpha_j^C})^2 - c^{\alpha_j^C}] = 0$. Denote

$$(3.1) \quad \tilde{\mu}_{\mathbf{d} \cap \delta, T}^\alpha = \frac{-k}{n-k} \tilde{\mu}_{\mathbf{d}, T}^\alpha + \tilde{\mu}_{\delta, T}^\alpha.$$

Remark 3.1. *Direct calculation confirms that, with $\alpha \in \mathbb{I}\mathbb{X}_{k,n}$,*

$$\mathbf{d}^k \tilde{\mu}_{\delta, T}^\alpha = 0, \quad \delta_k \tilde{\mu}_{\delta, T}^\alpha = (-1)^n \cdot 2 \kappa_T(\mathrm{d}x^{\alpha_1} \wedge \mathrm{d}x^{\alpha_2} \wedge \cdots \wedge \mathrm{d}x^{\alpha_k}),$$

$$\delta_k \tilde{\mu}_{\mathbf{d}, T}^\alpha = 0, \quad \mathbf{d}^k \tilde{\mu}_{\mathbf{d}, T}^\alpha = 2(-1)^{n(1+k)+1} \kappa_T^\delta(\mathrm{d}x^{\alpha_1} \wedge \cdots \wedge \mathrm{d}x^{\alpha_k}),$$

and

$$\mathbf{T}_k \tilde{\mu}_{\mathbf{d} \cap \delta, T}^\alpha = 2(-1)^n \begin{pmatrix} (-1)^{kn} \frac{k}{n-k} \kappa_T^\delta(\mathrm{d}x^{\alpha_1} \wedge \cdots \wedge \mathrm{d}x^{\alpha_k}) \\ \kappa_T(\mathrm{d}x^{\alpha_1} \wedge \cdots \wedge \mathrm{d}x^{\alpha_k}) \end{pmatrix}.$$

Denote

$$(3.2) \quad \mathcal{H}_{\mathbf{d}}^2 \Lambda^k(T) := \text{span}\{\tilde{\mu}_{\mathbf{d},T}^\alpha : \alpha \in \mathbb{I}\mathbb{X}_{k,n}\},$$

$$(3.3) \quad \mathcal{H}_{\delta}^2 \Lambda^k(T) := \text{span}\{\tilde{\mu}_{\delta,T}^\alpha : \alpha \in \mathbb{I}\mathbb{X}_{k,n}\},$$

and

$$(3.4) \quad \mathcal{H}_{\mathbf{d}\cap\delta}^2 \Lambda^k(T) := \text{span}\{\tilde{\mu}_{\mathbf{d}\cap\delta,T}^\alpha : \alpha \in \mathbb{I}\mathbb{X}_{k,n}\},$$

Remark 3.2. δ_k is bijective from $\mathcal{H}_{\delta}^2 \Lambda^k(T)$ onto $\kappa_T(\mathcal{P}_0 \Lambda^k(T))$, \mathbf{d}^k is bijective from $\mathcal{H}_{\mathbf{d}}^2 \Lambda^k(T)$ onto $\kappa_T^\delta(\mathcal{P}_0 \Lambda^k(T))$, and both \mathbf{d}^k and δ_k are bijective from $\mathcal{H}_{\mathbf{d}\cap\delta}^2 \Lambda^k(T)$ onto $\kappa_T^\delta(\mathcal{P}_0 \Lambda^k(T))$ and $\kappa_T(\mathcal{P}_0 \Lambda^k(T))$, respectively.

Now we introduce, for the $H\Lambda^k \cap H^* \Lambda^k$ space, an enriched trimmed space, defined by

$$(3.5) \quad \mathbf{P}_{\mathbf{d}\cap\delta} \Lambda^k(T) := \mathcal{P}_0 \Lambda^k(T) \oplus \kappa_T(\mathcal{P}_0 \Lambda^{k+1}(T)) \oplus \kappa_T^\delta(\mathcal{P}_0 \Lambda^{k-1}(T)) \oplus \text{span}\{\tilde{\mu}_{\mathbf{d}\cap\delta,T}^\alpha : \alpha \in \mathbb{I}\mathbb{X}_{k,n}\},$$

and denote

$$(3.6) \quad \mathbf{P}_{\delta \times \mathbf{d}}^k(T) := \mathcal{P}_1^{*,-} \Lambda^{k+1}(T) \times \mathcal{P}_1^- \Lambda^{k-1}(T).$$

Remark 3.3. The following identities hold:

$$(3.7) \quad \mathcal{N}(\mathbf{T}_k, \mathbf{P}_{\mathbf{d}\cap\delta} \Lambda^k(T)) = \mathcal{R}(\mathbf{T}_k^*, \mathbf{P}_{\delta \times \mathbf{d}}^k(T)), \quad \text{and} \quad \mathcal{R}(\mathbf{T}_k, \mathbf{P}_{\mathbf{d}\cap\delta} \Lambda^k(T)) = \mathcal{N}(\mathbf{T}_k^*, \mathbf{P}_{\delta \times \mathbf{d}}^k(T)).$$

Actually, for the first item,

$$\mathcal{N}(\mathbf{T}_k, \mathbf{P}_{\mathbf{d}\cap\delta} \Lambda^k(T)) = \mathcal{P}_0 \Lambda^k(T) = \mathcal{R}(\mathbf{T}_k^*, \mathbf{P}_{\delta \times \mathbf{d}}^k(T)),$$

and for the second

$$\begin{aligned} \mathcal{N}(\mathbf{T}_k^*, \mathbf{P}_{\delta \times \mathbf{d}}^k(T)) &= \mathcal{P}_0 \Lambda^{k+1}(T) \times \mathcal{P}_0 \Lambda^{k-1}(T) \\ &\oplus \text{span} \left\{ \left(\begin{array}{c} (-1)^{kn} \frac{k}{n-k} \kappa_T^\delta(\mathbf{d}\mathbf{x}^{\alpha_1} \wedge \cdots \wedge \mathbf{d}\mathbf{x}^{\alpha_k}) \\ \kappa_T(\mathbf{d}\mathbf{x}^{\alpha_1} \wedge \cdots \wedge \mathbf{d}\mathbf{x}^{\alpha_k}) \end{array} \right), \alpha \in \mathbb{I}\mathbb{X}_{k,n} \right\} = \mathcal{R}(\mathbf{T}_k, \mathbf{P}_{\mathbf{d}\cap\delta} \Lambda^k(T)). \end{aligned}$$

Remark 3.4. Direct calculation leads to that, given $\boldsymbol{\mu} \in \mathbf{P}_{\mathbf{d}\cap\delta} \Lambda^k(T)$, $\boldsymbol{\mu} = 0$ if and only if, for any

$$\begin{pmatrix} \boldsymbol{\eta} \\ \boldsymbol{\tau} \end{pmatrix} \in \mathbf{P}_{\delta \times \mathbf{d}}^k(T),$$

$$(3.8) \quad \langle \mathbf{d}^k \boldsymbol{\mu}, \boldsymbol{\eta} \rangle_{L^2 \Lambda^{k+1}(T)} + \langle \delta_k \boldsymbol{\mu}, \boldsymbol{\tau} \rangle_{L^2 \Lambda^{k-1}(T)} = \langle \boldsymbol{\mu}, (\delta_{k+1} \boldsymbol{\eta} + \mathbf{d}^{k-1} \boldsymbol{\tau}) \rangle_{L^2 \Lambda^k(T)}.$$

Meanwhile, given $\begin{pmatrix} \boldsymbol{\eta} \\ \boldsymbol{\tau} \end{pmatrix} \in \mathbf{P}_{\delta \times \mathbf{d}}^k(T)$, $\begin{pmatrix} \boldsymbol{\eta} \\ \boldsymbol{\tau} \end{pmatrix} = 0$ if and only if (3.8) holds for any $\boldsymbol{\mu} \in \mathbf{P}_{\mathbf{d}\cap\delta} \Lambda^k(T)$.

3.2. **Finite element space for $H\Lambda^k \cap H_0^*\Lambda^k$.** On the subdivision \mathcal{G}_h of Ω , define

$$(3.9) \quad V_h^{\mathbf{d}\cap\delta}\Lambda^k := \left\{ \boldsymbol{\mu}_h \in \mathbf{P}_{\mathbf{d}\cap\delta}\Lambda^k(\mathcal{G}_h), \text{ such that } \left\langle \mathbf{T}_{k,h}\boldsymbol{\mu}_h, \begin{pmatrix} \boldsymbol{\eta}_h \\ \boldsymbol{\tau}_h \end{pmatrix} \right\rangle = \left\langle \boldsymbol{\mu}_h, \mathbf{T}_{k,h}^* \begin{pmatrix} \boldsymbol{\eta}_h \\ \boldsymbol{\tau}_h \end{pmatrix} \right\rangle_{L^2\Lambda^k}, \right. \\ \left. \forall \begin{pmatrix} \boldsymbol{\eta}_h \\ \boldsymbol{\tau}_h \end{pmatrix} \in \mathbf{W}_{h0}^{*,\text{nc}}\Lambda^{k+1} \times \mathbf{W}_h\Lambda^{k-1} \right\}.$$

Here, we use $\left\langle \begin{pmatrix} \boldsymbol{\mu} \\ \boldsymbol{\varsigma} \end{pmatrix}, \begin{pmatrix} \boldsymbol{\eta} \\ \boldsymbol{\tau} \end{pmatrix} \right\rangle = \langle \boldsymbol{\mu}, \boldsymbol{\eta} \rangle_{L^2\Lambda^{k+1}} + \langle \boldsymbol{\varsigma}, \boldsymbol{\tau} \rangle_{L^2\Lambda^{k-1}}$ for $\begin{pmatrix} \boldsymbol{\mu} \\ \boldsymbol{\varsigma} \end{pmatrix}, \begin{pmatrix} \boldsymbol{\eta} \\ \boldsymbol{\tau} \end{pmatrix} \in \Lambda^{k+1} \times \Lambda^{k-1}$ to denote the L^2 inner product. Namely,

$$(3.10) \quad V_h^{\mathbf{d}\cap\delta}\Lambda^k = \left\{ \boldsymbol{\mu}_h \in \mathbf{P}_{\mathbf{d}\cap\delta}\Lambda^k(\mathcal{G}_h), \text{ such that } \langle \mathbf{d}_h^k\boldsymbol{\mu}_h, \boldsymbol{\eta}_h \rangle_{L^2\Lambda^{k+1}} = \langle \boldsymbol{\mu}_h, \boldsymbol{\delta}_{k+1,h}\boldsymbol{\eta}_h \rangle_{L^2\Lambda^k}, \right. \\ \left. \forall \boldsymbol{\eta}_h \in \mathbf{W}_{h0}^{*,\text{nc}}\Lambda^{k+1}, \text{ and } \langle \boldsymbol{\delta}_{k,h}\boldsymbol{\mu}_h, \boldsymbol{\tau}_h \rangle_{L^2\Lambda^{k-1}} = \langle \boldsymbol{\mu}_h, \mathbf{d}^{k-1}\boldsymbol{\tau}_h \rangle_{L^2\Lambda^k}, \forall \boldsymbol{\tau}_h \in \mathbf{W}_h\Lambda^{k-1} \right\}.$$

Therefore, on the other hand, according to Remark 3.4,

$$\mathbf{W}_{h0}^{*,\text{nc}}\Lambda^{k+1} \times \mathbf{W}_h\Lambda^{k-1} = \left\{ \begin{pmatrix} \boldsymbol{\eta}_h \\ \boldsymbol{\tau}_h \end{pmatrix} \in \mathbf{P}_{\delta \times \mathbf{d}}^k(\mathcal{G}_h) : \left\langle \mathbf{T}_{k,h}\boldsymbol{\mu}_h, \begin{pmatrix} \boldsymbol{\eta}_h \\ \boldsymbol{\tau}_h \end{pmatrix} \right\rangle = \left\langle \boldsymbol{\mu}_h, \mathbf{T}_{k,h}^* \begin{pmatrix} \boldsymbol{\eta}_h \\ \boldsymbol{\tau}_h \end{pmatrix} \right\rangle_{L^2\Lambda^k}, \boldsymbol{\mu}_h \in V_h^{\mathbf{d}\cap\delta}\Lambda^k \right\}.$$

The space $V_h^{\mathbf{d}\cap\delta}\Lambda^k$ possesses these characteristics.

Theorem 3.5. $\mathcal{N}(\mathbf{T}_{k,h}, V_h^{\mathbf{d}\cap\delta}\Lambda^k) = \mathfrak{H}_h\Lambda^k$.

Proof. Firstly, by Lemma 2.5 and by (3.10),

$$\mathfrak{H}_h\Lambda^k = \left\{ \boldsymbol{\mu}_h \in \mathcal{P}_0\Lambda^k(\mathcal{G}_h) : \langle \boldsymbol{\mu}_h, \boldsymbol{\delta}_{k+1,h}\boldsymbol{\eta}_h \rangle_{L^2\Lambda^k} = 0, \forall \boldsymbol{\eta}_h \in \mathbf{W}_{h0}^{*,\text{nc}}\Lambda^{k+1}, \right. \\ \left. \text{and } \langle \boldsymbol{\mu}_h, \mathbf{d}^{k-1}\boldsymbol{\tau}_h \rangle_{L^2\Lambda^k} = 0, \forall \boldsymbol{\tau}_h \in \mathbf{W}_h\Lambda^{k-1} \right\} = \left\{ \boldsymbol{\mu}_h \in \mathcal{P}_0\Lambda^k(\mathcal{G}_h) : \boldsymbol{\mu}_h \in V_h^{\mathbf{d}\cap\delta}\Lambda^k \right\}.$$

Each $\boldsymbol{\mu}_h \in \mathfrak{H}_h\Lambda^k$ is piecewise constant and satisfies $\mathbf{d}_h^k\boldsymbol{\mu}_h = \boldsymbol{\delta}_{k,h}\boldsymbol{\mu}_h = 0$, hence $\boldsymbol{\mu}_h \in \mathcal{N}(\mathbf{T}_{k,h}, V_h^{\mathbf{d}\cap\delta}\Lambda^k)$.

On the other hand, let $\boldsymbol{\mu}_h \in V_h^{\mathbf{d}\cap\delta}\Lambda^k$ with $\mathbf{d}_h^k\boldsymbol{\mu}_h = 0$ and $\boldsymbol{\delta}_{k,h}\boldsymbol{\mu}_h = 0$. On each cell T , $\boldsymbol{\mu}_h|_T \in \mathbf{P}_{\mathbf{d}\cap\delta}\Lambda^k(T)$ and $\mathbf{T}_k(\boldsymbol{\mu}_h|_T) = 0$, so Remark 3.3 gives $\boldsymbol{\mu}_h|_T \in \mathcal{P}_0\Lambda^k(T)$; thus $\boldsymbol{\mu}_h \in \mathcal{P}_0\Lambda^k(\mathcal{G}_h)$. Therefore, $\boldsymbol{\mu}_h \in \mathfrak{H}_h\Lambda^k$. This completes the proof. \square

Theorem 3.6. *There exists a constant $C_{k,n}$, depending on the regularity of \mathcal{G}_h , such that*

$$(3.11) \quad \|\boldsymbol{\mu}_h\|_{L^2\Lambda^k} \leq C_{k,n} (\|\mathbf{d}_h^k\boldsymbol{\mu}_h\|_{L^2\Lambda^{k+1}} + \|\boldsymbol{\delta}_{k,h}\boldsymbol{\mu}_h\|_{L^2\Lambda^{k-1}}), \quad \forall \boldsymbol{\mu}_h \in V_h^{\mathbf{d}\cap\delta}\Lambda^k \ominus^\perp \mathfrak{H}_h\Lambda^k.$$

Theorem 3.7. *The space $V_h^{\mathbf{d}\cap\delta}\Lambda^k$ admits a set of basis functions, which is each supported on no more than two cells.*

3.2.1. *Two- and three-dimensional realizations of $\mathbf{V}_h^{\text{d}\cap\delta}\Lambda^k$.* The construction (3.10) is illustrated below in vector calculus notation relevant to the cases tested in Section 6. The local enriched space $\mathbf{P}_{\text{d}\cap\delta}\Lambda^k(T)$ from Section 3.1 specializes to $P_{\text{rd}}(T)$ in 2D and $P_{\text{cd}}(T)$ in 3D.

Two dimensions ($n = 2, k = 1$). On a polygon $\Omega \subset \mathbb{R}^2$, we use ∇ , div , and rot in the usual way. We identify $H\Lambda^1(\Omega)$ with $H(\text{rot}, \Omega)$ and $H_0^*\Lambda^1(\Omega)$ with $H_0(\text{div}, \Omega)$. The the corresponding shape function spaces are:

- $P_{\text{rd}}(T) = \text{span} \left\{ \begin{pmatrix} 1 \\ 0 \end{pmatrix}, \begin{pmatrix} 0 \\ 1 \end{pmatrix}, \begin{pmatrix} x \\ y \end{pmatrix}, \begin{pmatrix} -y \\ x \end{pmatrix}, \begin{pmatrix} x^2 - y^2 \\ 0 \end{pmatrix}, \begin{pmatrix} 0 \\ x^2 - y^2 \end{pmatrix} \right\};$
- $\mathbf{P}_{\text{c}\times\text{g}} = \mathcal{P}_1(T) \times \mathcal{P}_1(T) = \text{span}\{1, x, y\} \times \text{span}\{1, x, y\}.$

Denote $P_{\text{rd}}(\mathcal{G}_h) := \prod_{T \in \mathcal{G}_h} P_{\text{rd}}(T)$. With \mathbb{V}_h^1 the continuous piecewise linear space and V_{h0}^{CR} the homogeneous Crouzeix–Raviart space, the space (3.10) becomes

$$(3.12) \quad \mathbf{V}_h^{\text{rd}} := \left\{ \boldsymbol{\mu}_h \in P_{\text{rd}}(\mathcal{G}_h) : (\text{rot}_h \boldsymbol{\mu}_h, \boldsymbol{\eta}_h) = \langle \boldsymbol{\mu}_h, \text{curl}_h \boldsymbol{\eta}_h \rangle, \forall \boldsymbol{\eta}_h \in V_{h0}^{\text{CR}}, \right. \\ \left. \text{and } (\text{div}_h \boldsymbol{\mu}_h, \boldsymbol{\tau}_h) = -\langle \boldsymbol{\mu}_h, \nabla_h \boldsymbol{\tau}_h \rangle, \forall \boldsymbol{\tau}_h \in \mathbb{V}_h^1 \right\}.$$

The local shape functions and the global basis functions are given explicitly in Appendix D.

Three dimensions ($n = 3, k = 2$). On a polyhedral domain $\Omega \subset \mathbb{R}^3$, we use ∇ , div , and curl in the usual way. The formulation for $H(\text{div}, \Omega) \cap H_0(\text{curl}, \Omega)$ corresponds to $H\Lambda^2(\Omega) \cap H_0^*\Lambda^2(\Omega)$. The corresponding shape function spaces are

- $P_{\text{cd}}(T) = \text{span} \left\{ \begin{pmatrix} 1 \\ 0 \\ 0 \end{pmatrix}, \begin{pmatrix} 0 \\ 1 \\ 0 \end{pmatrix}, \begin{pmatrix} 0 \\ 0 \\ 1 \end{pmatrix}, \begin{pmatrix} -y \\ x \\ 0 \end{pmatrix}, \begin{pmatrix} z \\ 0 \\ -x \end{pmatrix}, \begin{pmatrix} 0 \\ -z \\ y \end{pmatrix}, \begin{pmatrix} 2x^2 - y^2 - z^2 \\ 0 \\ 0 \end{pmatrix}, \begin{pmatrix} 0 \\ 2y^2 - x^2 - z^2 \\ 0 \end{pmatrix}, \begin{pmatrix} 0 \\ 0 \\ 2z^2 - x^2 - y^2 \end{pmatrix} \right\};$
- $P_{\text{g}\times\text{c}} = P_1(T) \times \text{Ned}(T) = \text{span}\{1, x, y, z\} \times \text{span} \left\{ \begin{pmatrix} 1 \\ 0 \\ 0 \end{pmatrix}, \begin{pmatrix} 0 \\ 1 \\ 0 \end{pmatrix}, \begin{pmatrix} 0 \\ 0 \\ 1 \end{pmatrix}, \begin{pmatrix} -y \\ x \\ 0 \end{pmatrix}, \begin{pmatrix} z \\ 0 \\ -x \end{pmatrix}, \begin{pmatrix} 0 \\ -z \\ y \end{pmatrix} \right\},$ where

$\text{Ned}(T)$ stands for the lowest-degree Nedelec element shape function space on T .

Denote $P_{\text{cd}}(\mathcal{G}_h) := \prod_{T \in \mathcal{G}_h} P_{\text{cd}}(T)$. With V_{h0}^{CR} and $\mathbb{V}_h^{\text{Ned}}$ the lowest-order Crouzeix–Raviart and Nedelec spaces, the specialization of (3.10) is

$$(3.13) \quad \mathbf{V}_h^{\text{cd}} := \left\{ \boldsymbol{\mu}_h \in P_{\text{cd}}(\mathcal{G}_h) : (\text{div}_h \boldsymbol{\mu}_h, \boldsymbol{\tau}_h) + \langle \boldsymbol{\mu}_h, \nabla_h \boldsymbol{\tau}_h \rangle = 0, \forall \boldsymbol{\tau}_h \in V_{h0}^{\text{CR}}, \right. \\ \left. \text{and } (\text{rot}_h \boldsymbol{\mu}_h, \boldsymbol{\eta}_h) - \langle \boldsymbol{\mu}_h, \text{curl}_h \boldsymbol{\eta}_h \rangle = 0, \forall \boldsymbol{\eta}_h \in \mathbb{V}_h^{\text{Ned}} \right\}.$$

The local shape functions and global basis functions are reported in Appendix E.

3.3. A primal finite element scheme for the Hodge-Laplace problem. We consider the finite element problem: find $\omega_h \in V_h^{\text{d}\cap\delta}\Lambda^k$, such that

$$(3.14) \quad \begin{cases} \langle \omega_h, \mathfrak{S}_h \rangle_{L^2\Lambda^k} = 0, & \forall \mathfrak{S}_h \in \mathfrak{S}_h\Lambda^k, \\ \langle \mathbf{d}_h^k \omega_h, \mathbf{d}_h^k \mu_h \rangle_{L^2\Lambda^{k+1}} + \langle \delta_{k,h} \omega_h, \delta_{k,h} \mu_h \rangle_{L^2\Lambda^{k-1}} = \langle \mathbf{f} - \mathbf{P}_{\mathfrak{S}_h\Lambda^k} \mathbf{f}, \mathbf{P}_h^k \mu_h \rangle_{L^2\Lambda^k}, & \forall \mu_h \in V_h^{\text{d}\cap\delta}\Lambda^k. \end{cases}$$

Here $\mathbf{P}_{\mathfrak{S}_h\Lambda^k}$ denotes the projection to $\mathfrak{S}_h\Lambda^k$, and \mathbf{P}_h^k denotes the projection to $\mathcal{P}_0\Lambda^k(\mathcal{G}_h)$.

Remark 3.8. *The use of \mathbf{P}_h^k on the test functions in the load term is not necessary, but it includes the influence of numerical quadrature and is frequently encountered since no later than [2]. The projector leads to a stable modification: for $\mathbf{f} \in L^2\Lambda^k$, replacing $\langle \mathbf{f}, \mu_h \rangle$ by $\langle \mathbf{f}, \mathbf{P}_h^k \mu_h \rangle$ introduces an $O(h)\|\mathbf{f}\|_{L^2\Lambda^k}$ perturbation, which is absorbed in the error analysis of Section 5 (cf. Lemma 5.1).*

By Theorem 3.6 the discrete Poincaré inequality, the system (3.14) is well posed.

The main result of this paper is the theorem below.

Theorem 3.9. *Let ω and ω_h be the solutions of (1.1) and (3.14), respectively. Then,*

$$\begin{aligned} & \|\omega - \omega_h\|_{L^2\Lambda^k} + \|\mathbf{d}^k \omega - \mathbf{d}_h^k \omega_h\|_{L^2\Lambda^{k+1}} + \|\delta_k \omega - \delta_{k,h} \omega_h\|_{L^2\Lambda^{k-1}} + \|\mathbf{P}_{\mathfrak{S}_h\Lambda^k} \mathbf{f} - \check{\mathfrak{S}}_h\|_{L^2\Lambda^k} \\ & \leq C \left(\inf_{\tau_h \in W_h\Lambda^{k-1}} \|\delta_k \omega - \tau_h\|_{\mathfrak{d}^{k-1}} + \inf_{\mu_h \in W_h\Lambda^k} \|\omega - \mu_h\|_{\mathfrak{d}^k} + \inf_{\mathfrak{S}_h \in \mathfrak{S}_h\Lambda^k} \|\mathbf{P}_{\mathfrak{S}_h\Lambda^k} \mathbf{f} - \mathfrak{S}_h\|_{L^2\Lambda^k} + h\|\mathbf{f}\|_{L^2\Lambda^k} \right); \end{aligned}$$

and further, with Ω being s -regular,

$$(3.15) \quad \|\omega - \omega_h\|_{L^2\Lambda^k} + \|\mathbf{d}^k \omega - \mathbf{d}_h^k \omega_h\|_{L^2\Lambda^{k+1}} + \|\delta_k \omega - \delta_{k,h} \omega_h\|_{L^2\Lambda^{k-1}} \leq Ch^s \|\mathbf{f}\|_{L^2\Lambda^k}.$$

4. PROOFS OF THEOREMS 3.6 AND 3.7

4.1. Some technical preparation.

Lemma 4.1. (*[21]*) *There exists a constant $C_{k,n}$, depending on the regularity of T , such that*

$$(4.1) \quad \|\mu\|_{L^2\Lambda^k(T)} \leq C_{k,n} h_T \|\mathbf{d}^k \mu\|_{L^2\Lambda^{k+1}(T)}, \quad \text{for } \mu \in \kappa_T(\mathcal{P}_0\Lambda^{k+1}(T)),$$

and

$$(4.2) \quad \|\mu\|_{L^2\Lambda^k(T)} \leq C_{k,n} h_T \|\delta_k \mu\|_{L^2\Lambda^{k+1}(T)} \quad \text{for } \mu \in \kappa_T^\delta(\mathcal{P}_0\Lambda^{k-1}(T)).$$

Lemma 4.2. *There exists a constant $C_{k,n}$, depending on the regularity of T , such that*

$$(4.3) \quad \|\mu\|_{L^2\Lambda^k(T)} \leq C_{k,n} h_T \|\delta_k \mu\|_{L^2\Lambda^{k-1}(T)}, \quad \text{for } \mu \in \mathcal{H}_\delta^2\Lambda^k(T),$$

and

$$(4.4) \quad \|\mu\|_{L^2\Lambda^k(T)} \leq C_{k,n} h_T \|\mathbf{d}^k \mu\|_{L^2\Lambda^{k+1}(T)}, \quad \text{for } \mu \in \mathcal{H}_\mathfrak{d}^2\Lambda^k(T).$$

Proof. For $\boldsymbol{\mu} = \sum_{\boldsymbol{\varepsilon} \in \mathbb{I}\mathbb{X}_{k,n}} C_{\boldsymbol{\varepsilon}} \tilde{\boldsymbol{\mu}}_{\boldsymbol{\varepsilon},T}^{\boldsymbol{\varepsilon}}$, by H^1 Poincaré inequality,

$$\|\boldsymbol{\mu}\|_{L^2\Lambda^k(T)}^2 \leq C_{k,n} h_T^2 \left\| \sum_{\boldsymbol{\varepsilon} \in \mathbb{I}\mathbb{X}_{k,n}} C_{\boldsymbol{\varepsilon}} \sum_{1 \leq j \leq k} \nabla(\tilde{x}^{\boldsymbol{\varepsilon}_j})^2 dx^{\boldsymbol{\varepsilon}_1} \wedge dx^{\boldsymbol{\varepsilon}_2} \wedge \cdots \wedge dx^{\boldsymbol{\varepsilon}_k} \right\|_{L^2\Lambda^k(T)}^2 \leq C_{k,n} h_T^4 |T| \sum_{\boldsymbol{\varepsilon} \in \mathbb{I}\mathbb{X}_{k,n}} C_{\boldsymbol{\varepsilon}}^2.$$

Note that $\boldsymbol{\delta}_k \boldsymbol{\mu} = 2(-1)^n \sum_{\boldsymbol{\varepsilon} \in \mathbb{I}\mathbb{X}_{k,n}} C_{\boldsymbol{\varepsilon}} \boldsymbol{\kappa}_T(dx^{\boldsymbol{\varepsilon}_1} \wedge \cdots \wedge dx^{\boldsymbol{\varepsilon}_k})$ and further $\mathbf{d}^{k-1} \boldsymbol{\delta}_k \boldsymbol{\mu} = 2k(-1)^n \sum_{\boldsymbol{\varepsilon} \in \mathbb{I}\mathbb{X}_{k,n}} C_{\boldsymbol{\varepsilon}} dx^{\boldsymbol{\varepsilon}_1} \wedge \cdots \wedge dx^{\boldsymbol{\varepsilon}_k}$. It follows by the inverse inequality that

$$4k^2 h_T^2 |T| \sum_{\boldsymbol{\varepsilon} \in \mathbb{I}\mathbb{X}_{k,n}} C_{\boldsymbol{\varepsilon}}^2 = h_T^2 \|\mathbf{d}^{k-1} \boldsymbol{\delta}_k \boldsymbol{\mu}\|_{L^2\Lambda^k(T)}^2 \leq C_{k,n} \|\boldsymbol{\delta}_k \boldsymbol{\mu}\|_{L^2\Lambda^{k-1}(T)}^2.$$

The proof of (4.3) is thus completed. Similarly can (4.4) be proved. \square

Lemma 4.3. *There exists a constant $C_{k,n}$, depending on the regularity of T , such that*

$$(4.5) \quad \|\boldsymbol{\mu}\|_{L^2\Lambda^k(T)} \leq C_{k,n} h_T \|\boldsymbol{\delta}_k \boldsymbol{\mu}\|_{L^2\Lambda^{k-1}(T)}, \text{ for } \boldsymbol{\mu} \in \boldsymbol{\kappa}_T^{\delta}(\mathcal{P}_0\Lambda^{k-1}(T)) + \mathcal{H}_{\delta}^2\Lambda^k(T),$$

and

$$(4.6) \quad \|\boldsymbol{\mu}\|_{L^2\Lambda^k(T)} \leq C_{k,n} h_T \|\mathbf{d}^k \boldsymbol{\mu}\|_{L^2\Lambda^{k+1}(T)}, \text{ for } \boldsymbol{\mu} \in \boldsymbol{\kappa}_T(\mathcal{P}_0\Lambda^{k+1}(T)) + \mathcal{H}_{\mathbf{d}}^2\Lambda^k(T).$$

Proof. Note that $\boldsymbol{\delta}_k(\boldsymbol{\kappa}_T^{\delta}(\mathcal{P}_0\Lambda^{k-1}(T)))$ and $\boldsymbol{\delta}_k(\mathcal{H}_{\delta}^2\Lambda^k(T))$ are orthogonal, and $\mathbf{d}^k(\boldsymbol{\kappa}_T(\mathcal{P}_0\Lambda^{k+1}(T)))$ and $\mathbf{d}^k(\mathcal{H}_{\mathbf{d}}^2\Lambda^k(T))$ are orthogonal. The lemma follows by Lemmas 4.1 and 4.2. \square

Denote by $\mathbf{P}_{0,T}^k$ the L^2 projection onto $\mathcal{P}_0\Lambda^k(T)$.

Lemma 4.4. *There exists a constant $C_{k,n}$, depending on the regularity of T , such that*

$$(4.7) \quad \|\boldsymbol{\mu}\|_{L^2\Lambda^k(T)} \leq C_{k,n} h_T (\|\boldsymbol{\delta}_k \boldsymbol{\mu}\|_{L^2\Lambda^{k-1}(T)} + \|\mathbf{d}^k \boldsymbol{\mu}\|_{L^2\Lambda^{k-1}(T)}),$$

$$\text{for } \boldsymbol{\mu} \in \boldsymbol{\kappa}_T^{\delta}(\mathcal{P}_0\Lambda^{k-1}(T)) + \boldsymbol{\kappa}_T(\mathcal{P}_0\Lambda^{k+1}(T)) + \mathcal{H}_{\delta}^2\Lambda^k(T) + \mathcal{H}_{\mathbf{d}}^2\Lambda^k(T),$$

and

$$(4.8) \quad \|\boldsymbol{\mu} - \mathbf{P}_{0,T}^k \boldsymbol{\mu}\|_{L^2\Lambda^k(T)} \leq C_{k,n} h_T (\|\boldsymbol{\delta}_k \boldsymbol{\mu}\|_{L^2\Lambda^{k-1}(T)} + \|\mathbf{d}^k \boldsymbol{\mu}\|_{L^2\Lambda^{k-1}(T)}),$$

$$\text{for } \boldsymbol{\mu} \in \mathcal{P}_0\Lambda^k(T) + \boldsymbol{\kappa}_T^{\delta}(\mathcal{P}_0\Lambda^{k-1}(T)) + \boldsymbol{\kappa}_T(\mathcal{P}_0\Lambda^{k+1}(T)) + \mathcal{H}_{\delta}^2\Lambda^k(T) + \mathcal{H}_{\mathbf{d}}^2\Lambda^k(T).$$

Proof. For $\boldsymbol{\mu} \in \boldsymbol{\kappa}_T^{\delta}(\mathcal{P}_0\Lambda^{k-1}(T)) + \boldsymbol{\kappa}_T(\mathcal{P}_0\Lambda^{k+1}(T)) + \mathcal{H}_{\delta}^2\Lambda^k(T) + \mathcal{H}_{\mathbf{d}}^2\Lambda^k(T)$, decompose $\boldsymbol{\mu} = \boldsymbol{\mu}_1 + \boldsymbol{\mu}_2$, such that $\boldsymbol{\mu}_1 \in \boldsymbol{\kappa}_T^{\delta}(\mathcal{P}_0\Lambda^{k-1}(T)) + \mathcal{H}_{\delta}^2\Lambda^k(T)$ and $\boldsymbol{\mu}_2 \in \boldsymbol{\kappa}_T(\mathcal{P}_0\Lambda^{k+1}(T)) + \mathcal{H}_{\mathbf{d}}^2\Lambda^k(T)$, then $\mathbf{d}^k \boldsymbol{\mu}_1 = 0$ and $\boldsymbol{\delta}_k \boldsymbol{\mu}_2 = 0$. Then (4.7) follows by Lemma 4.3. Similarly can (4.8) be proved. \square

Now we introduce the notations below for short:

$$(4.9) \quad \mathring{\mathbf{P}}_{\delta \times \mathbf{d}}^k(T) := \mathcal{N}(\mathbf{T}_k^*, \mathbf{P}_{\delta \times \mathbf{d}}^k(T)), \text{ and, } \mathring{\mathbf{P}}_{\delta \times \mathbf{d}}^k(\mathcal{G}_h) := \prod_{T \in \mathcal{G}_h} \mathring{\mathbf{P}}_{\delta \times \mathbf{d}}^k(T).$$

Lemma 4.5 (Helmholtz-type decomposition). *For $1 \leq k \leq n-1$, orthogonal in $L^2\Lambda^k$,*

$$(4.10) \quad \mathcal{P}_0\Lambda^k(\mathcal{G}_h) = \mathcal{R}(\mathbf{T}_{k,h}^*, \mathbf{W}_{h0}^{*,nc}\Lambda^{k+1} \times \mathbf{W}_h\Lambda^{k-1}) \oplus^\perp \mathcal{N}(\mathbf{T}_{k,h}, \mathbf{V}_h^{\mathbf{d}\cap\delta}\Lambda^k),$$

$$(4.11) \quad \mathring{\mathcal{P}}_{\delta \times \mathbf{d}}^k(\mathcal{G}_h) = \mathcal{N}(\mathbf{T}_{k,h}^*, \mathbf{W}_{h0}^{*,nc}\Lambda^{k+1} \times \mathbf{W}_h\Lambda^{k-1}) \oplus^\perp \mathcal{R}(\mathbf{T}_{k,h}, \mathbf{V}_h^{\mathbf{d}\cap\delta}\Lambda^k).$$

Proof. Clearly, $\mathcal{P}_0\Lambda^k(\mathcal{G}_h) \supset \mathcal{R}(\mathbf{T}_{k,h}^*, \mathbf{W}_{h0}^{*,nc}\Lambda^{k+1} \times \mathbf{W}_h\Lambda^{k-1}) \oplus^\perp \mathcal{N}(\mathbf{T}_{k,h}, \mathbf{V}_h^{\mathbf{d}\cap\delta}\Lambda^k)$. On the other hand,

given $\boldsymbol{\mu}_h \in \mathcal{P}_0\Lambda^k(\mathcal{G}_h) \ominus^\perp \mathcal{R}(\mathbf{T}_{k,h}^*, \mathbf{W}_{h0}^{*,nc}\Lambda^{k+1} \times \mathbf{W}_h\Lambda^{k-1})$, it holds for $\begin{pmatrix} \boldsymbol{\eta}_h \\ \boldsymbol{\tau}_h \end{pmatrix} \in \mathbf{W}_{h0}^{*,nc}\Lambda^{k+1} \times \mathbf{W}_h\Lambda^{k-1}$

that $\left\langle \boldsymbol{\mu}_h, \mathbf{T}_{k,h}^* \begin{pmatrix} \boldsymbol{\eta}_h \\ \boldsymbol{\tau}_h \end{pmatrix} \right\rangle_{L^2\Lambda^k} = 0 = \left\langle \mathbf{T}_{k,h}\boldsymbol{\mu}_h, \begin{pmatrix} \boldsymbol{\eta}_h \\ \boldsymbol{\tau}_h \end{pmatrix} \right\rangle$; then it follows that $\boldsymbol{\mu}_h \in \mathbf{V}_h^{\mathbf{d}\cap\delta}\Lambda^k$ and further

$\mathcal{N}(\mathbf{T}_{k,h}, \mathbf{V}_h^{\mathbf{d}\cap\delta}\Lambda^k)$. Hence (4.10) holds. The proof of (4.11) is analogous. \square

4.2. Proof of Theorem 3.6. Firstly, following [21], we introduce the notion **Poincaré inequality's criterion** of (\mathbf{T}, \mathbf{D}) . Let \mathbf{X} and \mathbf{Y} be two Hilbert spaces. For $(\mathbf{T}, \mathbf{D}) : \mathbf{X} \rightarrow \mathbf{Y}$ a closed operator, denote

$$\mathbf{D}^{\mathbf{T}} := \{\mathbf{v} \in \mathbf{D} : \langle \mathbf{v}, \mathbf{w} \rangle_{\mathbf{X}} = 0, \forall \mathbf{w} \in \mathcal{N}(\mathbf{T}, \mathbf{D})\}.$$

The **Poincaré inequality's criterion** of (\mathbf{T}, \mathbf{D}) is defined as

$$(4.12) \quad \text{pic}(\mathbf{T}, \mathbf{D}) := \begin{cases} \sup_{0 \neq \mathbf{v} \in \mathbf{D}^{\mathbf{T}}} \frac{\|\mathbf{v}\|_{\mathbf{X}}}{\|\mathbf{T}\mathbf{v}\|_{\mathbf{Y}}}, & \text{if } \mathbf{D}^{\mathbf{T}} \neq \{0\}; \\ 0, & \text{if } \mathbf{D}^{\mathbf{T}} = \{0\}. \end{cases}$$

If $\text{pic}(\mathbf{T}, \mathbf{D})$ is finite, then the Poincaré inequality holds for (\mathbf{T}, \mathbf{D}) , and $\text{pic}(\mathbf{T}, \mathbf{D})$ is precisely the best constant.

Lemma 4.6. (*[4] [21]*) *There exists a constant $C_{k,n}$, depending on the regularity of \mathcal{G}_h , such that*

$$\text{pic}(\mathbf{d}^k, \mathbf{W}_h\Lambda^k) \leq C_{k,n}, \quad \text{and}, \quad \text{pic}(\mathbf{d}^k, \mathbf{W}_{h0}\Lambda^k) \leq C_{k,n},$$

and

$$\text{pic}(\mathbf{d}_h^k, \mathbf{W}_h^{\text{nc}}\Lambda^k) \leq C_{k,n}, \quad \text{and}, \quad \text{pic}(\mathbf{d}_h^k, \mathbf{W}_{h0}^{\text{nc}}\Lambda^k) \leq C_{k,n}.$$

Throughout, the subscript \cdot_h denotes the piecewise operation on \mathcal{G}_h .

Remark 4.7. *By Lemma 4.6, it follows by definition that*

$$\text{pic}(\boldsymbol{\delta}_k, \mathbf{W}_h^*\Lambda^k) \leq C_{n-k,n}, \quad \text{and}, \quad \text{pic}(\boldsymbol{\delta}_k, \mathbf{W}_{h0}^*\Lambda^k) \leq C_{n-k,n},$$

and

$$\text{pic}(\boldsymbol{\delta}_{k,h}, \mathbf{W}_h^{*,nc}\Lambda^k) \leq C_{n-k,n}, \quad \text{and}, \quad \text{pic}(\boldsymbol{\delta}_{k,h}, \mathbf{W}_{h0}^{*,nc}\Lambda^k) \leq C_{n-k,n}.$$

Without ambiguity, we do not distinguish the generic constants $C_{n-k,n}$ and $C_{k,n}$ in the sequel.

Remark 4.8. By Lemma 2.5, $\mathcal{R}(\delta_{k+1,h}, \mathbf{W}_{h0}^{*,nc} \Lambda^{k+1})$ is orthogonal to $\mathcal{R}(\mathbf{d}_h^{k-1}, \mathbf{W}_h \Lambda^{k-1})$. Therefore, $\mathcal{N}(\mathbf{T}_{k,h}^*, \mathbf{W}_{h0}^{*,nc} \Lambda^{k+1} \times \mathbf{W}_h \Lambda^{k-1}) = \mathcal{N}(\delta_{k+1,h}, \mathbf{W}_{h0}^{*,nc} \Lambda^{k+1}) \times \mathcal{N}(\mathbf{d}_h^{k-1}, \mathbf{W}_h \Lambda^{k-1})$. Further,

$$(4.13) \quad \text{pic}(\mathbf{T}_{k,h}^*, \mathbf{W}_{h0}^{*,nc} \Lambda^{k+1} \times \mathbf{W}_h \Lambda^{k-1}) = \max(\text{pic}(\delta_{k+1,h}, \mathbf{W}_{h0}^{*,nc} \Lambda^{k+1}), \text{pic}(\mathbf{d}_h^{k-1}, \mathbf{W}_h \Lambda^{k-1})) \leq C_{k,n}.$$

Proof of Theorem 3.6. First, decompose $V_h^{\text{d}\cap\delta} \Lambda^k = (V_h^{\text{d}\cap\delta} \Lambda^k)^\perp \oplus \mathfrak{H}_h \Lambda^k$. Now, given $\mu_h \in (V_h^{\text{d}\cap\delta} \Lambda^k)^\perp$, decompose further $\mu_h = \hat{\mu}_h + \mu_h^\perp$, such that, with $\hat{\mu}_h \in \mathcal{P}_0 \Lambda^k(\mathcal{G}_h)$ and $\mu_h^\perp \in \mathbf{P}_{\text{d}\cap\delta} \Lambda^k(\mathcal{G}_h)$ being orthogonal to $\mathcal{P}_0 \Lambda^k(\mathcal{G}_h)$, i.e. $\mu_h^\perp \in \prod_{T \in \mathcal{G}_h} [\kappa_T^\delta(\mathcal{P}_0 \Lambda^{k-1}(T)) + \kappa_T(\mathcal{P}_0 \Lambda^{k+1}(T)) + \mathcal{H}_{\text{d}\cap\delta}^2 \Lambda^k(T)]$. It follows

that $\hat{\mu}_h = \mu_h - \mu_h^\perp$ is orthogonal to $\mathfrak{H}_h \Lambda^k$, and hence $\hat{\mu}_h \in \mathcal{R}(\mathbf{T}_{k,h}^*, \mathbf{W}_{h0}^{*,nc} \Lambda^{k+1} \times \mathbf{W}_h \Lambda^{k-1})$ by Lemma 4.5. Therefore,

$$\begin{aligned} \|\hat{\mu}_h\|_{L^2 \Lambda^k} &= \sup_{\begin{pmatrix} \eta_h \\ \tau_h \end{pmatrix} \in (\mathbf{W}_{h0}^{*,nc} \Lambda^{k+1} \times \mathbf{W}_h \Lambda^{k-1})^\perp} \frac{\left\langle \hat{\mu}_h, \mathbf{T}_{k,h}^* \begin{pmatrix} \eta_h \\ \tau_h \end{pmatrix} \right\rangle_{L^2 \Lambda^k}}{\left\| \mathbf{T}_{k,h}^* \begin{pmatrix} \eta_h \\ \tau_h \end{pmatrix} \right\|_{L^2 \Lambda^k}} \\ &= \sup_{\begin{pmatrix} \eta_h \\ \tau_h \end{pmatrix} \in (\mathbf{W}_{h0}^{*,nc} \Lambda^{k+1} \times \mathbf{W}_h \Lambda^{k-1})^\perp} \frac{\left\langle \mu_h^\perp, \mathbf{T}_{k,h}^* \begin{pmatrix} \eta_h \\ \tau_h \end{pmatrix} \right\rangle_{L^2 \Lambda^k} - \left\langle \mathbf{T}_{k,h} \mu_h^\perp, \begin{pmatrix} \eta_h \\ \tau_h \end{pmatrix} \right\rangle}{\left\| \mathbf{T}_{k,h}^* \begin{pmatrix} \eta_h \\ \tau_h \end{pmatrix} \right\|_{L^2 \Lambda^k}} \\ &\leq \|\mu_h^\perp\|_{L^2 \Lambda^k} + \|\mathbf{T}_{k,h} \mu_h^\perp\|_{L^2 \Lambda^{k+1} \times L^2 \Lambda^{k-1}} \text{pic}(\mathbf{T}_{k,h}^*, \mathbf{W}_{h0}^{*,nc} \Lambda^{k+1} \times \mathbf{W}_h \Lambda^{k-1}). \end{aligned}$$

By Lemma 4.4, $\|\mu_h^\perp\|_{L^2 \Lambda^k} \leq Ch(\|\mathbf{d}_h^k \mu_h^\perp\|_{L^2 \Lambda^{k+1}} + \|\delta_{k,h} \mu_h^\perp\|_{L^2 \Lambda^{k-1}})$. Hence, by (4.13),

$$\|\mu_h\|_{L^2 \Lambda^k} \leq ch \|\mathbf{T}_{k,h} \mu_h\|_{L^2 \Lambda^{k+1} \times L^2 \Lambda^{k-1}} + C_{k,n} \|\mathbf{T}_{k,h} \mu_h\|_{L^2 \Lambda^{k+1} \times L^2 \Lambda^{k-1}} \leq C_{k,n} \|\mathbf{T}_{k,h} \mu_h\|_{L^2 \Lambda^{k+1} \times L^2 \Lambda^{k-1}}.$$

The proof is completed. \square

4.3. Proof of Theorem 3.7. Given a triangle T , define the cell-wise interpolator

$$(4.14) \quad \mathbb{I}_T^{\text{d}\cap\delta} : H \Lambda^k \cap H^* \Lambda^k \rightarrow \mathbf{P}_{\text{d}\cap\delta} \Lambda^k(T)$$

such that

$$(4.15) \quad \begin{aligned} &\langle \mathbf{d}^k(\mathbb{I}_T^{\text{d}\cap\delta} \mu), \eta \rangle_{L^2 \Lambda^{k+1}(T)} + \langle \delta_k(\mathbb{I}_T^{\text{d}\cap\delta} \mu), \tau \rangle_{L^2 \Lambda^{k-1}(T)} - \langle \mathbb{I}_T^{\text{d}\cap\delta} \mu, (\delta_{k+1} \eta + \mathbf{d}^{k-1} \tau) \rangle_{L^2 \Lambda^k(T)} \\ &= \langle \mathbf{d}^k \mu, \eta \rangle_{L^2 \Lambda^{k+1}(T)} + \langle \delta_k \mu, \tau \rangle_{L^2 \Lambda^{k-1}(T)} - \langle \mu, (\delta_{k+1} \eta + \mathbf{d}^{k-1} \tau) \rangle_{L^2 \Lambda^k(T)} \quad \forall \begin{pmatrix} \eta \\ \tau \end{pmatrix} \in \mathbf{P}_{\delta \times \mathbf{d}}^k(T). \end{aligned}$$

Further, define two partial interpolators, by

$$(4.16) \quad \mathbb{I}_T^{\text{d}\setminus\delta} : H \Lambda^k \cap H^* \Lambda^k \rightarrow \mathbf{P}_{\text{d}\cap\delta} \Lambda^k(T)$$

such that

- for $\forall \boldsymbol{\eta} \in \mathcal{P}_1^{*,-} \Lambda^{k+1}(T)$,

$$\langle \mathbf{d}^k(\mathbb{I}_T^{\mathbf{d}\delta} \boldsymbol{\mu}), \boldsymbol{\eta} \rangle_{L^2 \Lambda^{k+1}(T)} - \langle \mathbb{I}_T^{\mathbf{d}\delta} \boldsymbol{\mu}, \boldsymbol{\delta}_{k+1} \boldsymbol{\eta} \rangle_{L^2 \Lambda^k(T)} = \langle \mathbf{d}^k \boldsymbol{\mu}, \boldsymbol{\eta} \rangle_{L^2 \Lambda^{k+1}(T)} - \langle \boldsymbol{\mu}, \boldsymbol{\delta}_{k+1} \boldsymbol{\eta} \rangle_{L^2 \Lambda^k(T)},$$

- and for $\forall \boldsymbol{\tau} \in \mathcal{P}_1^- \Lambda^{k-1}(T)$,

$$\langle \boldsymbol{\delta}_k(\mathbb{I}_T^{\mathbf{d}\delta} \boldsymbol{\mu}), \boldsymbol{\tau} \rangle_{L^2 \Lambda^{k-1}(T)} - \langle \mathbb{I}_T^{\mathbf{d}\delta} \boldsymbol{\mu}, \mathbf{d}^{k-1} \boldsymbol{\tau} \rangle_{L^2 \Lambda^k(T)} = 0,$$

and by

$$(4.17) \quad \mathbb{I}_T^{\delta \mathbf{d}} : H \Lambda^k \cap H^* \Lambda^k \rightarrow \mathbf{P}_{\mathbf{d} \cap \delta} \Lambda^k(T)$$

such that

- for $\forall \boldsymbol{\tau} \in \mathcal{P}_1^{*,-} \Lambda^{k+1}(T)$.

$$\langle \mathbf{d}^k(\mathbb{I}_T^{\delta \mathbf{d}} \boldsymbol{\mu}), \boldsymbol{\tau} \rangle_{L^2 \Lambda^{k+1}(T)} - \langle \mathbb{I}_T^{\delta \mathbf{d}} \boldsymbol{\mu}, \boldsymbol{\delta}_{k+1} \boldsymbol{\tau} \rangle_{L^2 \Lambda^k(T)} = 0,$$

- and for $\forall \boldsymbol{\eta} \in \mathcal{P}_1^- \Lambda^{k-1}(T)$,

$$\langle \boldsymbol{\delta}_k(\mathbb{I}_T^{\delta \mathbf{d}} \boldsymbol{\mu}), \boldsymbol{\eta} \rangle_{L^2 \Lambda^{k+1}(T)} - \langle \mathbb{I}_T^{\delta \mathbf{d}} \boldsymbol{\mu}, \mathbf{d}^{k-1} \boldsymbol{\eta} \rangle_{L^2 \Lambda^k(T)} = \langle \boldsymbol{\delta}_k \boldsymbol{\mu}, \boldsymbol{\eta} \rangle_{L^2 \Lambda^{k+1}(T)} - \langle \boldsymbol{\mu}, \mathbf{d}^{k-1} \boldsymbol{\eta} \rangle_{L^2 \Lambda^k(T)}.$$

Evidently, $\mathbb{I}_T^{\mathbf{d} \cap \delta}$ is well-posed by Remark 3.3, and $\mathbb{I}_T^{\mathbf{d}\delta}$ and $\mathbb{I}_T^{\delta \mathbf{d}}$ are both well-posed by (2.1).

Remark 4.9. $\mathbb{I}_T^{\mathbf{d}\delta}$ is bijective from $\mathcal{P}_1^- \Lambda^k(T)$ onto $\mathcal{R}(\mathbb{I}_T^{\mathbf{d}\delta}, \mathcal{P}_1^- \Lambda^k(T))$ and $\mathbb{I}_T^{\delta \mathbf{d}}$ is bijective from $\mathcal{P}_1^{*,-} \Lambda^k(T)$ onto $\mathcal{R}(\mathbb{I}_T^{\delta \mathbf{d}}, \mathcal{P}_1^{*,-} \Lambda^k(T))$. However, neither $\mathbb{I}_T^{\mathbf{d}\delta}$ or $\mathbb{I}_T^{\delta \mathbf{d}}$ is projective on $\mathcal{P}_0 \Lambda^k = \mathcal{P}_1^- \Lambda^k(T) \cap \mathcal{P}_1^{*,-} \Lambda^k(T)$.

Remark 4.10. It holds that $\mathbb{I}_T^{\mathbf{d} \cap \delta} = \mathbb{I}_T^{\mathbf{d}\delta} + \mathbb{I}_T^{\delta \mathbf{d}}$ and $\mathbf{P}_{\mathbf{d} \cap \delta} \Lambda^k(T) = \mathcal{R}(\mathbb{I}_T^{\mathbf{d}\delta}, \mathcal{P}_1^- \Lambda^k(T)) \oplus \mathcal{R}(\mathbb{I}_T^{\delta \mathbf{d}}, \mathcal{P}_1^{*,-} \Lambda^k(T))$.

Further, define two global partial interpolators, by

$$(4.18) \quad \mathbb{I}_h^{\mathbf{d}\delta} : \prod_{T \in \mathcal{G}_h} H \Lambda^k \cap H^* \Lambda^k(T) \rightarrow \prod_{T \in \mathcal{G}_h} \mathbf{P}_{\mathbf{d} \cap \delta} \Lambda^k(T)$$

such that

$$(4.19) \quad (\mathbb{I}_h^{\mathbf{d}\delta} \boldsymbol{\mu}_h)_T = \mathbb{I}_T^{\mathbf{d}\delta}(\boldsymbol{\mu}_h|_T), \quad \forall T \in \mathcal{G}_h,$$

and by

$$(4.20) \quad \mathbb{I}_h^{\delta \mathbf{d}} : \prod_{T \in \mathcal{G}_h} H \Lambda^k \cap H^* \Lambda^k(T) \rightarrow \prod_{T \in \mathcal{G}_h} \mathbf{P}_{\mathbf{d} \cap \delta} \Lambda^k(T),$$

such that

$$(4.21) \quad (\mathbb{I}_h^{\delta \mathbf{d}} \boldsymbol{\mu}_h)_T = \mathbb{I}_T^{\delta \mathbf{d}}(\boldsymbol{\mu}_h|_T), \quad \forall T \in \mathcal{G}_h.$$

Remark 4.11. $\mathbb{I}_h^{\mathbf{d}\setminus\delta}$ and $\mathbb{I}_h^{\delta\setminus\mathbf{d}}$ are injective on $\mathbf{W}_h\Lambda^k$ and $\mathbf{W}_{h0}^{*,\text{nc}}\Lambda^k$, respectively. Though, neither $\mathbb{I}_h^{\mathbf{d}\setminus\delta}$ or $\mathbb{I}_h^{\delta\setminus\mathbf{d}}$ is projective on $\mathbf{W}_h\Lambda^k \cap \mathbf{W}_{h0}^{*,\text{nc}}\Lambda^k \subset \mathcal{P}_0\Lambda^k(\mathcal{G}_h)$.

Theorem 4.12. $\mathbf{V}_h^{\mathbf{d}\cap\delta}\Lambda^k = \mathcal{R}(\mathbb{I}_h^{\mathbf{d}\setminus\delta}, \mathbf{W}_h\Lambda^k) \oplus \mathcal{R}(\mathbb{I}_h^{\delta\setminus\mathbf{d}}, \mathbf{W}_{h0}^{*,\text{nc}}\Lambda^k)$.

Proof. Clearly, $\mathcal{R}(\mathbb{I}_h^{\mathbf{d}\setminus\delta}, \mathbf{W}_h\Lambda^k) \subset \mathbf{V}_h^{\mathbf{d}\cap\delta}\Lambda^k$ and $\mathcal{R}(\mathbb{I}_h^{\delta\setminus\mathbf{d}}, \mathbf{W}_{h0}^{*,\text{nc}}\Lambda^k) \subset \mathbf{V}_h^{\mathbf{d}\cap\delta}\Lambda^k$. Hence

$$\mathbf{V}_h^{\mathbf{d}\cap\delta}\Lambda^k \supset \mathcal{R}(\mathbb{I}_h^{\mathbf{d}\setminus\delta}, \mathbf{W}_h\Lambda^k) \oplus \mathcal{R}(\mathbb{I}_h^{\delta\setminus\mathbf{d}}, \mathbf{W}_{h0}^{*,\text{nc}}\Lambda^k).$$

On the other hand,

$$\begin{aligned} & \mathbf{V}_h^{\mathbf{d}\cap\delta}\Lambda^k \\ &= \left\{ \boldsymbol{\mu}_h \in \mathbf{P}_{\mathbf{d}\cap\delta}\Lambda^k(\mathcal{G}_h) : \left\langle \mathbf{T}_{k,h}\boldsymbol{\mu}_h, \begin{pmatrix} \boldsymbol{\eta}_h \\ \boldsymbol{\tau}_h \end{pmatrix} \right\rangle = \left\langle \boldsymbol{\mu}_h, \mathbf{T}_{k,h}^* \begin{pmatrix} \boldsymbol{\eta}_h \\ \boldsymbol{\tau}_h \end{pmatrix} \right\rangle_{L^2\Lambda^k}, \forall \begin{pmatrix} \boldsymbol{\eta}_h \\ \boldsymbol{\tau}_h \end{pmatrix} \in \mathbf{W}_{h0}^{*,\text{nc}}\Lambda^{k+1} \times \mathbf{W}_h\Lambda^{k-1} \right\} \\ &= \left\{ \boldsymbol{\mu}_h \in \prod_{T \in \mathcal{G}_h} \left(\mathcal{R}(\mathbb{I}_T^{\mathbf{d}\setminus\delta}, \mathcal{P}_1^-\Lambda^k(T)) \oplus \mathcal{R}(\mathbb{I}_T^{\delta\setminus\mathbf{d}}, \mathcal{P}_1^{*-}\Lambda^k(T)) \right) : \right. \\ & \quad \left. \left\langle \mathbf{T}_{k,h}\boldsymbol{\mu}_h, \begin{pmatrix} \boldsymbol{\eta}_h \\ \boldsymbol{\tau}_h \end{pmatrix} \right\rangle = \left\langle \boldsymbol{\mu}_h, \mathbf{T}_{k,h}^* \begin{pmatrix} \boldsymbol{\eta}_h \\ \boldsymbol{\tau}_h \end{pmatrix} \right\rangle_{L^2\Lambda^k}, \forall \begin{pmatrix} \boldsymbol{\eta}_h \\ \boldsymbol{\tau}_h \end{pmatrix} \in \mathbf{W}_{h0}^{*,\text{nc}}\Lambda^{k+1} \times \mathbf{W}_h\Lambda^{k-1} \right\} \\ &= \left\{ \boldsymbol{\mu}_h \in \prod_{T \in \mathcal{G}_h} \left(\mathcal{R}(\mathbb{I}_T^{\mathbf{d}\setminus\delta}, \mathcal{P}_1^-\Lambda^k(T)) \right) : \langle \mathbf{d}_h^k \boldsymbol{\mu}_h, \boldsymbol{\eta}_h \rangle_{L^2\Lambda^{k+1}} = \langle \boldsymbol{\mu}_h, \boldsymbol{\delta}_{k+1,h} \boldsymbol{\eta}_h \rangle_{L^2\Lambda^k}, \forall \boldsymbol{\eta}_h \in \mathbf{W}_{h0}^{*,\text{nc}}\Lambda^{k+1} \right\} \\ & \quad \oplus \left\{ \boldsymbol{\mu}_h \in \prod_{T \in \mathcal{G}_h} \left(\mathcal{R}(\mathbb{I}_T^{\delta\setminus\mathbf{d}}, \mathcal{P}_1^{*-}\Lambda^k(T)) \right) : \langle \boldsymbol{\delta}_{k,h} \boldsymbol{\mu}_h, \boldsymbol{\tau}_h \rangle_{L^2\Lambda^{k-1}} = \langle \boldsymbol{\mu}_h, \mathbf{d}^{k-1} \boldsymbol{\tau}_h \rangle_{L^2\Lambda^k}, \forall \boldsymbol{\tau}_h \in \mathbf{W}_h\Lambda^{k-1} \right\} \\ &:= I_1 \oplus I_2. \end{aligned}$$

Denote by $\check{\mathbb{I}}_T^{\mathbf{d}\setminus\delta}$ the inverse of $\mathbb{I}_T^{\mathbf{d}\setminus\delta}$ from $\mathcal{R}(\mathbb{I}_T^{\mathbf{d}\setminus\delta}, \mathcal{P}_1^-\Lambda^k(T))$ onto $\mathcal{P}_1^-\Lambda^k(T)$, and $\check{\mathbb{I}}_h^{\mathbf{d}\setminus\delta}$ the piecewise combination of $\check{\mathbb{I}}_T^{\mathbf{d}\setminus\delta}$. Then given $\boldsymbol{\mu}_h \in I_1$, it follows that

$$\begin{aligned} & \sum_{T \in \mathcal{G}_h} \langle \mathbf{d}_h^k \check{\mathbb{I}}_h^{\mathbf{d}\setminus\delta} \boldsymbol{\mu}_h, \boldsymbol{\eta}_h \rangle_{L^2\Lambda^{k+1}(T)} - \langle \check{\mathbb{I}}_h^{\mathbf{d}\setminus\delta} \boldsymbol{\mu}_h, \boldsymbol{\delta}_{k+1,h} \boldsymbol{\eta}_h \rangle_{L^2\Lambda^k(T)} \\ &= \sum_{T \in \mathcal{G}_h} \langle \mathbf{d}_h^k \boldsymbol{\mu}_h, \boldsymbol{\eta}_h \rangle_{L^2\Lambda^{k+1}(T)} - \langle \boldsymbol{\mu}_h, \boldsymbol{\delta}_{k+1,h} \boldsymbol{\eta}_h \rangle_{L^2\Lambda^k(T)} = 0, \quad \forall \boldsymbol{\eta}_h \in \mathbf{W}_{h0}^{*,\text{nc}}\Lambda^{k+1}; \end{aligned}$$

namely $\check{\mathbb{I}}_h^{\mathbf{d}\setminus\delta} \boldsymbol{\mu}_h \in \mathbf{W}_h\Lambda^k$, and $\boldsymbol{\mu}_h \in \mathcal{R}(\mathbb{I}_h^{\mathbf{d}\setminus\delta}, \mathbf{W}_h\Lambda^k)$. Hence, $I_1 \subset \mathcal{R}(\mathbb{I}_h^{\mathbf{d}\setminus\delta}, \mathbf{W}_h\Lambda^k)$. Similarly $I_2 \subset \mathcal{R}(\mathbb{I}_h^{\delta\setminus\mathbf{d}}, \mathbf{W}_{h0}^{*,\text{nc}}\Lambda^k)$. It follows that $\mathbf{V}_h^{\mathbf{d}\cap\delta}\Lambda^k \subset \mathcal{R}(\mathbb{I}_h^{\mathbf{d}\setminus\delta}, \mathbf{W}_h\Lambda^k) \oplus \mathcal{R}(\mathbb{I}_h^{\delta\setminus\mathbf{d}}, \mathbf{W}_{h0}^{*,\text{nc}}\Lambda^k)$, and the proof is completed. \square

Proof of Theorem 3.7. It suffices to note that, given a set of linearly dependent basis functions of $\mathbf{W}_h\Lambda^k$ and a set of $\mathbf{W}_{h0}^{*,\text{nc}}\Lambda^k$, a set of linearly dependent basis functions of $\mathbf{V}_h^{\mathbf{d}\cap\delta}\Lambda^k$ follows. Actually, for example, given a set of basis functions $\{\boldsymbol{\eta}_h^j\}$ of $\mathbf{W}_h\Lambda^k$, the support of $\mathbb{I}_h^{\mathbf{d}\setminus\delta} \boldsymbol{\eta}_h^j$ does not

exceed the support of $\boldsymbol{\eta}_h^j$, and we only have to show that $\{\mathbb{I}_h^{\mathbf{d}\setminus\delta}\boldsymbol{\eta}_h^j\}$ are linearly independent. For this, provided that a linear combination of all these functions $\{\mathbb{I}_h^{\mathbf{d}\setminus\delta}\boldsymbol{\eta}_h^j\}$ vanishes everywhere, as $\mathbb{I}_h^{\mathbf{d}\setminus\delta}$ is piecewise bijective, it follows that the same combination of $\{\boldsymbol{\eta}_h^j\}$ vanishes everywhere. Therefore, by Theorem 4.12, an explicit set of basis functions of $\mathbf{V}_h^{\mathbf{d}\cap\delta}\Lambda^k$, each supported on no more than two cells, are constructed. \square

5. PROOF OF THEOREM 3.9

For the ease of theoretical analysis below, we introduce two auxiliary formulations, namely

- find $\boldsymbol{\omega} \in H\Lambda^k(\Omega) \cap H_0^*\Lambda^k(\Omega)$ and $\boldsymbol{\vartheta} \in \mathfrak{H}\Lambda^k$, such that, for any $\boldsymbol{\mu} \in H\Lambda^k(\Omega) \cap H_0^*\Lambda^k(\Omega)$ and $\boldsymbol{\varsigma} \in \mathfrak{H}\Lambda^k$,

$$(5.1) \quad \begin{cases} \langle \boldsymbol{\omega}, \boldsymbol{\varsigma} \rangle_{L^2\Lambda^k} = 0, \\ \langle \boldsymbol{\vartheta}, \boldsymbol{\mu} \rangle_{L^2\Lambda^k} + \langle \mathbf{d}^k \boldsymbol{\omega}, \mathbf{d}^k \boldsymbol{\mu} \rangle_{L^2\Lambda^{k+1}} + \langle \boldsymbol{\delta}_k \boldsymbol{\omega}, \boldsymbol{\delta}_k \boldsymbol{\mu} \rangle_{L^2\Lambda^{k-1}} = \langle \boldsymbol{f}, \boldsymbol{\mu} \rangle_{L^2\Lambda^k}; \end{cases}$$

- find $(\boldsymbol{\omega}_h, \boldsymbol{\vartheta}_h) \in \mathbf{V}_h^{\mathbf{d}\cap\delta}\Lambda^k \times \mathfrak{H}_h\Lambda^k$, such that, for any $\boldsymbol{\varsigma}_h \in \mathfrak{H}_h\Lambda^k$ and $\boldsymbol{\mu}_h \in \mathbf{V}_h^{\mathbf{d}\cap\delta}\Lambda^k$,

$$(5.2) \quad \begin{cases} \langle \boldsymbol{\omega}_h, \boldsymbol{\varsigma}_h \rangle_{L^2\Lambda^k} = 0, \\ \langle \boldsymbol{\vartheta}_h, \boldsymbol{\mu}_h \rangle_{L^2\Lambda^k} + \langle \mathbf{d}_h^k \boldsymbol{\omega}_h, \mathbf{d}_h^k \boldsymbol{\mu}_h \rangle_{L^2\Lambda^{k+1}} + \langle \boldsymbol{\delta}_{k,h} \boldsymbol{\omega}_h, \boldsymbol{\delta}_{k,h} \boldsymbol{\mu}_h \rangle_{L^2\Lambda^{k-1}} = \langle \boldsymbol{f}, \mathbf{P}_h^k \boldsymbol{\mu}_h \rangle_{L^2\Lambda^k}. \end{cases}$$

One readily verifies that (5.1) is equivalent to (1.1), and (3.14) is equivalent to (5.2).

Lemma 5.1. *Let $(\boldsymbol{\omega}_h, \boldsymbol{\vartheta}_h)$ solve (5.2) and let $(\hat{\boldsymbol{\omega}}_h, \hat{\boldsymbol{\vartheta}}_h)$ solve the same system with $\langle \boldsymbol{f}, \boldsymbol{\mu}_h \rangle_{L^2\Lambda^k}$ in place of $\langle \boldsymbol{f}, \mathbf{P}_h^k \boldsymbol{\mu}_h \rangle_{L^2\Lambda^k}$ on the right-hand side. Then*

$$\|\boldsymbol{\omega}_h - \hat{\boldsymbol{\omega}}_h\|_{L^2\Lambda^k} + \|\mathbf{T}_{k,h}(\boldsymbol{\omega}_h - \hat{\boldsymbol{\omega}}_h)\|_{L^2\Lambda^{k+1} \times L^2\Lambda^{k-1}} \leq Ch\|\boldsymbol{f}\|_{L^2\Lambda^k}.$$

Proof. The difference $\boldsymbol{\omega}_h - \hat{\boldsymbol{\omega}}_h$ satisfies $\langle \mathbf{T}_{k,h}(\boldsymbol{\omega}_h - \hat{\boldsymbol{\omega}}_h), \mathbf{T}_{k,h}\boldsymbol{\mu}_h \rangle = \langle \boldsymbol{f}, (\mathbf{I} - \mathbf{P}_h^k)\boldsymbol{\mu}_h \rangle_{L^2\Lambda^k}$ for all $\boldsymbol{\mu}_h \in \mathbf{V}_h^{\mathbf{d}\cap\delta}\Lambda^k$ orthogonal to $\mathfrak{H}_h\Lambda^k$. Then Lemma 4.4 yields the bound. \square

5.1. Auxiliary mixed formulations and their connections. We introduce several auxiliary problems in mixed formulations.

- (A) Denote by $\mathbf{P}_{\delta \times \mathbf{d}}^k(\mathcal{G}_h)$ the L^2 projection onto $\dot{\mathbf{P}}_{\delta \times \mathbf{d}}^k(\mathcal{G}_h)$, which is a combination of the piecewise projection to $\dot{\mathbf{P}}_{\delta \times \mathbf{d}}^k(T)$. We consider an auxiliary problem: find $(\bar{\boldsymbol{\omega}}_h, \bar{\boldsymbol{\zeta}}_h, \bar{\boldsymbol{\sigma}}_h, \bar{\boldsymbol{\vartheta}}_h) \in \mathcal{P}_0\Lambda^k(\mathcal{G}_h) \times \mathbf{W}_{h0}^{*,\text{nc}}\Lambda^{k+1} \times \mathbf{W}_h\Lambda^{k-1} \times \mathfrak{H}_h\Lambda^k$, such that, for $(\bar{\boldsymbol{\mu}}_h, \bar{\boldsymbol{\eta}}_h, \bar{\boldsymbol{\tau}}_h, \bar{\boldsymbol{\varsigma}}_h) \in \mathcal{P}_0\Lambda^k(\mathcal{G}_h) \times$

$$\begin{aligned}
& \mathbf{W}_{h0}^{*,nc} \Lambda^{k+1} \times \mathbf{W}_h \Lambda^{k-1} \times \mathfrak{S}_h \Lambda^k, \\
(5.3) \quad (\text{AP-I}) \quad & \left\{ \begin{array}{l} \langle \bar{\omega}_h, \bar{\mathfrak{S}}_h \rangle_{L^2 \Lambda^k} = 0, \\ \left\langle \mathbf{P}_{\delta \times d}^{\mathfrak{P}^k}(\mathcal{G}_h) \left(\begin{array}{c} \bar{\zeta}_h \\ \bar{\sigma}_h \end{array} \right), \left(\begin{array}{c} \bar{\eta}_h \\ \bar{\tau}_h \end{array} \right) \right\rangle_{L^2 \Lambda^k} - \left\langle \bar{\omega}_h, \mathbf{T}_{k,h}^* \left(\begin{array}{c} \bar{\eta}_h \\ \bar{\tau}_h \end{array} \right) \right\rangle_{L^2 \Lambda^k} = 0, \\ \langle \bar{\vartheta}_h, \bar{\mu}_h \rangle_{L^2 \Lambda^k} - \left\langle \bar{\mu}_h, \mathbf{T}_{k,h}^* \left(\begin{array}{c} \bar{\zeta}_h \\ \bar{\sigma}_h \end{array} \right) \right\rangle_{L^2 \Lambda^k} = \langle \mathbf{f}, \bar{\mu}_h \rangle_{L^2 \Lambda^k}. \end{array} \right.
\end{aligned}$$

$$\begin{aligned}
& \text{(B) find } (\bar{\omega}_h, \bar{\zeta}_h, \bar{\sigma}_h, \bar{\vartheta}_h) \in \mathcal{P}_0 \Lambda^k(\mathcal{G}_h) \times \mathbf{W}_{h0}^{*,nc} \Lambda^{k+1} \times \mathbf{W}_h \Lambda^{k-1} \times \mathfrak{S}_h \Lambda^k, \text{ such that, for } (\tilde{\mu}_h, \tilde{\eta}_h, \tilde{\tau}_h, \tilde{\zeta}_h) \in \\
& \mathcal{P}_0 \Lambda^k(\mathcal{G}_h) \times \mathbf{W}_{h0}^{*,nc} \Lambda^{k+1} \times \mathbf{W}_h \Lambda^{k-1} \times \mathfrak{S}_h \Lambda^k, \\
(5.4)
\end{aligned}$$

$$\begin{aligned}
(\text{AP-II}) \quad & \left\{ \begin{array}{l} \langle \tilde{\omega}_h, \tilde{\zeta}_h \rangle_{L^2 \Lambda^k} = 0 \\ \langle \mathbf{P}_h^{k+1} \tilde{\zeta}_h, \tilde{\eta}_h \rangle_{L^2 \Lambda^{k+1}} - \langle \tilde{\omega}_h, \delta_{k+1,h} \tilde{\eta}_h \rangle_{L^2 \Lambda^k} = 0 \\ \langle \mathbf{P}_h^{k-1} \tilde{\sigma}_h, \tilde{\tau}_h \rangle_{L^2 \Lambda^{k-1}} - \langle \tilde{\omega}_h, \mathbf{d}^{k-1} \tilde{\tau}_h \rangle_{L^2 \Lambda^k} = 0 \\ \langle \tilde{\vartheta}_h, \tilde{\mu}_h \rangle_{L^2 \Lambda^k} + \langle \delta_{k+1,h} \tilde{\zeta}_h, \tilde{\mu}_h \rangle_{L^2 \Lambda^k} + \langle \mathbf{d}^{k-1} \tilde{\sigma}_h, \tilde{\mu}_h \rangle_{L^2 \Lambda^k} = \langle \mathbf{f}, \tilde{\mu}_h \rangle_{L^2 \Lambda^k} \end{array} \right.
\end{aligned}$$

$$\begin{aligned}
& \text{(C) Find } (\hat{\vartheta}_h, \hat{\sigma}_h, \hat{\omega}_h) \in \mathfrak{S}_h \Lambda^k \times \mathbf{W}_h \Lambda^{k-1} \times \mathbf{W}_h \Lambda^k, \text{ such that, for } (\hat{\mathfrak{S}}_h, \hat{\tau}_h, \hat{\mu}_h) \in \mathfrak{S}_h \Lambda^k \times \mathbf{W}_h \Lambda^{k-1} \times \\
& \mathbf{W}_h \Lambda^k
\end{aligned}$$

$$\begin{aligned}
(5.5) \quad (\text{AP-III}) \quad & \left\{ \begin{array}{l} \langle \hat{\omega}_h, \hat{\mathfrak{S}}_h \rangle_{L^2 \Lambda^k} = 0 \\ \langle \mathbf{P}_h^{k-1} \hat{\sigma}_h, \mathbf{P}_h^{k-1} \hat{\tau}_h \rangle_{L^2 \Lambda^{k-1}} - \langle \hat{\omega}_h, \mathbf{d}^{k-1} \hat{\tau}_h \rangle_{L^2 \Lambda^k} = 0 \\ \langle \hat{\vartheta}_h, \hat{\mu}_h \rangle_{L^2 \Lambda^k} + \langle \mathbf{d}^{k-1} \hat{\sigma}_h, \hat{\mu}_h \rangle_{L^2 \Lambda^k} + \langle \mathbf{d}^k \hat{\omega}_h, \mathbf{d}^k \hat{\mu}_h \rangle_{L^2 \Lambda^{k+1}} = \langle \mathbf{f}, \mathbf{P}_h^k \hat{\mu}_h \rangle_{L^2 \Lambda^k} \end{array} \right.
\end{aligned}$$

$$\begin{aligned}
& \text{(D) Find } (\check{\vartheta}_h, \check{\sigma}_h, \check{\omega}_h) \in \mathfrak{S}_h \Lambda^k \times \mathbf{W}_h \Lambda^{k-1} \times \mathbf{W}_h \Lambda^k, \text{ such that, for } \check{\zeta}_h \in \mathfrak{S}_h \Lambda^k, \check{\tau}_h \in \mathbf{W}_h \Lambda^{k-1} \text{ and} \\
& \check{\mu}_h \in \mathbf{W}_h \Lambda^k,
\end{aligned}$$

$$\begin{aligned}
(5.6) \quad (\text{AP-IV}) \quad & \left\{ \begin{array}{l} \langle \check{\omega}_h, \check{\zeta}_h \rangle_{L^2 \Lambda^k} = 0 \\ \langle \check{\sigma}_h, \check{\tau}_h \rangle_{L^2 \Lambda^{k-1}} - \langle \check{\omega}_h, \mathbf{d}^{k-1} \check{\tau}_h \rangle_{L^2 \Lambda^k} = 0 \\ \langle \check{\vartheta}_h, \check{\mu}_h \rangle_{L^2 \Lambda^k} + \langle \mathbf{d}^{k-1} \check{\sigma}_h, \check{\mu}_h \rangle_{L^2 \Lambda^k} + \langle \mathbf{d}^k \check{\omega}_h, \mathbf{d}^k \check{\mu}_h \rangle_{L^2 \Lambda^{k+1}} = \langle \mathbf{f}, \check{\mu}_h \rangle_{L^2 \Lambda^k}. \end{array} \right.
\end{aligned}$$

Lemma 5.2. *The problem (5.3) is well-posed. Further, let (ω_h, ϑ_h) be the solution of (5.2). Then*

$$(5.7) \quad \mathbf{T}_{k,h} \omega_h = \mathbf{P}_{\delta \times d}^{\mathfrak{P}^k}(\mathcal{G}_h) \left(\begin{array}{c} \bar{\zeta}_h \\ \bar{\sigma}_h \end{array} \right), \quad \text{and } \bar{\omega}_h = \mathbf{P}_h^k \omega_h.$$

Proof. We are to verify Brezzi's conditions. Firstly, for any $\bar{\mathfrak{S}}_h \in \mathfrak{S}_h \Lambda^k$ and $\left(\begin{array}{c} \bar{\eta}_h \\ \bar{\tau}_h \end{array} \right) \in \mathbf{W}_{h0}^{*,nc} \Lambda^{k+1} \times \mathbf{W}_h \Lambda^{k-1}$, such that $\langle \bar{\mathfrak{S}}_h, \bar{\mu}_h \rangle_{L^2 \Lambda^k} = \left\langle \bar{\mu}_h, \mathbf{T}_{k,h}^* \left(\begin{array}{c} \bar{\eta}_h \\ \bar{\tau}_h \end{array} \right) \right\rangle_{L^2 \Lambda^k}$, $\forall \bar{\mu}_h \in \mathcal{P}_0 \Lambda^k(\mathcal{G}_h)$, it holds that $\bar{\mathfrak{S}}_h = 0$, $\mathbf{d}^{k-1} \bar{\tau}_h = 0$ and $\delta_{k+1,h} \bar{\eta}_h = 0$, and further $\bar{\tau}_h \in \mathcal{P}_0 \Lambda^{k-1}(\mathcal{G}_h)$ and $\bar{\eta}_h \in \mathcal{P}_0 \Lambda^{k+1}(\mathcal{G}_h)$. Therefore, $\left\langle \mathbf{P}_{\delta \times d}^{\mathfrak{P}^k}(\mathcal{G}_h) \left(\begin{array}{c} \bar{\eta}_h \\ \bar{\tau}_h \end{array} \right), \left(\begin{array}{c} \bar{\eta}_h \\ \bar{\tau}_h \end{array} \right) \right\rangle_{L^2 \Lambda^k} = \left\langle \left(\begin{array}{c} \bar{\eta}_h \\ \bar{\tau}_h \end{array} \right), \left(\begin{array}{c} \bar{\eta}_h \\ \bar{\tau}_h \end{array} \right) \right\rangle_{L^2 \Lambda^k}$, and the coercivity follows. On the other hand, given

any $\bar{\boldsymbol{\mu}}_h \in \mathcal{P}_0\Lambda^k(\mathcal{G}_h)$, by the Hodge decomposition of $\mathcal{P}_0\Lambda^k(\mathcal{G}_h)$ and the Poincaré inequalities on $\mathbf{W}_h\Lambda^{k-1}$ and $\mathbf{W}_{h0}^{*,\text{nc}}\Lambda^{k+1}$, there exists a $\bar{\boldsymbol{\varsigma}}_h \in \boldsymbol{\mathfrak{H}}_h\Lambda^k$, a $\bar{\boldsymbol{\tau}}_h \in \mathbf{W}_h\Lambda^{k-1}$ and an $\bar{\boldsymbol{\eta}}_h \in \mathbf{W}_{h0}^{*,\text{nc}}\Lambda^{k+1}$, such that $\bar{\boldsymbol{\mu}}_h = \bar{\boldsymbol{\varsigma}}_h + \mathbf{d}^{k-1}\bar{\boldsymbol{\tau}}_h + \boldsymbol{\delta}_{k+1,h}\bar{\boldsymbol{\eta}}_h$, and $\|\bar{\boldsymbol{\tau}}_h\|_{L^2\Lambda^{k-1}} + \|\bar{\boldsymbol{\eta}}_h\|_{L^2\Lambda^{k+1}} \leq C\|\bar{\boldsymbol{\mu}}_h\|_{L^2\Lambda^k}$. Then Brezzi's conditions for (5.3) are verified. For any $\mathbf{f} \in L^2\Lambda^k$, the system (5.3) admits a unique solution.

As $(\boldsymbol{\omega}_h, \boldsymbol{\vartheta}_h)$ is the solution of (5.2), with $\begin{pmatrix} \boldsymbol{\zeta}_h \\ \boldsymbol{\sigma}_h \end{pmatrix} \in \mathbf{W}_{h0}^{*,\text{nc}}\Lambda^{k+1} \times \mathbf{W}_h\Lambda^{k-1}$, it holds that

$$(5.8) \quad \langle \boldsymbol{\vartheta}_h, \boldsymbol{\mu}_h \rangle_{L^2\Lambda^k} + \langle \mathbf{T}_{k,h}\boldsymbol{\omega}_h, \mathbf{T}_{k,h}\boldsymbol{\mu}_h \rangle \\ + \left\langle \mathbf{T}_{k,h}\boldsymbol{\mu}_h, \begin{pmatrix} \boldsymbol{\zeta}_h \\ \boldsymbol{\sigma}_h \end{pmatrix} \right\rangle - \left\langle \boldsymbol{\mu}_h, \mathbf{T}_{k,h}^* \begin{pmatrix} \boldsymbol{\zeta}_h \\ \boldsymbol{\sigma}_h \end{pmatrix} \right\rangle_{L^2\Lambda^k} = \langle \mathbf{P}_h^k \mathbf{f}, \boldsymbol{\mu}_h \rangle_{L^2\Lambda^k}, \forall \boldsymbol{\mu}_h \in \mathbf{P}_{\mathbf{d}\cap\delta}\Lambda^k(\mathcal{G}_h).$$

Then, for $\boldsymbol{\mu}_h \in \mathcal{P}_0\Lambda^k(\mathcal{G}_h)$,

$$\langle \boldsymbol{\vartheta}_h, \boldsymbol{\mu}_h \rangle_{L^2\Lambda^k} - \left\langle \boldsymbol{\mu}_h, \mathbf{T}_{k,h}^* \begin{pmatrix} \boldsymbol{\zeta}_h \\ \boldsymbol{\sigma}_h \end{pmatrix} \right\rangle = \langle \mathbf{f}, \boldsymbol{\mu}_h \rangle_{L^2\Lambda^k}.$$

Namely

$$\mathbf{T}_{k,h}^* \begin{pmatrix} \boldsymbol{\zeta}_h \\ \boldsymbol{\sigma}_h \end{pmatrix} = \mathbf{P}_h^k \mathbf{f} - \mathbf{P}_{\boldsymbol{\mathfrak{H}}_h} \mathbf{f}, \mathbf{P}_{\boldsymbol{\mathfrak{H}}_h} \text{ being the projection to } \boldsymbol{\mathfrak{H}}_h.$$

It follows then

$$\mathbf{T}_{k,h}\boldsymbol{\omega}_h = \mathbf{P}_{\mathbf{P}_{\delta \times \mathbf{d}}^k(\mathcal{G}_h)} \begin{pmatrix} \boldsymbol{\zeta}_h \\ \boldsymbol{\sigma}_h \end{pmatrix}.$$

Noting that

$$\left\langle \mathbf{T}_{k,h}\boldsymbol{\omega}_h, \begin{pmatrix} \boldsymbol{\eta}_h \\ \boldsymbol{\tau}_h \end{pmatrix} \right\rangle = \left\langle \boldsymbol{\omega}_h, \mathbf{T}_{k,h}^* \begin{pmatrix} \boldsymbol{\eta}_h \\ \boldsymbol{\tau}_h \end{pmatrix} \right\rangle_{L^2\Lambda^k}, \forall \begin{pmatrix} \boldsymbol{\eta}_h \\ \boldsymbol{\tau}_h \end{pmatrix} \in \mathbf{W}_{h0}^{*,\text{nc}}\Lambda^{k+1} \times \mathbf{W}_h\Lambda^{k-1},$$

we have further

$$\left\langle \mathbf{P}_{\mathbf{P}_{\delta \times \mathbf{d}}^k(\mathcal{G}_h)} \begin{pmatrix} \boldsymbol{\zeta}_h \\ \boldsymbol{\sigma}_h \end{pmatrix}, \begin{pmatrix} \boldsymbol{\eta}_h \\ \boldsymbol{\tau}_h \end{pmatrix} \right\rangle = \left\langle \boldsymbol{\omega}_h, \mathbf{T}_{k,h}^* \begin{pmatrix} \boldsymbol{\eta}_h \\ \boldsymbol{\tau}_h \end{pmatrix} \right\rangle_{L^2\Lambda^k}, \forall \begin{pmatrix} \boldsymbol{\eta}_h \\ \boldsymbol{\tau}_h \end{pmatrix} \in \mathbf{W}_{h0}^{*,\text{nc}}\Lambda^{k+1} \times \mathbf{W}_h\Lambda^{k-1}.$$

Therefore, $(\mathbf{P}_h^k \boldsymbol{\omega}_h, \boldsymbol{\vartheta}_h, \boldsymbol{\sigma}_h, \boldsymbol{\zeta}_h)$ solves (5.3), and (5.7) follows. The proof is completed. \square

Remark 5.3. *It follows easily that*

$$\|\boldsymbol{\omega}_h - \bar{\boldsymbol{\omega}}_h\|_{L^2\Lambda^k} + \|\mathbf{d}_h^k \boldsymbol{\omega}_h - \bar{\boldsymbol{\zeta}}_h\|_{L^2\Lambda^{k+1}} + \|\boldsymbol{\delta}_{k,h}\boldsymbol{\omega}_h - \bar{\boldsymbol{\sigma}}_h\|_{L^2\Lambda^{k-1}} \leq Ch\|\mathbf{f}\|_{L^2\Lambda^k}.$$

By the same virtue, we can prove the lemmas below.

Lemma 5.4. *The system (5.4) is well-posed. Further, let $(\bar{\omega}_h, \bar{\zeta}_h, \bar{\sigma}_h, \bar{\vartheta}_h)$ and $(\tilde{\omega}_h, \tilde{\zeta}_h, \tilde{\sigma}_h, \tilde{\vartheta}_h)$ be the solutions of (5.3) and (5.4), respectively. Then $\bar{\vartheta}_h = \tilde{\vartheta}_h$, and*

$$(5.9) \quad \|\bar{\omega}_h - \tilde{\omega}_h\|_{L^2\Lambda^k} + \|\bar{\zeta}_h - \tilde{\zeta}_h\|_{\delta_{k+1,h}} + \|\bar{\sigma}_h - \tilde{\sigma}_h\|_{\mathbf{d}^{k-1}} \leq Ch\|f\|_{L^2\Lambda^k}.$$

Lemma 5.5. *The system (5.5) is well-posed. Further, let $(\tilde{\omega}_h, \tilde{\zeta}_h, \tilde{\sigma}_h, \tilde{\vartheta}_h)$ and $(\hat{\vartheta}_h, \hat{\sigma}_h, \hat{\omega}_h)$ be the solutions of (5.4) and (5.5), respectively. Then*

$$\hat{\vartheta}_h = \tilde{\vartheta}_h, \quad \tilde{\omega}_h = \mathbf{P}_h^k \hat{\omega}_h, \quad \tilde{\sigma}_h = \hat{\sigma}_h, \quad \text{and} \quad \mathbf{d}^k \hat{\omega}_h = \mathbf{P}_h^{k+1} \tilde{\zeta}_h.$$

Lemma 5.6. *The system (5.6) is well-posed. Let $(\hat{\vartheta}_h, \hat{\sigma}_h, \hat{\omega}_h)$ and $(\check{\vartheta}_h, \check{\sigma}_h, \check{\omega}_h)$ be the solutions of (5.5) and (5.6), respectively. Then $\hat{\vartheta}_h = \check{\vartheta}_h$, and*

$$(5.10) \quad \|\hat{\sigma}_h - \check{\sigma}_h\|_{\mathbf{d}^{k-1}} + \|\hat{\omega}_h - \check{\omega}_h\|_{\mathbf{d}^{k+1}} \leq Ch\|f\|_{L^2\Lambda^k}.$$

Proposition 5.7. *Let $f \in L^2\Lambda^k(\Omega)$. Let (ω_h, ϑ_h) be the solution of (5.2). Let $(\check{\vartheta}_h, \check{\sigma}_h, \check{\omega}_h)$ be the solution of (5.6). Then there exists a constant $C > 0$, independent of h , such that*

$$(5.11) \quad \|\omega_h - \check{\omega}_h\|_{L^2\Lambda^k} + \left\| \mathbf{T}_{k,h} \omega_h - \begin{pmatrix} \mathbf{d}_h^k \check{\omega}_h \\ \check{\sigma}_h \end{pmatrix} \right\|_{L^2\Lambda^{k+1} \times L^2\Lambda^{k-1}} \leq Ch\|f\|_{L^2\Lambda^k}.$$

Proof. Let $(\bar{\omega}_h, \bar{\zeta}_h, \bar{\sigma}_h, \bar{\vartheta}_h)$, $(\tilde{\omega}_h, \tilde{\zeta}_h, \tilde{\sigma}_h, \tilde{\vartheta}_h)$ and $(\hat{\vartheta}_h, \hat{\sigma}_h, \hat{\omega}_h)$ be the solutions of (5.3), (5.4) and (5.5), respectively. By Remark 5.3 and Lemma 5.4, $\bar{\vartheta}_h = \tilde{\vartheta}_h$ and

$$\|\bar{\omega}_h - \tilde{\omega}_h\|_{L^2\Lambda^k} + \|\bar{\zeta}_h - \tilde{\zeta}_h\|_{\delta_{k+1,h}} + \|\bar{\sigma}_h - \tilde{\sigma}_h\|_{\mathbf{d}^{k-1}} \leq Ch\|f\|_{L^2\Lambda^k}.$$

By Lemma 5.5, $\hat{\vartheta}_h = \tilde{\vartheta}_h$, $\tilde{\omega}_h = \mathbf{P}_h^k \hat{\omega}_h$, $\tilde{\sigma}_h = \hat{\sigma}_h$, and $\mathbf{d}_h^k \hat{\omega}_h = \mathbf{P}_h^{k+1} \tilde{\zeta}_h$. By Lemma 5.6, $\hat{\vartheta}_h = \check{\vartheta}_h$ and

$$\|\hat{\sigma}_h - \check{\sigma}_h\|_{\mathbf{d}^{k-1}} + \|\hat{\omega}_h - \check{\omega}_h\|_{\mathbf{d}^k} \leq Ch\|f\|_{L^2\Lambda^k}.$$

The estimate (5.11) follows by summing these bounds and applying the triangle inequality. \square

Remark 5.8. *Let ω_h solve (3.14). Since (3.14) and (5.2) are equivalent, the same bound (5.11) holds if ω_h there is replaced by the solution of (3.14).*

5.2. Proof of Theorem 3.9. Corresponding to (5.6), an equivalent mixed formulation of the Hodge-Laplace problem reads: find $(\check{\vartheta}, \check{\sigma}, \check{\omega}) \in \mathfrak{H}\Lambda^k \times H\Lambda^{k-1} \times H\Lambda^k$ such that

$$(5.12) \quad \begin{cases} \langle \check{\omega}, \boldsymbol{\zeta} \rangle_{L^2\Lambda^k} & = 0 & \forall \boldsymbol{\zeta} \in \mathfrak{H}\Lambda^k \\ \langle \check{\sigma}, \boldsymbol{\tau} \rangle_{L^2\Lambda^{k-1}} - \langle \check{\omega}, \mathbf{d}^{k-1} \boldsymbol{\tau} \rangle_{L^2\Lambda^k} & = 0 & \forall \boldsymbol{\tau} \in H\Lambda^{k-1} \\ \langle \check{\vartheta}, \boldsymbol{\mu} \rangle_{L^2\Lambda^k} + \langle \mathbf{d}^{k-1} \check{\sigma}, \boldsymbol{\mu}_h \rangle_{L^2\Lambda^k} + \langle \mathbf{d}^k \check{\omega}, \mathbf{d}^k \boldsymbol{\mu} \rangle_{L^2\Lambda^{k+1}} & = \langle f, \boldsymbol{\mu} \rangle_{L^2\Lambda^k} & \forall \boldsymbol{\mu} \in H\Lambda^k, \end{cases}$$

Note that (5.12) is the classical mixed formulation of the Hodge-Laplace problem and (5.6) is the corresponding discretization of (5.12).

Lemma 5.9. [4, (7.17), (7.30) and Theorem 7.10] Let $(\check{\boldsymbol{\vartheta}}, \check{\boldsymbol{\sigma}}, \check{\boldsymbol{\omega}})$ and $(\check{\boldsymbol{\vartheta}}_h, \check{\boldsymbol{\sigma}}_h, \check{\boldsymbol{\omega}}_h)$ be the solutions of (5.12) and (5.6), respectively. Then,

$$\begin{aligned} & \|\check{\boldsymbol{\sigma}} - \check{\boldsymbol{\sigma}}_h\|_{\mathbf{d}^{k-1}} + \|\check{\boldsymbol{\omega}} - \check{\boldsymbol{\omega}}_h\|_{\mathbf{d}^k} + \|\check{\boldsymbol{\vartheta}} - \check{\boldsymbol{\vartheta}}_h\|_{L^2\Lambda^k} \\ & \leq C \left(\inf_{\boldsymbol{\tau}_h \in \mathbf{W}_h\Lambda^{k-1}} \|\check{\boldsymbol{\sigma}} - \boldsymbol{\tau}_h\|_{\mathbf{d}^{k-1}} + \inf_{\boldsymbol{\mu}_h \in \mathbf{W}_h\Lambda^k} \|\check{\boldsymbol{\omega}} - \boldsymbol{\mu}_h\|_{\mathbf{d}^k} + \inf_{\boldsymbol{s}_h \in \mathfrak{H}_h\Lambda^k} \|\check{\boldsymbol{\vartheta}} - \boldsymbol{s}_h\|_{L^2\Lambda^k} + h\|\mathbf{f}\|_{L^2\Lambda^k} \right); \end{aligned}$$

and further, with Ω being s -regular,

$$\|\check{\boldsymbol{\sigma}} - \check{\boldsymbol{\sigma}}_h\|_{L^2\Lambda^k} + \|\check{\boldsymbol{\omega}} - \check{\boldsymbol{\omega}}_h\|_{\mathbf{d}^k} + \|\check{\boldsymbol{\vartheta}} - \check{\boldsymbol{\vartheta}}_h\|_{L^2\Lambda^k} \leq Ch^s\|\mathbf{f}\|_{L^2\Lambda^k}.$$

Proof of Theorem 3.9. Let $\boldsymbol{\omega}$ and $\boldsymbol{\omega}_h$ be the solutions of (1.1) and (3.14), respectively. Let $(\check{\boldsymbol{\vartheta}}, \check{\boldsymbol{\sigma}}, \check{\boldsymbol{\omega}})$ and $(\check{\boldsymbol{\vartheta}}_h, \check{\boldsymbol{\sigma}}_h, \check{\boldsymbol{\omega}}_h)$ be the solutions of (5.12) and (5.6), respectively. Then $\boldsymbol{\omega} = \check{\boldsymbol{\omega}}$. By Remark 5.8 and Proposition 5.7,

$$(5.13) \quad \|\boldsymbol{\omega}_h - \check{\boldsymbol{\omega}}_h\|_{L^2\Lambda^k} + \left\| \mathbf{T}_{k,h}\boldsymbol{\omega}_h - \begin{pmatrix} \mathbf{d}_h^k \check{\boldsymbol{\omega}}_h \\ \check{\boldsymbol{\sigma}}_h \end{pmatrix} \right\|_{L^2\Lambda^{k+1} \times L^2\Lambda^{k-1}} \leq Ch\|\mathbf{f}\|_{L^2\Lambda^k}.$$

Therefore,

$$\|\boldsymbol{\omega} - \boldsymbol{\omega}_h\|_{L^2\Lambda^k} \leq \|\boldsymbol{\omega} - \check{\boldsymbol{\omega}}_h\|_{L^2\Lambda^k} + \|\check{\boldsymbol{\omega}}_h - \boldsymbol{\omega}_h\|_{L^2\Lambda^k} \leq \|\boldsymbol{\omega} - \check{\boldsymbol{\omega}}_h\|_{L^2\Lambda^k} + Ch\|\mathbf{f}\|_{L^2\Lambda^k}.$$

Moreover,

$$\begin{aligned} & \|\mathbf{d}^k\boldsymbol{\omega} - \mathbf{d}_h^k\boldsymbol{\omega}_h\|_{L^2\Lambda^{k+1}} + \|\boldsymbol{\delta}_k\boldsymbol{\omega} - \boldsymbol{\delta}_{k,h}\boldsymbol{\omega}_h\|_{L^2\Lambda^{k-1}} \leq \|\mathbf{d}^k\check{\boldsymbol{\omega}} - \mathbf{d}_h^k\check{\boldsymbol{\omega}}_h\|_{L^2\Lambda^{k+1}} + \|\check{\boldsymbol{\sigma}} - \check{\boldsymbol{\sigma}}_h\|_{L^2\Lambda^{k-1}} \\ & + \|\mathbf{d}_h^k\check{\boldsymbol{\omega}}_h - \mathbf{d}_h^k\hat{\boldsymbol{\omega}}_h\|_{L^2\Lambda^{k+1}} + \|\check{\boldsymbol{\sigma}}_h - \hat{\boldsymbol{\sigma}}_h\|_{L^2\Lambda^{k-1}} + \|\mathbf{d}_h^k\hat{\boldsymbol{\omega}}_h - \tilde{\boldsymbol{\zeta}}_h\|_{L^2\Lambda^{k+1}} + \|\hat{\boldsymbol{\sigma}}_h - \tilde{\boldsymbol{\sigma}}_h\|_{L^2\Lambda^{k-1}} \\ & + \|\tilde{\boldsymbol{\zeta}}_h - \bar{\boldsymbol{\zeta}}_h\|_{L^2\Lambda^{k+1}} + \|\tilde{\boldsymbol{\sigma}}_h - \bar{\boldsymbol{\sigma}}_h\|_{L^2\Lambda^{k-1}} + \|\bar{\boldsymbol{\zeta}}_h - \mathbf{d}_h^k\boldsymbol{\omega}_h\|_{L^2\Lambda^{k+1}} + \|\bar{\boldsymbol{\sigma}}_h - \boldsymbol{\delta}_{k,h}\boldsymbol{\omega}_h\|_{L^2\Lambda^{k-1}} \\ & \leq \|\mathbf{d}^k\check{\boldsymbol{\omega}} - \mathbf{d}_h^k\check{\boldsymbol{\omega}}_h\|_{L^2\Lambda^{k+1}} + \|\check{\boldsymbol{\sigma}} - \check{\boldsymbol{\sigma}}_h\|_{L^2\Lambda^{k-1}} + Ch\|\mathbf{f}\|_{L^2\Lambda^k}, \end{aligned}$$

where the last inequality follows from Remark 5.3, Lemmas 5.4, 5.5, and 5.6, and the identity $\boldsymbol{\omega} = \check{\boldsymbol{\omega}}$ together with the link between (1.1) and (5.12). The proof is completed by Lemma 5.9. \square

Remark 5.10. *The continuous primal and mixed Hodge–Laplace formulations are equivalent; therefore, an estimation of (5.13)-type, not necessarily identical, can be a necessary condition so that $\boldsymbol{\omega}_h$ converges to $\boldsymbol{\omega}$. This is why this indirect analysis routine is utilized here.*

6. NUMERICAL EXPERIMENTS

6.1. Overview. In this section, we use the two- and three- dimensional $H(\text{div}) \cap H(\text{curl})$ problem to test the spaces $\mathbf{V}_h^{\mathbf{d} \cap \check{\boldsymbol{\delta}}} \Lambda^k$, the specific formulations of which are given in Subsection 3.2.1. To particularly illustrate the performance with respect to the complicated topology of the domain, we focus ourselves on eigenvalue problems and compare with standard mixed FEEC discretizations.

Particularly, Subsection 6.2 treats $n = 2$ and Subsections 6.3 treats $n = 3$ (both including domains with nontrivial topology).

To keep a reasonable length of the paper, we report the manufactured-solution boundary-value tests in Appendix F, and counterexamples using vector Lagrange and vector Crouzeix–Raviart elements are given in Appendices A and B.

6.2. Two-dimensional tests. For $\Omega \subset \mathbb{R}^2$ a polygon, we consider the following eigenvalue problem: find $(\lambda, \omega \neq 0) \in \mathbb{R} \times H(\text{rot}, \Omega) \cap H_0(\text{div}, \Omega)$ such that

$$(6.1) \quad (\text{div}\omega, \text{div}\tau) + (\text{rot}\omega, \text{rot}\tau) = \lambda(\omega, \tau), \quad \forall \tau \in H(\text{rot}, \Omega) \cap H_0(\text{div}, \Omega).$$

The finite element space \mathbf{V}_h^{rd} is defined in (3.12) (Subsection 3.2.1); the cell-wise and locally supported global basis functions can be found in Appendix D. The primal discretization of (6.1) is to find $(\lambda_h, \omega_h \neq 0) \in \mathbb{R} \times \mathbf{V}_h^{\text{rd}}$, such that

$$(6.2) \quad (\text{div}_h \omega_h, \text{div}_h \tau_h) + (\text{rot}_h \omega_h, \text{rot}_h \tau_h) = \lambda_h(\omega_h, \tau_h), \quad \forall \tau_h \in \mathbf{V}_h^{\text{rd}}.$$

To verify the computation results, we use the standard mixed formulation for reference: find $(\lambda, \sigma, u \neq 0) \in \mathbb{R} \times H^1(\Omega) \times H(\text{rot}, \Omega)$ such that

$$(6.3) \quad \begin{cases} (\sigma, \tau) - (u, \text{grad}\tau) = 0 & \forall \tau \in H^1(\Omega) \\ (\text{grad}\sigma, v) + (\text{rot}u, \text{rot}v) = \lambda(u, v) & \forall v \in H(\text{rot}, \Omega). \end{cases}$$

Its classical discretization is to find

$$(\lambda_h, \sigma_h, u_h \neq 0) \in \mathbb{R} \times \mathbb{V}_h^1 \times \mathbb{V}_h^{\text{Ned}},$$

such that

$$(6.4) \quad \begin{cases} (\sigma_h, \tau_h) - (u_h, \text{grad}\tau_h) = 0, & \forall \tau_h \in \mathbb{V}_h^1, \\ (\text{grad}\sigma_h, v_h) + (\text{rot}u_h, \text{rot}v_h) = \lambda_h(u_h, v_h), & \forall v_h \in \mathbb{V}_h^{\text{Ned}}, \end{cases}$$

where $\mathbb{V}_h^{\text{Ned}}$ is the lowest-degree Nedelec element space for $H(\text{rot}, \Omega)$.

We compute the ten smallest eigenvalues using the primal formulation (6.2) with the \mathbf{V}_h^{rd} element and the mixed formulation (6.4) with the classical mixed element on three domains, namely

- Square domain: $\Omega_S = [0, 1]^2$.
- L-shaped domain: $\Omega_L = [0, 1]^2 \setminus ((0.5, 1) \times (0, 0.5))$; see Figure 1.
- Square domain with an interior hole: $\Omega_H = [0, 1]^2 \setminus [0.5, 0.75]^2$; see Figure 2.

Tables 1–6 record the computed eigenvalues, where L denotes the mesh level. The eigenvalues computed by (6.2) agree closely with those computed by (6.4). In particular, on the third domain Ω_H , the first Betti number \mathbf{b}_1 is 1, and 0 appears as a simple eigenvalue for both (6.2) and (6.4).

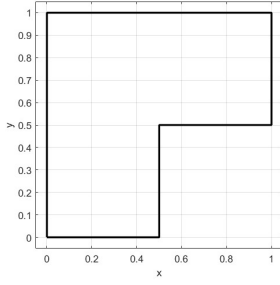


FIGURE 1. Computational domain for the L-shaped example.

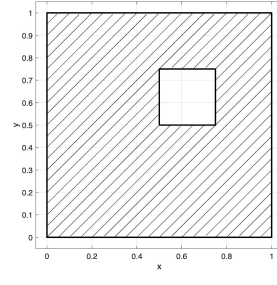


FIGURE 2. Computational domain for the square example with an interior hole.

L	λ_h^1	λ_h^2	λ_h^3	λ_h^4	λ_h^5	λ_h^6	λ_h^7	λ_h^8	λ_h^9	λ_h^{10}
1	10.188	10.188	18.982	20.516	44.578	44.578	45.776	45.776	55.394	55.394
2	9.949	9.949	19.549	19.930	40.753	40.753	48.447	48.447	50.837	50.837
3	9.889	9.889	19.692	19.787	39.796	39.796	49.122	49.122	49.718	49.718
4	9.875	9.875	19.727	19.751	39.558	39.558	49.292	49.292	49.440	49.440

TABLE 1. Computed eigenvalues on $\Omega_S = [0, 1]^2$, using (6.2).

L	λ_h^1	λ_h^2	λ_h^3	λ_h^4	λ_h^5	λ_h^6	λ_h^7	λ_h^8	λ_h^9	λ_h^{10}
1	10.211	10.211	19.398	20.608	45.012	45.012	48.291	48.291	56.070	56.070
2	9.954	9.954	19.655	19.952	40.843	40.843	49.100	49.100	50.977	50.977
3	9.891	9.891	19.718	19.792	39.817	39.817	49.287	49.287	49.751	49.751
4	9.875	9.875	19.734	19.752	39.563	39.563	49.333	49.333	49.449	49.449

TABLE 2. Computed eigenvalues on $\Omega_S = [0, 1]^2$, using (6.4).

L	λ_h^1	λ_h^2	λ_h^3	λ_h^4	λ_h^5	λ_h^6	λ_h^7	λ_h^8	λ_h^9	λ_h^{10}
1	6.412	14.621	34.269	44.578	44.578	51.021	55.628	58.114	67.036	91.817
2	6.076	14.264	37.143	40.753	40.753	46.927	52.346	59.443	75.928	82.064
3	5.966	14.169	38.075	39.796	39.796	45.900	50.863	60.444	78.197	79.722
4	5.926	14.144	38.387	39.558	39.558	45.643	50.458	60.701	78.767	79.147

TABLE 3. Computed eigenvalues on Ω_L (Figure 1) using (6.2).

L	λ_h^1	λ_h^2	λ_h^3	λ_h^4	λ_h^5	λ_h^6	λ_h^7	λ_h^8	λ_h^9	λ_h^{10}
1	6.421	14.667	35.592	45.012	45.012	51.592	58.859	59.559	73.337	93.723
2	6.078	14.275	37.520	40.843	40.843	47.047	52.495	60.436	77.594	82.432
3	5.966	14.172	38.174	39.817	39.817	45.928	50.898	60.694	78.618	79.808
4	5.926	14.145	38.412	39.563	39.563	45.651	50.467	60.764	78.872	79.169

TABLE 4. Computed eigenvalues on Ω_L (Figure 1) using (6.4).

L	λ_h^1	λ_h^2	λ_h^3	λ_h^4	λ_h^5	λ_h^6	λ_h^7	λ_h^8	λ_h^9	λ_h^{10}
1	0.000	8.707	8.931	19.531	33.867	41.637	45.949	53.379	53.732	55.952
2	0.000	8.216	8.406	18.918	36.748	40.149	42.097	48.935	53.802	72.364
3	0.000	8.049	8.225	18.732	35.954	37.763	42.731	49.967	52.093	60.796
4	0.000	7.989	8.160	18.676	34.948	38.091	42.453	46.388	49.654	59.727

TABLE 5. Computed eigenvalues on Ω_H (Figure 2) using (6.2). The method can correctly capture the zero eigenvalue associated with the topology of the domain.

L	λ_h^1	λ_h^2	λ_h^3	λ_h^4	λ_h^5	λ_h^6	λ_h^7	λ_h^8	λ_h^9	λ_h^{10}
1	0.000	8.724	8.949	19.614	35.146	42.014	46.384	54.127	56.354	56.373
2	0.000	8.219	8.410	18.937	36.788	37.128	41.756	48.474	51.643	58.173
3	0.000	8.050	8.226	18.737	35.375	37.838	40.569	47.091	50.374	58.802
4	0.000	7.989	8.160	18.677	34.951	38.105	40.255	46.722	50.049	59.025

TABLE 6. Computed eigenvalues on Ω_H (Figure 2) using (6.4).

Overall, the proposed element gives eigenvalue approximations that are consistent with those obtained from the mixed formulation on all tested two-dimensional domains. In particular, the zero eigenvalue associated with the topology of the multiply connected domain is correctly captured by both methods. The present results therefore provide evidence that the proposed element is well suited to the primal eigenvalue formulation considered here. The agreement is observed not only on the simply connected square domain, but also on the nonconvex L-shaped domain and on the multiply connected domain with an interior hole. This is noteworthy in view of the known difficulty of designing nonconforming primal discretizations for curl–curl type problems. For example, Brenner-Sun-Cui [11] observed that a naive CR-type weakly continuous P_1 discretization of the two-dimensional curl–curl problem fails to converge unless additional consistency terms controlling the tangential and normal jumps are included.

6.3. Three-dimensional tests. Let $\Omega \subset \mathbb{R}^3$ be a polyhedral domain.

6.3.1. The case $H(\operatorname{div}, \Omega) \cap H_0(\operatorname{curl}, \Omega)$. In the first case, we consider eigenvalue problem associated with the space $H(\operatorname{div}, \Omega) \cap H_0(\operatorname{curl}, \Omega)$. The primal weak formulation is to find $(\lambda, \omega) \in \mathbb{R} \times H(\operatorname{div}, \Omega) \cap H_0(\operatorname{curl}, \Omega)$ such that

$$(6.5) \quad (\operatorname{div} \omega, \operatorname{div} \tau) + (\operatorname{curl} \omega, \operatorname{curl} \tau) = \lambda(\omega, \tau), \quad \forall \tau \in H(\operatorname{div}, \Omega) \cap H_0(\operatorname{curl}, \Omega).$$

For $H(\operatorname{div}, \Omega) \cap H_0(\operatorname{curl}, \Omega)$ the finite element space is $\mathbf{V}_h^{\operatorname{cd}}$ in (3.13) (see Appendix E for the cell-wise and locally supported global basis functions). The discrete primal weak formulation is to find

$$(\lambda_h, \omega_h) \in \mathbb{R} \times \mathbf{V}_h^{\operatorname{cd}}, \quad \omega_h \neq 0,$$

such that

$$(6.6) \quad (\operatorname{div}_h \omega_h, \operatorname{div}_h \tau_h) + (\operatorname{curl}_h \omega_h, \operatorname{curl}_h \tau_h) = \lambda_h(\omega_h, \tau_h), \quad \forall \tau_h \in \mathbb{V}_h^{\text{ed}}.$$

The corresponding mixed formulation is to find $(\lambda, \sigma, u) \in \mathbb{R} \times H(\operatorname{curl}, \Omega) \times H(\operatorname{div}, \Omega)$ such that

$$(6.7) \quad \begin{cases} (\sigma, \tau) - (u, \operatorname{curl} \tau) = 0 & \forall \tau \in H(\operatorname{curl}, \Omega) \\ (\operatorname{curl} \sigma, v) + (\operatorname{div} u, \operatorname{div} v) = \lambda(u, v) & \forall v \in H(\operatorname{div}, \Omega) \end{cases}$$

The discrete mixed formulation is to find

$$(\lambda_h, \sigma_h, u_h) \in \mathbb{R} \times \mathbb{V}_h^{\text{Ned}} \times \mathbb{V}_h^{\text{RT}}, \quad u_h \neq 0,$$

such that

$$(6.8) \quad \begin{cases} (\sigma_h, \tau_h) - (u_h, \operatorname{curl} \tau_h) = 0, & \forall \tau_h \in \mathbb{V}_h^{\text{Ned}}, \\ (\operatorname{curl} \sigma_h, v_h) + (\operatorname{div} u_h, \operatorname{div} v_h) = \lambda_h(u_h, v_h), & \forall v_h \in \mathbb{V}_h^{\text{RT}}. \end{cases}$$

We compute the eigenvalues on a representative non-simply connected domain $\Omega_1 = [0, 1]^3 \setminus ((0.25, 0.5) \times (0.25, 0.5) \times [0, 1])$ (see Figure 3) and compare them with those obtained from the mixed formulation on the same meshes. Unless otherwise stated, the smallest ten eigenvalues are reported; the results are presented in Tables 7–8.

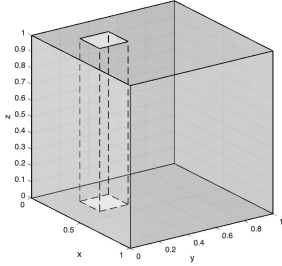


FIGURE 3. Computational domain Ω_1 : the cube with a rectangular through-hole.

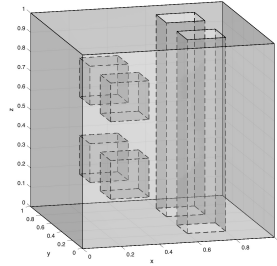


FIGURE 4. Computational domain Ω_2 : the cube with four enclosed rectangular cavities and two through-holes.

L	λ_h^1	λ_h^2	λ_h^3	λ_h^4	λ_h^5	λ_h^6	λ_h^7	λ_h^8	λ_h^9	λ_h^{10}
1	9.139	18.149	18.443	28.730	33.144	33.664	41.078	43.122	44.284	44.695
2	9.602	17.967	18.150	28.632	36.483	37.620	45.080	45.776	46.381	46.735
3	9.774	17.879	18.047	28.562	37.588	38.907	44.883	47.269	47.345	47.363
4	9.834	17.845	18.011	28.535	38.007	39.288	44.734	47.380	47.520	47.869

TABLE 7. Computed eigenvalues on Ω_1 shown in Figure 3, using the primal weak formulation (6.6).

L	λ_h^1	λ_h^2	λ_h^3	λ_h^4	λ_h^5	λ_h^6	λ_h^7	λ_h^8	λ_h^9	λ_h^{10}
1	9.200	18.419	18.613	29.282	33.983	34.524	44.736	45.095	45.181	45.894
2	9.618	18.032	18.193	28.765	36.726	37.864	45.417	46.772	46.945	46.990
3	9.778	17.895	18.058	28.595	37.652	38.969	44.965	47.390	47.411	47.552
4	9.835	17.849	18.014	28.543	38.024	39.304	44.754	47.410	47.537	47.895

TABLE 8. Computed eigenvalues on Ω_1 shown in Figure 3, using the mixed formulation (6.8).

Convergence of the discrepancies between the two formulations. To further quantify the agreement between the proposed element and the mixed formulation, we compare the corresponding numerical eigenvalues and eigenvectors on Ω_1 .

For the eigenvalue comparison, we consider the first ten computed eigenvalues and compute

$$|\lambda_i^{\text{mix}} - \lambda_i^{\text{new}}|, \quad i = 1, \dots, 10$$

where λ_i^{mix} and λ_i^{new} denote the corresponding eigenvalues computed by the mixed formulation and the proposed element, respectively. The corresponding log–log plots are shown in Figures 5a.

For the eigenvector comparison, we consider the eigenvectors associated with the first ten computed eigenvalues on Ω_1 . The errors are measured in the L^2 norm and in the combined $H(\text{div})$ – $H(\text{curl})$ norm,

$$\|u_i^{\text{mix}} - u_i^{\text{new}}\|_{L^2}, \quad |u_i^{\text{mix}} - u_i^{\text{new}}|_{H(\text{div})+H(\text{curl})}, \quad i = 1, \dots, 10.$$

The results are displayed in Figures 5b, 5c.

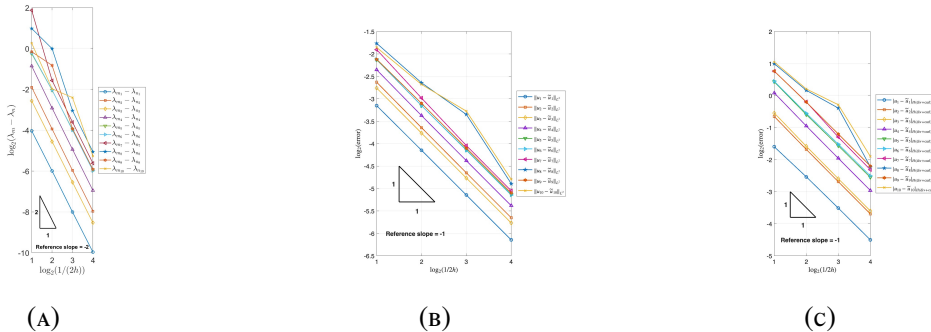


FIGURE 5. (a) Log–log plots of the differences between the first ten eigenvalues computed by the mixed formulation and the proposed element on Ω_1 ; (b) Errors between the first ten matched eigenvectors computed by the mixed formulation and the proposed element in the L^2 norm on Ω_1 ; (c) Errors between the first ten matched eigenvectors computed by the mixed formulation and the proposed element in the combined $H(\text{div})$ – $H(\text{curl})$ norm on Ω_1 .

The log–log plots show that the discrepancies between the two formulations decrease as the mesh is refined. This provides an additional consistency check: not only do the two methods produce close eigenvalue tables on each fixed mesh, but their eigenvalue and eigenvector approximations also become increasingly consistent under mesh refinement.

6.3.2. *Influence of topology associated with the boundary condition.* For comparison, we also consider the space $H(\text{curl}, \Omega) \cap H_0(\text{div}, \Omega)$. It corresponds to $H\Lambda^1 \cap H_0^*\Lambda^1$, and leads to Hodge-Laplace problems on Λ^1 . The first Betti number b_1 influence its computation.

We consider the eigenvalue problem: find $(\lambda, \omega) \in \mathbb{R} \times H(\text{curl}, \Omega) \cap H_0(\text{div}, \Omega)$ such that

$$(6.9) \quad (\text{div}\omega, \text{div}\mu) + (\text{curl}\omega, \text{curl}\mu) = \lambda(\omega, \mu), \quad \forall \mu \in H(\text{curl}, \Omega) \cap H_0(\text{div}, \Omega)$$

To compare and illustrate the influence of the boundary condition, we just make slight modification on \mathbf{V}_h^{cd} , rather than define directly the space $\mathbf{V}_h^{\text{d}\cap\delta^*}\Lambda^1$. Denote by $\mathbb{V}_{h0}^{\text{Ned}}$ the Nedelec element space on \mathcal{T}_h with homogeneous boundary condition and by V_h^{CR} the Crouzeix-Raviart element space on \mathcal{T}_h . The finite element space reads:

$$(6.10) \quad \mathbf{V}_h^{\text{cd}} := \left\{ \mu_h \in P_{\text{rd}}(\mathcal{G}_h) : (\text{div}_h \mu_h, \tau_h) = -(\mu_h, \nabla_h \tau_h), \quad \forall \tau_h \in \mathbb{V}_h^{\text{CR}}, \right. \\ \left. \text{and } (\text{rot}_h \mu_h, \eta_h) = \langle \mu_h, \text{curl} \eta_h \rangle, \quad \forall \eta_h \in V_{h0}^{\text{Ned}} \right\}.$$

We remark here that the homogeneous boundary condition for the adjoint partner is transferred from the Crouzeix-Raviart element space side to the Nedelec element space side compared to \mathbf{V}_h^{cd} .

The discrete primal weak formulation is to find

$$(\lambda_h, \omega_h) \in \mathbb{R} \times \mathbf{V}_h^{\text{cd}}, \quad \omega_h \neq 0,$$

such that

$$(6.11) \quad (\text{div}_h \omega_h, \text{div}_h \mu_h) + (\text{curl}_h \omega_h, \text{curl}_h \mu_h) = \lambda_h(\omega_h, \mu_h), \quad \forall \mu_h \in \mathbf{V}_h^{\text{cd}}.$$

The corresponding mixed formulation is to find $(\lambda, \sigma, u) \in \mathbb{R} \times H^1(\Omega) \times H(\text{curl}, \Omega)$ such that

$$(6.12) \quad \begin{cases} (\sigma, \tau) - (u, \text{grad}\tau) = 0 & \forall \tau \in H^1(\Omega) \\ (\text{grad}\sigma, v) + (\text{curl}u, \text{curl}v) = \lambda(u, v) & \forall v \in H(\text{curl}, \Omega) \end{cases}$$

The discrete mixed formulation is to find

$$(\lambda_h, \sigma_h, u_h) \in \mathbb{R} \times \mathbb{V}_h^1 \times \mathbb{V}_h^{\text{Ned}}, \quad u_h \neq 0,$$

such that

$$(6.13) \quad \begin{cases} (\sigma_h, \tau_h) - (u_h, \text{grad}\tau_h) = 0, & \forall \tau_h \in \mathbb{V}_h^1, \\ (\text{grad}\sigma_h, v_h) + (\text{curl}u_h, \text{curl}v_h) = \lambda_h(u_h, v_h), & \forall v_h \in \mathbb{V}_h^{\text{Ned}}. \end{cases}$$

For this type of boundary condition, the number of zero eigenvalues is determined by the first Betti number b_1 of the domain.

To examine the influence of boundary conditions on the numerical results, we consider $\Omega_2 = [0, 1]^3 \setminus [(0.2, 0.4) \times Y \times Y \cup (0.6, 0.8) \times Y \times (0, 1)]$, $Y = (0.2, 0.4) \cup (0.6, 0.8)$. This domain combines cavity-type and handle-type topological features, and is illustrated in Figure 4. Its first Betti number $b_1 = 2$ and second Betti number $b_2 = 4$. Tables 9 and 10 report the computed eigenvalues under the boundary condition $H_0(\text{rot}, \Omega) \cap H(\text{div}, \Omega)$, while the results under the boundary condition $H_0(\text{div}, \Omega) \cap H(\text{rot}, \Omega)$ are presented in Tables 11–12.

L	λ_h^1	λ_h^2	λ_h^3	λ_h^4	λ_h^5	λ_h^6	λ_h^7	λ_h^8	λ_h^9	λ_h^{10}
1	0.000	0.000	0.000	0.000	9.124	9.140	17.248	17.381	26.886	27.005
2	0.000	0.000	0.000	0.000	9.407	9.513	16.579	16.698	26.023	26.193
3	0.000	0.000	0.000	0.000	9.492	9.674	16.242	16.359	25.367	25.813
4	0.000	0.000	0.000	0.000	9.515	9.734	16.094	16.213	25.036	25.651

TABLE 9. Computed eigenvalues on Ω_2 shown in Figure 4, using the primal weak formulation (6.6).

L	λ_h^1	λ_h^2	λ_h^3	λ_h^4	λ_h^5	λ_h^6	λ_h^7	λ_h^8	λ_h^9	λ_h^{10}
1	0.000	0.000	0.000	0.000	9.162	9.179	17.343	17.537	27.162	27.351
2	0.000	0.000	0.000	0.000	9.417	9.523	16.604	16.731	26.092	26.269
3	0.000	0.000	0.000	0.000	9.494	9.676	16.248	16.367	25.384	25.830
4	0.000	0.000	0.000	0.000	9.515	9.734	16.096	16.215	25.040	25.655

TABLE 10. Computed eigenvalues on Ω_2 shown in Figure 4, using the mixed formulation (6.8).

L	λ_h^1	λ_h^2	λ_h^3	λ_h^4	λ_h^5	λ_h^6	λ_h^7	λ_h^8	λ_h^9	λ_h^{10}
1	0.000	0.000	6.958	7.338	8.507	8.736	8.973	13.233	13.417	16.041
2	0.000	0.000	7.491	7.767	9.122	9.252	9.385	14.783	14.840	16.796
3	0.000	0.000	7.711	7.954	9.353	9.367	9.627	15.477	15.580	17.100
4	0.000	0.000	7.799	8.031	9.390	9.464	9.717	15.784	15.899	17.218

TABLE 11. Computed eigenvalues on Ω_2 shown in Figure 4, using the primal weak formulation (6.11).

As in the cases of Ω_1 , we further compare the numerical eigenvalues and eigenvectors produced by the primal weak formulation (6.6) and the mixed formulation (6.8). The positive eigenvalues among the first ten computed eigenvalues, together with the associated eigenvectors, are considered in the comparison. The corresponding results are presented in Figure 6.

L	λ_h^1	λ_h^2	λ_h^3	λ_h^4	λ_h^5	λ_h^6	λ_h^7	λ_h^8	λ_h^9	λ_h^{10}
1	0.000	0.000	8.825	8.974	9.162	9.179	9.889	17.343	17.537	19.520
2	0.000	0.000	8.302	8.489	9.417	9.523	9.605	16.604	16.731	18.126
3	0.000	0.000	8.042	8.250	9.488	9.494	9.676	16.248	16.367	17.597
4	0.000	0.000	7.930	8.148	9.441	9.515	9.734	16.096	16.215	17.404

TABLE 12. Computed eigenvalues on Ω_2 shown in Figure 4, using the mixed formulation (6.13).

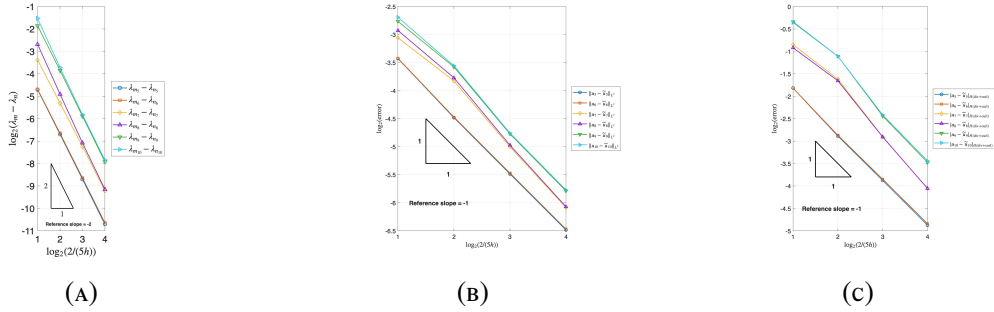


FIGURE 6. (a) Log–log plots of the differences between the first six positive eigenvalues computed by the mixed formulation and the proposed element on Ω_2 ; (b) Errors between the corresponding six matched eigenvectors computed by the mixed formulation and the proposed element in the L^2 norm on Ω_2 ; (c) Errors between the corresponding six matched eigenvectors computed by the mixed formulation and the proposed element in the combined $H(\text{div})$ – $H(\text{curl})$ norm on Ω_2 .

Summary. For all tested three-dimensional domains, the eigenvalues computed by the proposed element agree well with those obtained from the mixed formulation. The agreement remains valid for domains with nontrivial topology. In particular, for the domain with multiple cavities and through-holes, the proposed element correctly captures the expected zero eigenvalues associated with the corresponding Betti number. It is also worth noting that, whenever zero eigenvalues occur, either simple or multiple, we further compared the corresponding zero eigenspaces computed by the proposed element and by the mixed element. The comparison shows that the two discretizations give exactly the same eigenspace associated with the eigenvalue 0, up to roundoff error. This demonstrates that the proposed element preserves the relevant topological structure of the continuous problem.

7. CONCLUDING REMARKS

In this paper, we constructed a unified nonconforming primal finite element framework for the Hodge-Laplace problem on $H\Lambda^k \cap H_0^*\Lambda^k$, for any $n \geq 2$ and $1 \leq k \leq n - 1$ on simplicial meshes. The construction is based on adjoint continuity: instead of imposing trace continuity directly, the space is defined by discrete adjoint identities against Whitney-type test spaces. This construction

preserves the key FEEC structures needed for topology-sensitive problems. In particular, discrete harmonic forms are recovered as the joint kernel of the discrete exterior derivative and codifferential, the discrete Poincaré inequality holds uniformly in h , and the resulting primal scheme is well posed. By linking the primal scheme to a classical mixed FEEC discretization, we obtain the error estimate in Theorem 3.9, including the $O(h^s)$ rate on s -regular domains. The numerical eigenvalue tests in Section 6 (including domains with nontrivial topology) are consistent with the theoretical structure and with mixed-method reference results.

A systematic higher-order extension that preserves the same adjoint continuity and topological robustness will still be of interest, particularly for smoother solutions and hp/adaptive settings. For the topology-sensitive domains emphasized here, however, the error rate is fundamentally constrained by solution regularity: on s -regular domains, the dominant behavior is $O(h^s)$ regardless of polynomial enrichment beyond degree one. In this sense, the present low-degree construction is already aligned with the regularity-limited regime addressed in Theorem 3.9 as well as Theorem 7.10 of [4]. At the same time, the space remains non-Ciarlet type in nature, so basis construction and implementation rely on the adjoint-constraint framework rather than standard nodal continuity machinery. On the computational side, robust preconditioners and conditioning estimates adapted to the discrete Hodge decomposition are needed for large-scale solvers. It is also natural to investigate whether the same adjoint-construction strategy can be transferred to other coupled systems, such as Stokes, Maxwell, and linear elasticity.

REFERENCES

- [1] Douglas N Arnold. *Finite element exterior calculus*. SIAM, 2018.
- [2] Douglas N Arnold and Franco Brezzi. Mixed and nonconforming finite element methods: implementation, post-processing and error estimates. *RAIRO-Modélisation Mathématique et Analyse Numérique*, 19(1):7–32, 1985.
- [3] Douglas Arnold, Richard Falk, and Ragnar Winther. Finite element exterior calculus: from Hodge theory to numerical stability. *Bulletin of the American Mathematical Society*, 47(2):281–354, 2010.
- [4] Douglas N Arnold, Richard S Falk, and Ragnar Winther. Finite element exterior calculus, homological techniques, and applications. *Acta Numerica*, 15:1–155, 2006.
- [5] Mary Barker. *A Nonconforming Finite Element Method for the 2D Vector Laplacian*. PhD thesis, Washington University in St. Louis, 2022.
- [6] Mary Barker, Shuhao Cao, and Ari Stern. A nonconforming primal hybrid finite element method for the two-dimensional vector Laplacian. *The SMAI Journal of Computational Mathematics*, 10:85–106, 2024.
- [7] KJ Bathe, C Nitikitpaiboon, and X Wang. A mixed displacement-based finite element formulation for acoustic fluid-structure interaction. *Computers & Structures*, 56(2-3):225–237, 1995.
- [8] Alfredo Bermúdez and Rodolfo Rodríguez. Finite element computation of the vibration modes of a fluid-solid system. *Computer Methods in Applied Mechanics and Engineering*, 119(3-4):355–370, 1994.
- [9] Susanne C Brenner, Jintao Cui, Fengyan Li, and L-Y Sung. A nonconforming finite element method for a two-dimensional curl-curl and grad-div problem. *Numerische Mathematik*, 109(4):509–533, 2008.

- [10] Susanne C Brenner and Li-Yeng Sung. A quadratic nonconforming vector finite element for $H(\text{curl}; \omega) \cap H(\text{div}; \omega)$. *Applied Mathematics Letters*, 22:892–896, 2009.
- [11] Susanne C Brenner, Li-yeng Sung, and Jintao Cui. An interior penalty method for a two dimensional curl-curl and grad-div problem. *ANZIAM Journal*, 50:C947–C975, 2008.
- [12] Philippe G Ciarlet. *The finite element method for elliptic problems*. North-Holland, Amsterdam, 1978.
- [13] Michel Crouzeix and P-A Raviart. Conforming and nonconforming finite element methods for solving the stationary Stokes equations I. *Revue française d'automatique informatique recherche opérationnelle. Mathématique*, 7(R3):33–75, 1973.
- [14] Lourenço Beirão da Veiga, Franco Brezzi, L Donatella Marini, and Alessandro Russo. Virtual element approximations of the vector potential formulation of magnetostatic problems. *The SMAI Journal of computational mathematics*, 4:399–416, 2018.
- [15] Mohamed Ali Hamdi, Yves Ousset, and Georges Verchery. A displacement method for the analysis of vibrations of coupled fluid-structure systems. *International Journal for Numerical Methods in Engineering*, 13(1):139–150, 1978.
- [16] Ralf Hiptmair. Finite elements in computational electromagnetism. *Acta Numerica*, 11:237–339, 2002.
- [17] Jeonghun Lee and Ragnar Winther. Local coderivatives and approximation of Hodge Laplace problems. *Mathematics of Computation*, 87(314):2709–2735, 2018.
- [18] Jean-Marie Mirebeau. Nonconforming vector finite elements for $H(\text{curl}; \omega) \cap H(\text{div}; \omega)$. *Applied Mathematics Letters*, 25(3):369–373, 2012.
- [19] Peter Monk. *Finite element methods for Maxwell's equations*. Oxford University Press, 2003.
- [20] Pierre-Arnaud Raviart and Jean-Marie Thomas. A mixed finite element method for 2-nd order elliptic problems. In *Mathematical Aspects of Finite Element Methods*, pages 292–315. Springer, 1977.
- [21] Shuo Zhang. A nonconforming framework for finite element exterior calculus. *IMA Journal of Numerical Analysis*, online, 2026.

GUIDE TO THE APPENDICES

Appendices A and B document eigenvalue counterexamples with vector Lagrange and vector Crouzeix–Raviart elements; they supplement the proposed-element and mixed results in Section 6. Appendix C illustrates the adjoint partner spaces $\mathbf{W}_h^{r*,nc} \Lambda^k$ used in (3.10); Appendices D and E give explicit basis constructions for the proposed trial space $\mathbf{V}_h^{d \cap \delta} \Lambda^1$ and $\mathbf{V}_h^{d \cap \delta} \Lambda^2$ in two and three dimensions, respectively. Appendix F reports manufactured-solution boundary-value tests on $[0, 1]^2$ and $[0, 1]^3$, including log–log plots of mesh-refinement errors.

APPENDIX A. EIGENVALUE RESULTS OBTAINED BY THE VECTOR LAGRANGE ELEMENT

This appendix collects supplementary eigenvalue results for the linear vector Lagrange element, to be compared with the proposed-element and mixed results in Section 6.

A.1. Two-dimensional vector Lagrange discretization and results. In two dimensions, the vector Lagrange space is used as a replacement for the proposed space V_h^{rd} in (6.2), which discretizes the primal formulation (6.1).

Let

$$S_{h,2D}^{\text{Lag}} = \{v_h \in H^1(\Omega) : v_h|_T \in \mathbb{P}_1(T), \forall T \in \mathcal{G}_h\}.$$

For the two-dimensional primal formulation (6.1), we define

$$V_{h,2D}^{\text{Lag}} = [S_{h,2D}^{\text{Lag}}]^2 \cap (H(\text{rot}, \Omega) \cap H_0(\text{div}, \Omega)).$$

The corresponding vector Lagrange discretization is to find

$$(\lambda_h, \omega_h) \in \mathbb{R} \times V_{h,2D}^{\text{Lag}}, \quad \omega_h \neq 0,$$

such that

$$(A.1) \quad (\text{div} \omega_h, \text{div} \tau_h) + (\text{rot} \omega_h, \text{rot} \tau_h) = \lambda_h(\omega_h, \tau_h), \quad \forall \tau_h \in V_{h,2D}^{\text{Lag}}.$$

The corresponding two-dimensional eigenvalue results are reported below.

L	λ_h^1	λ_h^2	λ_h^3	λ_h^4	λ_h^5	λ_h^6	λ_h^7	λ_h^8	λ_h^9	λ_h^{10}
1	10.211	10.211	20.608	20.608	45.012	45.012	56.070	56.070	56.070	56.070
2	9.954	9.954	19.952	19.952	40.843	40.843	50.977	50.977	50.977	50.977
3	9.891	9.891	19.792	19.792	39.817	39.817	49.751	49.751	49.751	49.751
4	9.875	9.875	19.752	19.752	39.563	39.563	49.449	49.449	49.449	49.449

TABLE 13. Computed eigenvalues on $\Omega = [0, 1]^2$ using the vector Lagrange discretization (A.1), corresponding to the two-dimensional primal formulation (6.1).

L	λ_h^1	λ_h^2	λ_h^3	λ_h^4	λ_h^5	λ_h^6	λ_h^7	λ_h^8	λ_h^9	λ_h^{10}
1	17.418	17.418	45.012	45.012	52.760	52.760	80.195	80.195	93.723	93.723
2	15.731	15.731	40.843	40.843	47.644	47.644	67.110	67.110	82.432	82.432
3	15.026	15.026	39.817	39.817	46.282	46.282	63.522	63.522	79.808	79.808
4	14.664	14.664	39.563	39.563	45.870	45.870	62.209	62.209	79.169	79.169

TABLE 14. Computed eigenvalues on the L-shaped domain shown in Figure 1 using the vector Lagrange discretization (A.1), corresponding to the two-dimensional primal formulation (6.1).

A.2. Three-dimensional vector Lagrange discretization and results. In three dimensions, we consider the primal formulation with respect to $H(\text{div}, \Omega) \cap H_0(\text{curl}, \Omega)$. The vector Lagrange space is used as a replacement for the proposed space V_h^{rd} in (6.6), which discretizes the primal formulation (6.5).

L	λ_h^1	λ_h^2	λ_h^3	λ_h^4	λ_h^5	λ_h^6	λ_h^7	λ_h^8	λ_h^9	λ_h^{10}
1	19.407	19.407	39.473	39.473	52.977	52.977	71.814	71.814	89.737	89.737
2	17.451	17.451	31.855	31.855	46.680	46.680	56.952	56.952	74.032	74.032
3	16.594	16.594	28.731	28.731	44.767	44.767	53.076	53.076	69.231	69.231
4	16.136	16.136	27.107	27.107	44.057	44.057	51.652	51.652	67.177	67.177

TABLE 15. Computed eigenvalues on the square domain with an interior hole shown in Figure 2 using the vector Lagrange discretization (A.1), corresponding to the two-dimensional primal formulation (6.1).

Let

$$S_{h,3D}^{\text{Lag}} = \{v_h \in H^1(\Omega) : v_h|_T \in \mathbb{P}_1(T), \forall T \in \mathcal{G}_h\}.$$

For the three-dimensional primal formulation with respect to $H(\text{div}, \Omega) \cap H_0(\text{curl}, \Omega)$, we define

$$\mathbf{V}_{h,3D}^{\text{Lag}} = [S_{h,3D}^{\text{Lag}}]^3 \cap (H(\text{div}, \Omega) \cap H_0(\text{curl}, \Omega)).$$

The corresponding vector Lagrange discretization is to find

$$(\lambda_h, \omega_h) \in \mathbb{R} \times \mathbf{V}_{h,3D}^{\text{Lag}}, \quad \omega_h \neq 0,$$

such that

$$(A.2) \quad (\text{div}\omega_h, \text{div}\tau_h) + (\text{curl}\omega_h, \text{curl}\tau_h) = \lambda_h(\omega_h, \tau_h), \quad \forall \tau_h \in \mathbf{V}_{h,3D}^{\text{Lag}}.$$

The corresponding three-dimensional eigenvalue results are reported below.

L	λ_h^1	λ_h^2	λ_h^3	λ_h^4	λ_h^5	λ_h^6	λ_h^7	λ_h^8	λ_h^9	λ_h^{10}
1	22.838	22.838	22.838	37.293	37.293	37.293	62.453	62.453	62.453	71.457
2	20.503	20.503	20.503	31.509	31.509	31.509	52.609	52.609	52.609	54.575
3	19.930	19.930	19.930	30.084	30.084	30.084	50.165	50.165	50.165	50.630
4	19.787	19.787	19.787	29.728	29.728	29.728	49.552	49.552	49.552	49.667

TABLE 16. Computed eigenvalues on $\Omega = [0, 1]^3$ using the vector Lagrange discretization (A.2), corresponding to the three-dimensional primal formulation with respect to $H(\text{div}, \Omega) \cap H_0(\text{curl}, \Omega)$, namely (6.5).

L	λ_h^1	λ_h^2	λ_h^3	λ_h^4	λ_h^5	λ_h^6	λ_h^7	λ_h^8	λ_h^9	λ_h^{10}
1	22.721	23.634	25.790	28.346	36.700	40.694	56.825	57.045	63.791	68.227
2	13.030	18.518	20.541	22.443	30.541	33.227	35.167	38.375	46.014	49.681
3	4.634	12.735	15.612	18.327	21.557	26.625	28.629	30.702	31.754	35.672
4	1.341	3.708	9.613	9.784	9.933	14.384	14.404	16.443	20.643	21.309

TABLE 17. Computed eigenvalues on Ω_1 shown in Figure 3 using the vector Lagrange discretization (A.2), corresponding to the three-dimensional primal formulation with respect to $H(\text{div}, \Omega) \cap H_0(\text{curl}, \Omega)$, namely (6.5).

L	λ_h^1	λ_h^2	λ_h^3	λ_h^4	λ_h^5	λ_h^6	λ_h^7	λ_h^8	λ_h^9	λ_h^{10}
1	21.085	21.351	22.319	25.715	33.602	34.655	51.717	54.819	59.254	60.737
2	13.179	16.340	17.601	19.744	22.272	27.151	29.351	31.654	32.334	41.989
3	4.918	7.508	11.822	11.965	14.570	14.994	15.168	18.498	21.025	21.263
4	1.448	2.141	3.500	4.176	5.100	6.810	6.850	8.104	8.344	8.958

TABLE 18. Computed eigenvalues on Ω_2 shown in Figure 4 using the vector Lagrange discretization (A.2), corresponding to the three-dimensional primal formulation with respect to $H(\text{div}, \Omega) \cap H_0(\text{curl}, \Omega)$, namely (6.5).

A.3. Summary of the vector Lagrange element. The vector Lagrange element gives reasonable eigenvalue approximations on convex domains, such as the square and the cube. However, this favorable behavior does not persist on nonconvex or multiply connected domains, where the computed spectra deviate significantly from the expected results. In particular, on the perforated square Ω_H (Figure 2), where the first Betti number is 1, the smallest computed eigenvalue at mesh level $L = 4$ is $\lambda_h^1 \approx 16.1$ (Table 15), whereas both the proposed element and the mixed formulation in Section 6 correctly capture a simple zero eigenvalue (Tables 5 and 6). More generally, the method does not reliably reproduce the zero eigenvalues associated with the topology of the domain. Therefore, although the vector Lagrange element may be effective on convex domains, it is not robust as a general discretization for the eigenvalue problems considered here.

APPENDIX B. EIGENVALUE RESULTS OBTAINED BY THE VECTOR CROUZEIX–RAVIART ELEMENT

This appendix reports eigenvalue computations based on the vector Crouzeix–Raviart element, to be compared with the proposed-element and mixed results in Section 6. We remark that relevant numerical experiments concerning the Crouzeix–Raviart element were reported by [9].

B.1. Two-dimensional vector Crouzeix–Raviart discretizations and results. In two dimensions, the continuous space is

$$V_{2D} = H_0(\text{div}; \Omega) \cap H(\text{rot}; \Omega).$$

Let \mathcal{F}_h^i and \mathcal{F}_h^b denote the sets of interior and boundary edges of \mathcal{G}_h , respectively. The scalar Crouzeix–Raviart space is defined by

$$CR_h = \left\{ v_h \in L^2(\Omega) : v_h|_T \in \mathbb{P}_1(T), \forall T \in \mathcal{G}_h, \int_F \llbracket v_h \rrbracket ds = 0, \forall F \in \mathcal{F}_h^i \right\}.$$

The two-dimensional vector Crouzeix–Raviart space used for $H_0(\text{div}; \Omega) \cap H(\text{rot}; \Omega)$ is

$$\mathbf{V}_{h,2D}^{\text{CR}} = \left\{ \mathbf{v}_h \in [CR_h]^2 : \int_F \mathbf{v}_h \cdot \mathbf{n} ds = 0, \forall F \in \mathcal{F}_h^b \right\}.$$

B.1.1. *Direct discretization.* The direct vector Crouzeix–Raviart discretization is to find

$$(\lambda_h, \mathbf{u}_h) \in \mathbb{R} \times \mathbf{V}_{h,2D}^{\text{CR}}, \quad \mathbf{u}_h \neq \mathbf{0},$$

such that

$$(B.1) \quad a_{h,2D}(\mathbf{u}_h, \mathbf{v}_h) = \lambda_h(\mathbf{u}_h, \mathbf{v}_h), \quad \forall \mathbf{v}_h \in \mathbf{V}_{h,2D}^{\text{CR}},$$

where

$$a_{h,2D}(\mathbf{u}_h, \mathbf{v}_h) = \sum_{T \in \mathcal{G}_h} \int_T (\operatorname{div} \mathbf{u}_h \operatorname{div} \mathbf{v}_h + \operatorname{rot} \mathbf{u}_h \operatorname{rot} \mathbf{v}_h).$$

The corresponding two-dimensional eigenvalue results are listed below.

L	λ_h^1	λ_h^2	λ_h^3	λ_h^4	λ_h^5	λ_h^6	λ_h^7	λ_h^8	λ_h^9	λ_h^{10}
1	19.568	19.568	38.797	38.797	76.056	76.056	94.284	94.284	94.284	94.284
2	19.697	19.697	39.309	39.309	78.271	78.271	97.629	97.629	97.629	97.629
3	19.729	19.729	39.436	39.436	78.787	78.787	98.431	98.431	98.431	98.431
4	19.737	19.737	39.468	39.468	78.915	78.915	98.630	98.630	98.630	98.630

TABLE 19. Computed eigenvalues on $\Omega = [0, 1]^2$, using (B.1).

L	λ_h^1	λ_h^2	λ_h^3	λ_h^4	λ_h^5	λ_h^6	λ_h^7	λ_h^8	λ_h^9	λ_h^{10}
1	10.931	28.089	69.092	76.056	76.056	87.522	92.974	116.905	146.675	146.675
2	11.462	28.211	74.346	78.271	78.271	90.240	98.357	120.230	155.188	155.188
3	11.670	28.255	76.116	78.787	78.787	90.896	99.872	121.217	157.236	157.236
4	11.752	28.267	76.744	78.915	78.915	91.060	100.341	121.484	157.744	157.744

TABLE 20. Computed eigenvalues on the L-shaped domain shown in Figure 1, using (B.1).

L	λ_h^1	λ_h^2	λ_h^3	λ_h^4	λ_h^5	λ_h^6	λ_h^7	λ_h^8	λ_h^9	λ_h^{10}
1	14.641	14.837	36.549	60.880	68.017	76.117	87.467	97.405	109.834	121.091
2	15.401	15.680	36.985	66.630	73.489	79.027	91.424	99.031	115.414	144.318
3	15.706	16.018	37.179	68.454	75.419	79.868	92.593	99.632	117.314	148.538
4	15.827	16.152	37.254	69.095	76.120	80.130	92.961	99.808	117.959	149.491

TABLE 21. Computed eigenvalues on the square domain with an interior hole shown in Figure 2, using (B.1).

B.1.2. ∇ -formulation. The ∇ -formulation with the vector Crouzeix–Raviart element is to find

$$(\lambda_h, \mathbf{u}_h) \in \mathbb{R} \times \mathbf{V}_{h,2D}^{\text{CR}}, \quad \mathbf{u}_h \neq \mathbf{0},$$

such that

$$(B.2) \quad b_{h,2D}(\mathbf{u}_h, \mathbf{v}_h) = \lambda_h(\mathbf{u}_h, \mathbf{v}_h), \quad \forall \mathbf{v}_h \in \mathbf{V}_{h,2D}^{\text{CR}},$$

where

$$b_{h,2D}(\mathbf{u}_h, \mathbf{v}_h) = \sum_{T \in \mathcal{G}_h} \int_T \nabla \mathbf{u}_h : \nabla \mathbf{v}_h.$$

The corresponding two-dimensional eigenvalue results are listed below.

L	λ_h^1	λ_h^2	λ_h^3	λ_h^4	λ_h^5	λ_h^6	λ_h^7	λ_h^8	λ_h^9	λ_h^{10}
1	9.827	9.827	19.061	19.061	38.797	38.797	46.236	46.236	46.236	46.236
2	9.859	9.859	19.570	19.570	39.309	39.309	48.575	48.575	48.575	48.575
3	9.867	9.867	19.697	19.697	39.436	39.436	49.155	49.155	49.155	49.155
4	9.869	9.869	19.729	19.729	39.468	39.468	49.300	49.300	49.300	49.300

TABLE 22. Computed eigenvalues on $\Omega = [0, 1]^2$, using (B.2).

L	λ_h^1	λ_h^2	λ_h^3	λ_h^4	λ_h^5	λ_h^6	λ_h^7	λ_h^8	λ_h^9	λ_h^{10}
1	12.358	12.358	38.797	38.797	42.589	42.589	52.532	52.532	68.016	68.016
2	12.996	12.996	39.309	39.309	44.472	44.472	57.086	57.086	76.242	76.242
3	13.402	13.402	39.436	39.436	45.075	45.075	58.794	58.794	78.280	78.280
4	13.664	13.664	39.468	39.468	45.304	45.304	59.602	59.602	78.788	78.788

TABLE 23. Computed eigenvalues on the L-shaped domain shown in Figure 1, using (B.2).

L	λ_h^1	λ_h^2	λ_h^3	λ_h^4	λ_h^5	λ_h^6	λ_h^7	λ_h^8	λ_h^9	λ_h^{10}
1	12.797	12.797	16.934	16.934	40.379	40.379	43.852	43.852	52.459	52.459
2	13.765	13.765	19.564	19.564	41.688	41.688	46.869	46.869	57.918	57.918
3	14.377	14.377	21.333	21.333	42.333	42.333	48.195	48.195	60.565	60.565
4	14.763	14.763	22.515	22.515	42.699	42.699	48.907	48.907	62.059	62.059

TABLE 24. Computed eigenvalues on the square domain with an interior hole shown in Figure 2, using (B.2).

B.2. Three-dimensional vector Crouzeix–Raviart discretizations and results. In three dimensions, the continuous space is

$$\mathbf{V}_{3D} = H(\operatorname{div}; \Omega) \cap H_0(\operatorname{curl}; \Omega).$$

Let \mathcal{F}_h^i and \mathcal{F}_h^b denote the sets of interior and boundary faces of \mathcal{G}_h , respectively. The scalar Crouzeix–Raviart space is defined by

$$CR_h = \left\{ v_h \in L^2(\Omega) : v_h|_T \in \mathbb{P}_1(T), \forall T \in \mathcal{G}_h, \int_F \llbracket v_h \rrbracket ds = 0, \forall F \in \mathcal{F}_h^i \right\}.$$

The three-dimensional vector Crouzeix–Raviart space used for $H(\operatorname{div}; \Omega) \cap H_0(\operatorname{curl}; \Omega)$ is

$$\mathbf{V}_{h,3D}^{\text{CR}} = \left\{ \mathbf{v}_h \in [CR_h]^3 : \int_F \mathbf{v}_h \times \mathbf{n} ds = \mathbf{0}, \forall F \in \mathcal{F}_h^b \right\}.$$

B.2.1. Direct discretization. The direct vector Crouzeix–Raviart discretization is to find

$$(\lambda_h, \mathbf{u}_h) \in \mathbb{R} \times \mathbf{V}_{h,3D}^{\text{CR}}, \quad \mathbf{u}_h \neq \mathbf{0},$$

such that

$$(B.3) \quad a_{h,3D}(\mathbf{u}_h, \mathbf{v}_h) = \lambda_h(\mathbf{u}_h, \mathbf{v}_h), \quad \forall \mathbf{v}_h \in \mathbf{V}_{h,3D}^{\text{CR}},$$

where

$$a_{h,3D}(\mathbf{u}_h, \mathbf{v}_h) = \sum_{T \in \mathcal{G}_h} \int_T (\operatorname{div} \mathbf{u}_h \operatorname{div} \mathbf{v}_h + (\nabla \times \mathbf{u}_h) \cdot (\nabla \times \mathbf{v}_h)).$$

The corresponding three-dimensional eigenvalue results are listed below.

L	λ_h^1	λ_h^2	λ_h^3	λ_h^4	λ_h^5	λ_h^6	λ_h^7	λ_h^8	λ_h^9	λ_h^{10}
1	23.835	23.835	26.341	36.609	36.609	46.154	53.202	53.202	60.000	65.876
2	20.434	23.349	23.349	28.762	28.762	30.438	32.339	32.339	33.718	33.718
3	22.066	26.198	26.198	35.663	35.663	51.299	52.055	52.055	59.355	59.355
4	22.503	26.994	26.994	37.274	37.274	58.071	58.830	58.830	65.948	65.948

TABLE 25. Computed eigenvalues on $\Omega = [0, 1]^3$, using (B.3).

L	λ_h^1	λ_h^2	λ_h^3	λ_h^4	λ_h^5	λ_h^6	λ_h^7	λ_h^8	λ_h^9	λ_h^{10}
1	9.423	19.933	21.729	29.581	34.689	39.819	43.040	45.321	45.897	47.059
2	11.492	21.160	23.390	36.338	43.749	46.256	52.659	55.647	58.888	59.267
3	12.292	21.620	24.007	36.787	48.429	48.496	55.216	57.656	62.524	62.644
4	12.658	22.915	23.970	37.775	49.861	50.241	58.615	59.734	62.799	63.228

TABLE 26. Computed eigenvalues on Ω_1 shown in Figure 3, using (B.3).

L	λ_h^1	λ_h^2	λ_h^3	λ_h^4	λ_h^5	λ_h^6	λ_h^7	λ_h^8	λ_h^9	λ_h^{10}
1	9.102	9.563	17.980	19.241	27.206	30.054	31.158	32.072	37.370	37.417
2	11.143	11.218	19.042	20.559	29.944	31.842	39.702	41.147	41.472	42.476
3	11.882	12.043	19.541	21.175	31.164	32.585	41.897	42.714	43.185	45.981
4	12.237	12.403	20.551	21.201	31.961	33.436	43.797	43.842	44.084	47.260

TABLE 27. Computed eigenvalues on Ω_2 shown in Figure 4, using (B.3).

B.2.2. ∇ -formulation. The ∇ -formulation with the vector Crouzeix–Raviart element is to find

$$(\lambda_h, \mathbf{u}_h) \in \mathbb{R} \times \mathbf{V}_{h,3D}^{\text{CR}}, \quad \mathbf{u}_h \neq \mathbf{0},$$

such that

$$(B.4) \quad b_{h,3D}(\mathbf{u}_h, \mathbf{v}_h) = \lambda_h(\mathbf{u}_h, \mathbf{v}_h), \quad \forall \mathbf{v}_h \in \mathbf{V}_{h,3D}^{\text{CR}},$$

where

$$b_{h,3D}(\mathbf{u}_h, \mathbf{v}_h) = \sum_{T \in \mathcal{G}_h} \int_T \nabla \mathbf{u}_h : \nabla \mathbf{v}_h.$$

The corresponding three-dimensional eigenvalue results are listed below.

L	λ_h^1	λ_h^2	λ_h^3	λ_h^4	λ_h^5	λ_h^6	λ_h^7	λ_h^8	λ_h^9	λ_h^{10}
1	16.917	16.917	16.917	25.090	25.090	25.090	28.268	28.268	28.268	28.935
2	19.000	19.000	19.000	28.383	28.383	28.383	43.302	43.302	43.967	43.967
3	19.552	19.552	19.552	29.295	29.295	29.295	47.774	47.774	47.967	47.967
4	19.692	19.692	19.692	29.530	29.530	29.530	48.951	48.951	49.001	49.001

TABLE 28. Computed eigenvalues on $\Omega = [0, 1]^3$, using (B.4).

L	λ_h^1	λ_h^2	λ_h^3	λ_h^4	λ_h^5	λ_h^6	λ_h^7	λ_h^8	λ_h^9	λ_h^{10}
1	21.648	21.648	25.798	25.798	32.095	41.235	44.819	44.819	46.230	46.230
2	23.300	23.300	28.924	28.924	36.188	45.870	50.100	50.100	51.594	51.594
3	24.116	24.116	30.926	30.926	37.569	47.391	51.799	51.799	53.391	53.391
4	24.570	24.570	32.223	32.223	38.027	47.884	52.443	52.443	54.096	54.096

TABLE 29. Computed eigenvalues on Ω_1 shown in Figure 3, using (B.4).

L	λ_h^1	λ_h^2	λ_h^3	λ_h^4	λ_h^5	λ_h^6	λ_h^7	λ_h^8	λ_h^9	λ_h^{10}
1	29.254	30.565	31.455	32.531	41.934	43.680	44.674	45.642	51.309	54.097
2	34.945	37.077	37.370	39.956	53.783	54.480	55.317	58.571	59.404	63.649
3	38.923	41.335	41.482	44.644	59.485	59.846	64.118	65.595	68.301	69.247
4	41.618	44.104	44.210	47.533	62.806	63.072	67.109	71.168	71.907	72.432

TABLE 30. Computed eigenvalues on Ω_2 shown in Figure 4, using (B.4).

B.3. Summary of the vector Crouzeix–Raviart element. The direct primal discretization using the vector Crouzeix–Raviart element does not yield satisfactory eigenvalue approximations for the present problem. The computed spectra show noticeable discrepancies from those obtained by the proposed element and the mixed formulation. In contrast, the ∇ -formulation with the vector Crouzeix–Raviart element gives reasonable approximations on convex domains. However, this favorable behavior does not persist uniformly on nonconvex or topologically more complicated domains. For example, on Ω_H neither the direct discretization (Table 21) nor the ∇ -formulation (Table 24) produces a zero eigenvalue, in contrast to Section 6. These observations suggest that, although the ∇ -formulation may be effective in the convex case, the direct use of the vector Crouzeix–Raviart element in the primal formulation is not reliable as a general discretization for the present eigenvalue problem.

APPENDIX C. ILLUSTRATION OF BASIS FUNCTIONS OF $\mathbf{W}_h^{*,\text{nc}} \Lambda^k$ IN TWO AND THREE DIMENSIONS

This appendix illustrates the basis functions of nonconforming Whitney spaces $\mathbf{W}_h^{*,\text{nc}} \Lambda^k$ defined in [21] used in the adjoint continuity constraints (3.10). The two- and three-dimensional realizations are below; note that, the choice of the two cells of the supports of the basis functions is not unique, and they are not necessarily adjacent to each other. In two dimensions, $\mathbf{RT}_h^{\text{nc}}$ coincides with the adjoint partner $\mathbf{W}_{h0}^{*,\text{nc}} \Lambda^1$ under the vector proxy used in (3.12).

C.1. $\mathbf{W}_h^{*,\text{nc}} \Lambda^1$ in 2D revisited. Let \mathbb{V}_h^1 denote the continuous piecewise linear element space, and $\underline{\mathbb{V}}_h^{\text{RT}}$ denote the Raviart-Thomas [20] element space of lowest degree on \mathcal{G}_h . Denote $\mathbb{V}_{h0}^1 := \mathbb{V}_h^1 \cap H_0^1(\Omega)$ and $\underline{\mathbb{V}}_{h0}^{\text{RT}} := \underline{\mathbb{V}}_h^{\text{RT}} \cap H_0(\text{div}, \Omega)$.

On a triangle T , denote the space of the lowest-degree Raviart-Thomas shape functions by $\mathbf{RT}(T) := \text{span} \{ \underline{\alpha} + \beta \underline{x} : \underline{\alpha} \in \mathbb{R}^2, \beta \in \mathbb{R} \}$. Then

$$(C.1) \quad \mathcal{R}(\text{div}, \mathbf{RT}(T)) = \mathbb{R} = \mathcal{N}(\nabla, P_1(T)), \quad \text{and} \quad \mathcal{N}(\text{div}, \mathbf{RT}(T)) = \mathbb{R}^2 = \mathcal{R}(\nabla, P_1(T)).$$

Denote $\mathbf{RT}(\mathcal{G}_h) := \bigoplus_{T \in \mathcal{G}_h} E_T^\Omega \mathbf{RT}(T)$. We define the nonconforming finite element spaces

$$(C.2) \quad \mathbf{RT}_h^{\text{nc}} := \left\{ \underline{\mathcal{T}}_h \in \mathbf{RT}(\mathcal{G}_h) : \sum_{T \in \mathcal{G}_h} (\underline{\mathcal{T}}_h, \nabla \mathbf{v}_h)_T + (\text{div} \underline{\mathcal{T}}_h, \mathbf{v}_h)_T = 0, \quad \forall \mathbf{v}_h \in \mathbb{V}_{h0}^1 \right\},$$

and

$$(C.3) \quad \mathbf{RT}_{h0}^{\text{nc}} := \left\{ \underline{\mathcal{T}}_h \in \mathbf{RT}(\mathcal{G}_h) : \sum_{T \in \mathcal{G}_h} (\underline{\mathcal{T}}_h, \nabla \mathbf{v}_h)_T + (\text{div} \underline{\mathcal{T}}_h, \mathbf{v}_h)_T = 0, \quad \forall \mathbf{v}_h \in \mathbb{V}_h^1 \right\}.$$

Figure 7 shows a representative global basis function of $\mathbb{RT}_h^{\text{nc}}$.

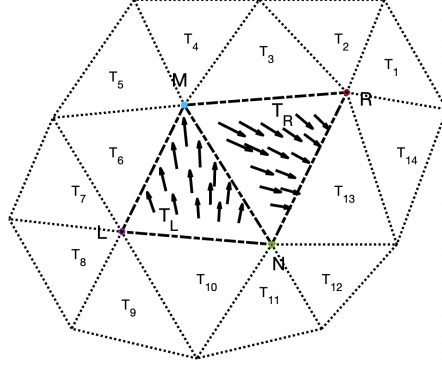


FIGURE 7. Profile of a representative global basis function in $\mathbb{RT}_h^{\text{nc}}$, supported on two cells T_L and T_R .

C.2. $W_h^{*,\text{nc}}\Lambda^2$ in 3D revisited. Let $\Omega \subset \mathbb{R}^3$ be a polyhedral domain, and let \mathcal{G}_h be a tetrahedral partition of Ω . Under the three-dimensional vector proxy, the lowest-order Whitney 1-form space is identified with the lowest-order Nedelec edge element space of the first kind. We denote this space by V_h^{Ned} , and set

$$V_{h0}^{\text{Ned}} := V_h^{\text{Ned}} \cap H_0(\text{curl}, \Omega).$$

On a tetrahedron T , the corresponding local Nedelec shape-function space is

$$\mathbf{Ned}(T) = \{ \mathbf{a} + \mathbf{b} \times \mathbf{x} : \mathbf{a}, \mathbf{b} \in \mathbb{R}^3 \}.$$

Meanwhile, $\mathbf{Ned}(T)$ represents $\mathcal{P}_1^{*-} \Lambda^2(T)$ under the vector proxy, and δ_2 is essentially curl. Namely, $W_h^{*,\text{nc}}\Lambda^2$ is essentially a nonconforming $H(\text{curl})$ finite element space. In the sequel, we denote it by \mathbb{N}_h^{nc} , and define it by

$$(C.4) \quad \mathbb{N}_h^{\text{nc}} := \left\{ \boldsymbol{\mu}_h \in \mathbb{N}(\mathcal{G}_h) : \sum_{T \in \mathcal{G}_h} [(\text{curl} \boldsymbol{\mu}_h, \boldsymbol{\tau}_h)_T - (\boldsymbol{\mu}_h, \text{curl} \boldsymbol{\tau}_h)_T] = 0, \forall \boldsymbol{\tau}_h \in V_{h0}^{\text{Ned}} \right\}.$$

Similarly, the space with the homogeneous boundary condition is defined by

$$(C.5) \quad \mathbb{N}_{h0}^{\text{nc}} := \left\{ \boldsymbol{\mu}_h \in \mathbb{N}(\mathcal{G}_h) : \sum_{T \in \mathcal{G}_h} [(\text{curl} \boldsymbol{\mu}_h, \boldsymbol{\tau}_h)_T - (\boldsymbol{\mu}_h, \text{curl} \boldsymbol{\tau}_h)_T] = 0, \forall \boldsymbol{\tau}_h \in V_h^{\text{Ned}} \right\}.$$

Figure 8 shows a typical global basis function in \mathbb{N}_h^{nc} , whose support consists of two adjacent tetrahedra sharing an edge. Again, we note that the two cells in the support are not necessarily adjacent to each other.

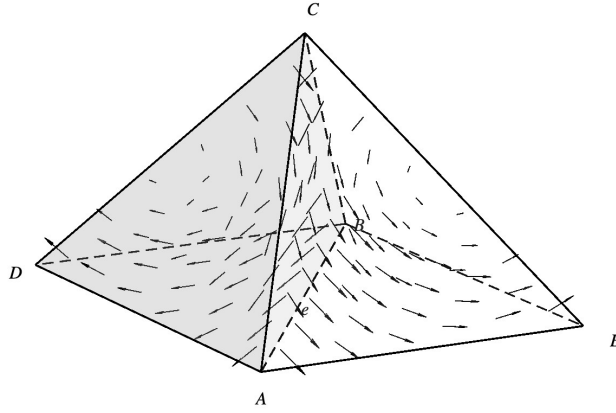


FIGURE 8. A global basis function of the three-dimensional dual nonconforming space \mathbb{N}_h^{nc} . The support consists of two adjacent tetrahedra sharing the edge e .

APPENDIX D. BASIS FUNCTIONS OF THE TWO-DIMENSIONAL NONCONFORMING SPACE (3.12) FOR $H(\text{rot}, \Omega) \cap H_0(\text{div}, \Omega)$

This section reports explicit cell-wise and patch-wise basis functions for $\mathbf{V}_h^{\text{rd}} = \mathbf{V}_h^{\text{d}\cap\delta^{\circ}} \Lambda^1$ in two dimensions, supporting the proof of Theorem 3.7.

Let

$$A = \int_T \tilde{x}^2 dx, \quad B = \int_T \tilde{y}^2 dx, \quad C = \int_T \tilde{x}\tilde{y} dx.$$

Define

$$\mathbf{M}_T(\tilde{x}, \tilde{y}) = \frac{1}{2(A+B)} \begin{bmatrix} \tilde{x}^2 - \tilde{y}^2 + \frac{3B-A}{|T|} & -\frac{2C}{|T|} \\ -\frac{2C}{|T|} & -\tilde{x}^2 + \tilde{y}^2 + \frac{3A-B}{|T|} \end{bmatrix},$$

and

$$P_T(\tilde{x}, \tilde{y}) = \frac{1}{4(A+B)} \begin{bmatrix} -\frac{2C}{|T|} & -\tilde{x}^2 + \tilde{y}^2 + \frac{3A-B}{|T|} \\ -\tilde{x}^2 + \tilde{y}^2 + \frac{A-3B}{|T|} & \frac{2C}{|T|} \end{bmatrix}.$$

Then the six local basis functions of $\mathbf{P}_{\mathbf{d}\cap\delta}\Lambda^1(T)$ are given by

$$(D.1) \quad \begin{aligned} \boldsymbol{\varrho}_i^T &= \frac{1}{2|T|} \begin{pmatrix} \tilde{x} \\ \tilde{y} \end{pmatrix} + \mathbf{M}_T(\tilde{x}, \tilde{y}) \begin{pmatrix} \tilde{x}_i \\ \tilde{y}_i \end{pmatrix}, \\ \boldsymbol{\varsigma}_i^T &= -\frac{1}{2|T|} \begin{pmatrix} \tilde{y} \\ -\tilde{x} \end{pmatrix} + P_T(\tilde{x}, \tilde{y}) \begin{pmatrix} \tilde{x}_i \\ \tilde{y}_i \end{pmatrix}, \quad i = 1, 2, 3. \end{aligned}$$

Then,

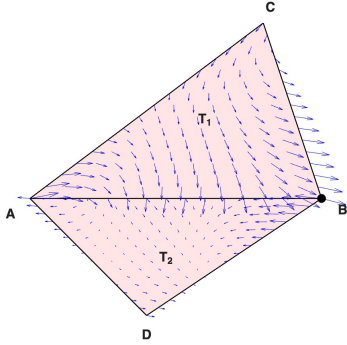
$$P_{\text{rd}}(T) = \text{span}\{\boldsymbol{\varrho}_i^T, \boldsymbol{\varsigma}_i^T\}_{i=1}^3$$

and

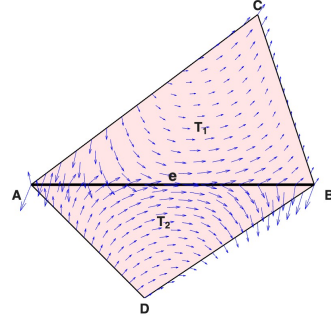
$$(D.2) \quad (\text{rot}\boldsymbol{\varrho}_i^T, 1 - 2\lambda_j)_T - (\boldsymbol{\varrho}_i^T, \text{curl}(1 - 2\lambda_j))_T = 0, \quad (\text{div}\boldsymbol{\varrho}_i^T, \lambda_j)_T + (\boldsymbol{\varrho}_i^T, \nabla\lambda_j)_T = \delta_{ij}, \quad i, j = 1 : 3$$

and

$$(D.3) \quad (\text{rot}\boldsymbol{\varsigma}_i^T, 1 - 2\lambda_j)_T - (\boldsymbol{\varsigma}_i^T, \text{curl}(1 - 2\lambda_j))_T = \delta_{ij}, \quad (\text{div}\boldsymbol{\varsigma}_i^T, \lambda_j)_T + (\boldsymbol{\varsigma}_i^T, \nabla\lambda_j)_T = 0, \quad i, j = 1 : 3$$



(A) Point-associated global basis function $\boldsymbol{\varrho}^T$



(B) Edge-associated global basis function $\boldsymbol{\varsigma}^T$

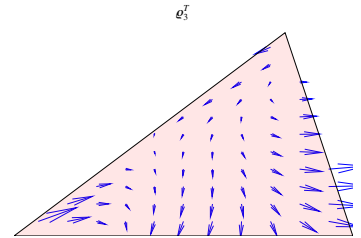
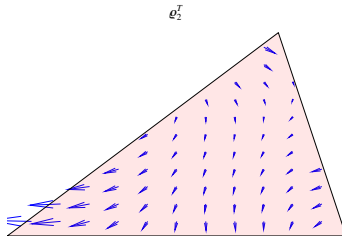
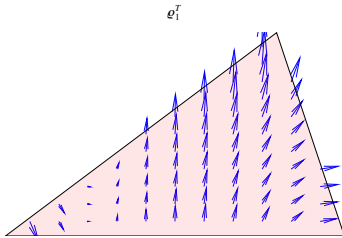
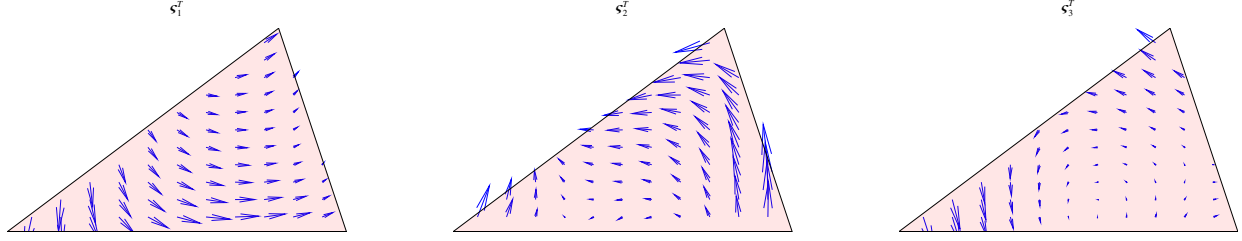


FIGURE 10. Local basis functions $\boldsymbol{\varrho}_1^T - \boldsymbol{\varrho}_3^T$.

FIGURE 11. Local basis functions $\mathfrak{S}_1^T - \mathfrak{S}_3^T$.

Remark D.1. The explicit basis functions \mathfrak{Q}_i^T and \mathfrak{S}_i^T can be written out by these 3 steps.

First, by Remark 3.3, we can write out $\omega_1 = \begin{pmatrix} \bar{x} \\ \bar{y} \end{pmatrix}$, $\omega_2 = \begin{pmatrix} \bar{y} \\ -\bar{x} \end{pmatrix}$, $\omega_3 = \begin{pmatrix} \bar{x}^2 - \bar{y}^2 + M \\ 0 \end{pmatrix}$, $\omega_4 = \begin{pmatrix} 0 \\ \bar{x}^2 - \bar{y}^2 + M \end{pmatrix}$, $\omega_5 = \begin{pmatrix} 1 \\ 0 \end{pmatrix}$, $\omega_6 = \begin{pmatrix} 0 \\ 1 \end{pmatrix}$ and $(s_1, \eta_1) = \frac{1}{2|T|} \begin{pmatrix} 1 \\ 0 \end{pmatrix}$, $(s_2, \eta_2) = -\frac{1}{2|T|} \begin{pmatrix} 0 \\ 1 \end{pmatrix}$, $(s_3, \eta_3) = \frac{1}{2(A+B)} \begin{pmatrix} \bar{x} \\ \bar{y} \end{pmatrix}$, $(s_4, \eta_4) = -\frac{1}{2(A+B)} \begin{pmatrix} \bar{y} \\ -\bar{x} \end{pmatrix}$, $(s_5, \eta_5) = \frac{1}{|T|} \left(\frac{1}{2} \begin{pmatrix} \bar{x} \\ -\bar{y} \end{pmatrix} + \frac{B-A}{2(A+B)} \begin{pmatrix} \bar{x} \\ \bar{y} \end{pmatrix} + \frac{C}{A+B} \begin{pmatrix} \bar{y} \\ -\bar{x} \end{pmatrix} \right)$, $(s_6, \eta_6) = \frac{1}{|T|} \left(\frac{1}{2} \begin{pmatrix} \bar{y} \\ \bar{x} \end{pmatrix} + \frac{C}{A+B} \begin{pmatrix} \bar{x} \\ \bar{y} \end{pmatrix} + \frac{A-B}{2(A+B)} \begin{pmatrix} \bar{y} \\ -\bar{x} \end{pmatrix} \right)$, so that

$$(D.4) \quad (\operatorname{div} \omega_i, s_j)_T + (\omega_i, \nabla s_j)_T + (\operatorname{rot} \omega_i, \eta_j)_T - (\omega_i, \operatorname{curl} \eta_j)_T = \delta_{i,j}.$$

Set

$$\begin{bmatrix} (s_1, \eta_1) \\ (s_2, \eta_2) \\ (s_3, \eta_3) \\ (s_4, \eta_4) \\ (s_5, \eta_5) \\ (s_6, \eta_6) \end{bmatrix} = \overline{M} \begin{bmatrix} (\lambda_1, 0) \\ (\lambda_2, 0) \\ (\lambda_3, 0) \\ (0, 1 - 2\lambda_1) \\ (0, 1 - 2\lambda_2) \\ (0, 1 - 2\lambda_3) \end{bmatrix} = \overline{M} \begin{bmatrix} (\tilde{s}_1, \tilde{\eta}_1) \\ (\tilde{s}_2, \tilde{\eta}_2) \\ (\tilde{s}_3, \tilde{\eta}_3) \\ (\tilde{s}_4, \tilde{\eta}_4) \\ (\tilde{s}_5, \tilde{\eta}_5) \\ (\tilde{s}_6, \tilde{\eta}_6) \end{bmatrix}$$

and

$$(\tilde{\omega}_1, \tilde{\omega}_2, \dots, \tilde{\omega}_6) = (\omega_1, \omega_2, \dots, \omega_6) \overline{M}.$$

Then

$$(\operatorname{div} \tilde{\omega}_i, \tilde{s}_j)_T + (\tilde{\omega}_i, \nabla \tilde{s}_j)_T + (\operatorname{rot} \tilde{\omega}_i, \tilde{\eta}_j)_T - (\tilde{\omega}_i, \operatorname{curl} \tilde{\eta}_j)_T = \delta_{i,j}.$$

APPENDIX E. BASIS FUNCTIONS OF THE THREE-DIMENSIONAL NONCONFORMING SPACE (3.13) FOR

$$H(\operatorname{div}, \Omega) \cap H_0(\operatorname{curl}, \Omega)$$

This section reports the explicit basis functions in three dimensions.

Let

$$A = \int_T \bar{x}^2 dx, \quad B = \int_T \bar{y}^2 dx, \quad C = \int_T \bar{z}^2 dx,$$

and

$$D = \int_T \bar{x}\bar{y} dx, \quad E = \int_T \bar{x}\bar{z} dx, \quad F = \int_T \bar{y}\bar{z} dx.$$

Set

$$\mathbf{G} = \begin{pmatrix} 4A + B + C & 3D & 3E \\ 3D & A + 4B + C & 3F \\ 3E & 3F & A + B + 4C \end{pmatrix}, \quad \mathbf{R} = \mathbf{G}^{-1}.$$

Let

$$\tilde{\mathbf{x}} = \begin{pmatrix} \tilde{x} \\ \tilde{y} \\ \tilde{z} \end{pmatrix}, \quad \tilde{\mathbf{x}}_i = \begin{pmatrix} \tilde{x}_i \\ \tilde{y}_i \\ \tilde{z}_i \end{pmatrix}, \quad i = 1, \dots, 4.$$

Define

$$\mathbf{Q}_T(\tilde{\mathbf{x}}) = \begin{pmatrix} 2\tilde{x}^2 - \tilde{y}^2 - \tilde{z}^2 & 0 & 0 \\ 0 & 2\tilde{y}^2 - \tilde{x}^2 - \tilde{z}^2 & 0 \\ 0 & 0 & 2\tilde{z}^2 - \tilde{x}^2 - \tilde{y}^2 \end{pmatrix},$$

and

$$\mathbf{H}_T = \begin{pmatrix} 7B + 7C - 2A & 0 & 0 \\ 0 & 7A + 7C - 2B & 0 \\ 0 & 0 & 7A + 7B - 2C \end{pmatrix}.$$

Define

$$\mathbf{M}_T(\tilde{\mathbf{x}}) = -\frac{1}{3}\mathbf{Q}_T(\tilde{\mathbf{x}})\mathbf{R} - \frac{1}{9|T|}\mathbf{H}_T\mathbf{R} + \frac{1}{9|T|}\mathbf{I}_3.$$

Then the four face-associated local basis functions are given by

$$(E.1) \quad \boldsymbol{\varrho}_i^T = \frac{1}{3|T|}\tilde{\mathbf{x}} + \mathbf{M}_T(\tilde{\mathbf{x}})\tilde{\mathbf{x}}_i, \quad i = 1, \dots, 4.$$

For each edge (i, j) , $1 \leq i < j \leq 4$, define

$$\mathbf{d}_{ij} = \tilde{\mathbf{x}}_j - \tilde{\mathbf{x}}_i, \quad \boldsymbol{\eta}_{ij} = \tilde{\mathbf{x}}_i \times \tilde{\mathbf{x}}_j.$$

Define

$$\mathbf{N}_T(\tilde{\mathbf{x}}) = \frac{1}{2}\mathbf{Q}_T(\tilde{\mathbf{x}})\mathbf{R} + \frac{1}{6|T|}\mathbf{H}_T\mathbf{R} - \frac{2}{3|T|}\mathbf{I}_3.$$

The six edge-associated local basis functions are given by

$$(E.2) \quad \boldsymbol{s}_{ij}^T = \frac{1}{2|T|}(\mathbf{d}_{ij} \times \tilde{\mathbf{x}}) + \mathbf{N}_T(\tilde{\mathbf{x}})\boldsymbol{\eta}_{ij}, \quad 1 \leq i < j \leq 4.$$

Then,

$$P_{cd}(T) = \text{span}\{\boldsymbol{\varrho}_1^T, \boldsymbol{\varrho}_2^T, \boldsymbol{\varrho}_3^T, \boldsymbol{\varrho}_4^T, \boldsymbol{s}_{12}^T, \boldsymbol{s}_{13}^T, \boldsymbol{s}_{14}^T, \boldsymbol{s}_{23}^T, \boldsymbol{s}_{24}^T, \boldsymbol{s}_{34}^T\}.$$

Let

$$\mathcal{E}_T = \{(1, 2), (1, 3), (1, 4), (2, 3), (2, 4), (3, 4)\}.$$

The local functions satisfy

$$(E.3) \quad (\operatorname{curl} \boldsymbol{\varrho}_i^T, N_{pq}) - (\boldsymbol{\varrho}_i^T, \operatorname{curl} N_{pq}) = 0, \quad (\operatorname{div} \boldsymbol{\varrho}_i^T, 1 - 2\lambda_k) + (\boldsymbol{\varrho}_i^T, \nabla(1 - 2\lambda_k)) = \delta_{ik},$$

for $i, k = 1, \dots, 4$ and $(p, q) \in \mathcal{E}_T$, and

$$(E.4) \quad (\operatorname{curl} \boldsymbol{\varsigma}_{ij}^T, N_{pq}) - (\boldsymbol{\varsigma}_{ij}^T, \operatorname{curl} N_{pq}) = \delta_{(i,j),(p,q)}, \quad (\operatorname{div} \boldsymbol{\varsigma}_{ij}^T, 1 - 2\lambda_k) + (\boldsymbol{\varsigma}_{ij}^T, \nabla(1 - 2\lambda_k)) = 0,$$

for $(i, j), (p, q) \in \mathcal{E}_T$ and $k = 1, \dots, 4$.

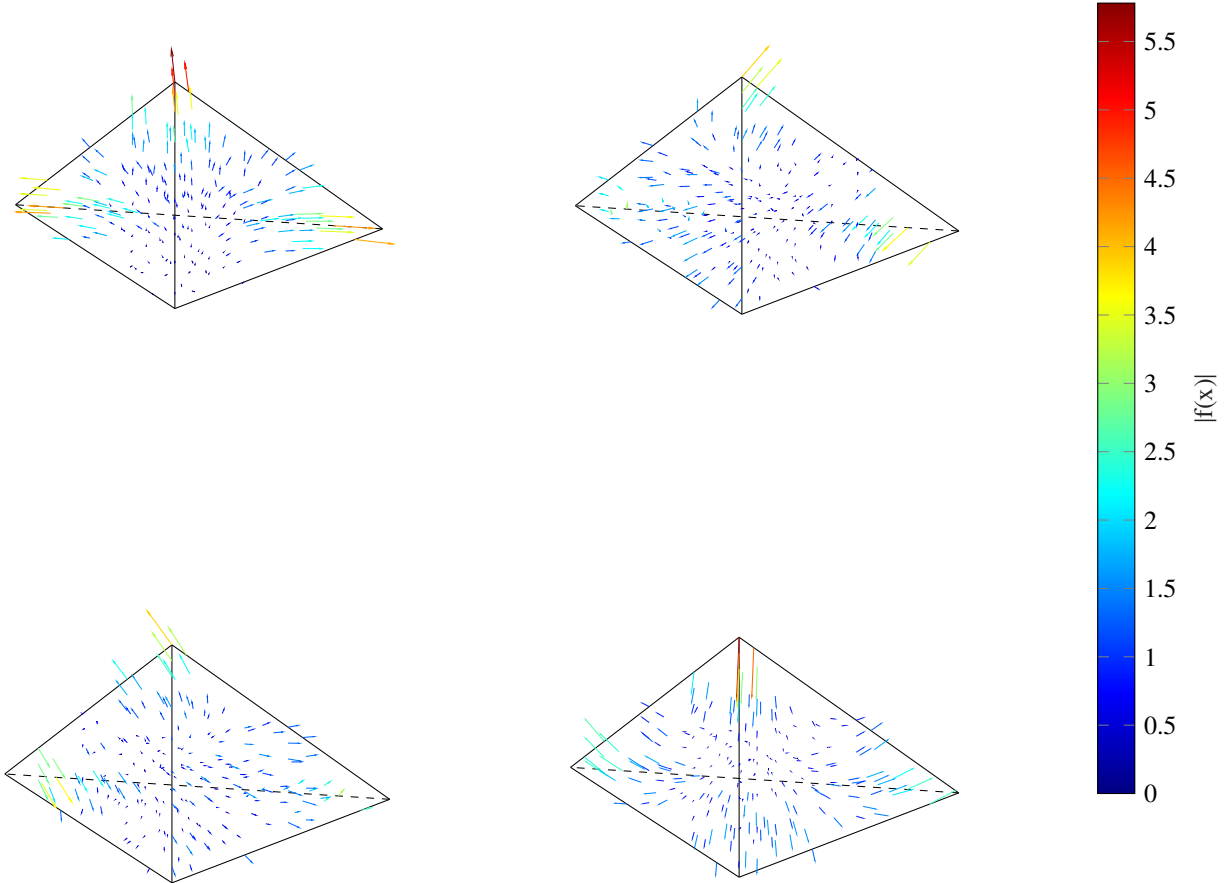
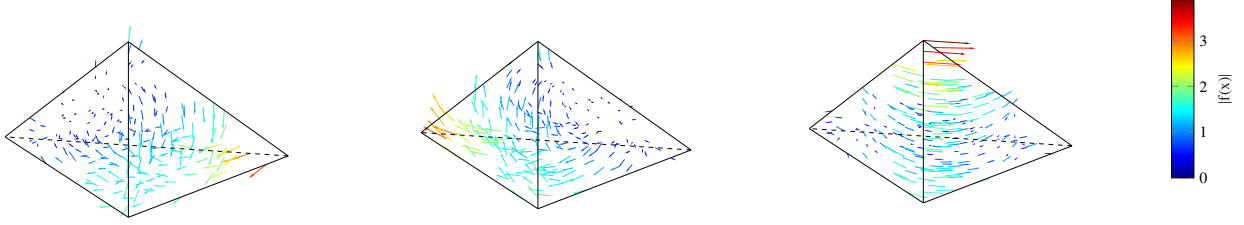
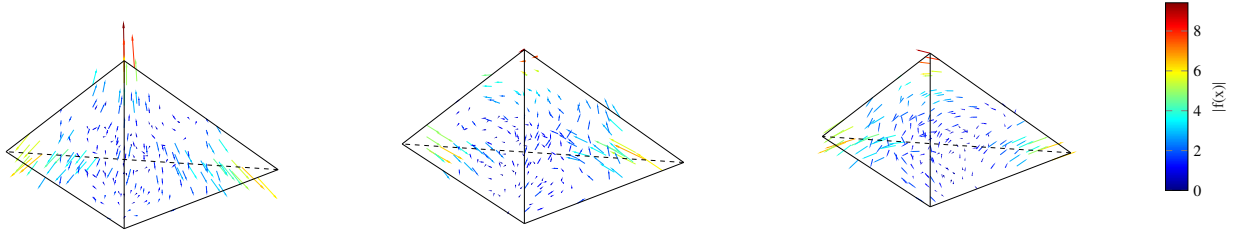


FIGURE 12. Local basis function $\boldsymbol{\varrho}_1^T - \boldsymbol{\varrho}_4^T$

Remark E.1. The explicit basis functions $\boldsymbol{\varrho}^T$ and $\boldsymbol{\varsigma}^T$ can be constructed through the following three steps.

FIGURE 13. Local basis function \mathfrak{S}_{12}^T , \mathfrak{S}_{13}^T , and \mathfrak{S}_{14}^T FIGURE 14. Local basis function \mathfrak{S}_{23}^T , \mathfrak{S}_{24}^T , and \mathfrak{S}_{34}^T

Let T be a tetrahedron. Denote by $\{\psi_j\}_{j=1}^4$ the Crouzeix–Raviart basis functions and by

$$\{\tau_{12}, \tau_{13}, \tau_{14}, \tau_{23}, \tau_{24}, \tau_{34}\}$$

the Nedelec basis functions associated with the ordered edges

$$\mathcal{E}_T = \{(12), (13), (14), (23), (24), (34)\}.$$

We seek functions

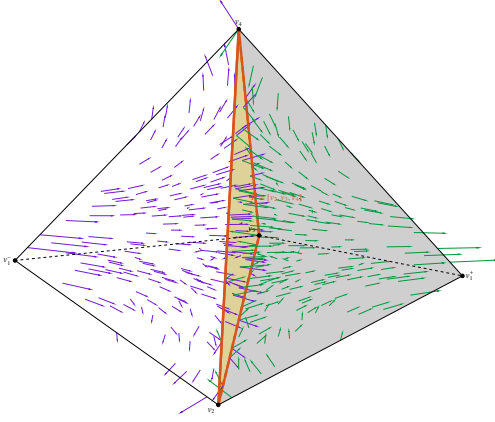
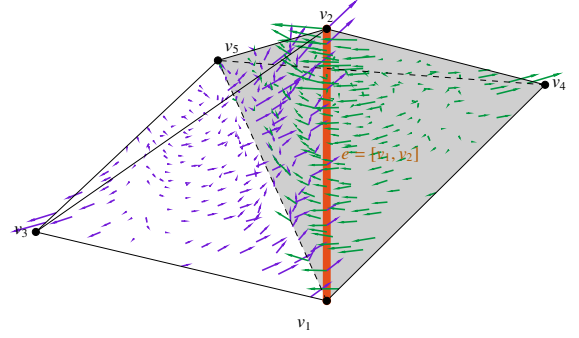
$$\tilde{\omega}_1, \dots, \tilde{\omega}_4, \quad \tilde{\omega}_{12}, \tilde{\omega}_{13}, \tilde{\omega}_{14}, \tilde{\omega}_{23}, \tilde{\omega}_{24}, \tilde{\omega}_{34} \in P_{\text{rd}}(T),$$

such that

$$(E.5) \quad \int_T (\operatorname{div} \tilde{\omega} \psi_j + \tilde{\omega} \cdot \nabla \psi_j) dx = \begin{cases} \delta_{ij}, & \tilde{\omega} = \tilde{\omega}_i, \quad i = 1, \dots, 4, \\ 0, & \tilde{\omega} = \tilde{\omega}_{mn}, \quad (mn) \in \mathcal{E}_T, \end{cases} \quad j = 1, \dots, 4,$$

and

$$(E.6) \quad \int_T (\operatorname{curl} \tilde{\omega} \cdot \tau_{pq} - \tilde{\omega} \cdot \operatorname{curl} \tau_{pq}) dx = \begin{cases} 0, & \tilde{\omega} = \tilde{\omega}_i, \quad i = 1, \dots, 4, \\ \delta_{(mn), (pq)}, & \tilde{\omega} = \tilde{\omega}_{mn}, \quad (mn) \in \mathcal{E}_T, \end{cases} \quad (pq) \in \mathcal{E}_T.$$

(a) Face-associated global basis function ϱ^T (b) Edge-associated global basis function ς^T

Here $\delta_{(mn),(pq)}$ denotes the Kronecker delta with respect to the ordered edge indices.

We first introduce the following ordered basis of $P_{\text{rd}}(T)$:

$$\omega_1 = \begin{pmatrix} \tilde{x} \\ \tilde{y} \\ \tilde{z} \end{pmatrix}, \omega_2 = \begin{pmatrix} 0 \\ -\tilde{z} \\ \tilde{y} \end{pmatrix}, \omega_3 = \begin{pmatrix} \tilde{z} \\ 0 \\ -\tilde{x} \end{pmatrix}, \omega_4 = \begin{pmatrix} -\tilde{y} \\ \tilde{x} \\ 0 \end{pmatrix},$$

$$\omega_5 = \begin{pmatrix} 2\tilde{x}^2 - (\tilde{y}^2 + \tilde{z}^2) + \frac{B+C-2A}{V} \\ 0 \\ 0 \end{pmatrix}, \omega_6 = \begin{pmatrix} 0 \\ 2\tilde{y}^2 - (\tilde{x}^2 + \tilde{z}^2) + \frac{A+C-2B}{V} \\ 0 \end{pmatrix},$$

$$\omega_7 = \begin{pmatrix} 0 \\ 0 \\ 2\tilde{z}^2 - (\tilde{x}^2 + \tilde{y}^2) + \frac{A+B-2C}{V} \end{pmatrix}, \omega_8 = \begin{pmatrix} 1 \\ 0 \\ 0 \end{pmatrix}, \omega_9 = \begin{pmatrix} 0 \\ 1 \\ 0 \end{pmatrix}, \omega_{10} = \begin{pmatrix} 0 \\ 0 \\ 1 \end{pmatrix}.$$

We also introduce the following ordered basis for the auxiliary product space:

$$\begin{aligned}
(\psi, \eta)_1 &= \left(1, \begin{pmatrix} 0 \\ 0 \\ 0 \end{pmatrix}\right), & (\psi, \eta)_2 &= \left(0, \begin{pmatrix} 1 \\ 0 \\ 0 \end{pmatrix}\right), & (\psi, \eta)_3 &= \left(0, \begin{pmatrix} 0 \\ 1 \\ 0 \end{pmatrix}\right), & (\psi, \eta)_4 &= \left(0, \begin{pmatrix} 0 \\ 0 \\ 1 \end{pmatrix}\right), \\
(\psi, \eta)_5 &= \left(2\bar{x}, \begin{pmatrix} 0 \\ -\bar{z} \\ \bar{y} \end{pmatrix}\right), & (\psi, \eta)_6 &= \left(2\bar{y}, \begin{pmatrix} \bar{z} \\ 0 \\ -\bar{x} \end{pmatrix}\right), & (\psi, \eta)_7 &= \left(2\bar{z}, \begin{pmatrix} -\bar{y} \\ \bar{x} \\ 0 \end{pmatrix}\right), \\
(\psi, \eta)_8 &= \left(2\bar{x}, \begin{pmatrix} 0 \\ \bar{z} \\ -\bar{y} \end{pmatrix}\right), & (\psi, \eta)_9 &= \left(2\bar{y}, \begin{pmatrix} -\bar{z} \\ 0 \\ \bar{x} \end{pmatrix}\right), & (\psi, \eta)_{10} &= \left(2\bar{z}, \begin{pmatrix} \bar{y} \\ -\bar{x} \\ 0 \end{pmatrix}\right).
\end{aligned}$$

For $\omega \in P_{\text{rd}}(T)$ and (ψ, η) in the above auxiliary product space, define

$$(E.7) \quad T\omega := (\text{div } \omega, \text{curl } \omega), \quad T^*(\psi, \eta) := \nabla\psi - \text{curl } \eta.$$

The associated bilinear form is given by

$$(E.8) \quad a(\omega, (\psi, \eta)) := (\text{div } \omega, \psi)_T + (\text{curl } \omega, \eta)_T + (\omega, \nabla\psi - \text{curl } \eta)_T.$$

The corresponding L^2 pairing matrix is

$$L_1 = \begin{bmatrix}
3V & 0 & 0 & 0 & 0 & 0 & 0 & 0 & 0 & 0 & 0 \\
0 & 2V & 0 & 0 & 0 & 0 & 0 & 0 & 0 & 0 & 0 \\
0 & 0 & 2V & 0 & 0 & 0 & 0 & 0 & 0 & 0 & 0 \\
0 & 0 & 0 & 2V & 0 & 0 & 0 & 0 & 0 & 0 & 0 \\
0 & 0 & 0 & 0 & 8A + 2B + 2C & 6D & 6E & 8A - 2B - 2C & 10D & 10E & 10E \\
0 & 0 & 0 & 0 & 6D & 8B + 2A + 2C & 6F & 10D & 8B - 2A - 2C & 10F & 10F \\
0 & 0 & 0 & 0 & 6E & 6F & 8C + 2A + 2B & 10E & 10F & 8C - 2A - 2B & 8C - 2A - 2B \\
0 & 0 & 0 & 0 & 0 & 0 & 0 & 4V & 0 & 0 & 0 \\
0 & 0 & 0 & 0 & 0 & 0 & 0 & 0 & 4V & 0 & 0 \\
0 & 0 & 0 & 0 & 0 & 0 & 0 & 0 & 0 & 4V & 4V
\end{bmatrix}.$$

Its inverse is

$$L_2 = \begin{bmatrix}
\frac{1}{3V} & 0_{1 \times 3} & 0_{1 \times 3} & 0_{1 \times 3} \\
0_{3 \times 1} & \frac{1}{2V}I_3 & 0_{3 \times 3} & 0_{3 \times 3} \\
0_{3 \times 1} & 0_{3 \times 3} & \frac{1}{2}R & \frac{M}{2}R - \frac{5}{12V}I_3 \\
0_{3 \times 1} & 0_{3 \times 3} & 0_{3 \times 3} & \frac{1}{4V}I_3
\end{bmatrix}.$$

Here I_3 denotes the 3×3 identity matrix,

$$M = \frac{4(A + B + C)}{3V},$$

and

$$\mathbf{R} = (r_{ij})_{i,j=1}^3 = \mathbf{G}^{-1},$$

where

$$\mathbf{G} = \begin{pmatrix} 4A + B + C & 3D & 3E \\ 3D & A + 4B + C & 3F \\ 3E & 3F & A + B + 4C \end{pmatrix}.$$

In the second step, the auxiliary product-space basis is represented in terms of the Crouzeix–Raviart and Nedelec basis functions. To write the corresponding representation matrix compactly, let

$$\tilde{\mathbf{x}}_i = (\tilde{x}_i, \tilde{y}_i, \tilde{z}_i)^T, \quad i = 1, \dots, 4,$$

and define

$$\mathbf{X} = [\tilde{\mathbf{x}}_1 \quad \tilde{\mathbf{x}}_2 \quad \tilde{\mathbf{x}}_3 \quad \tilde{\mathbf{x}}_4].$$

For the ordered edges

$$(12), (13), (14), (23), (24), (34),$$

set

$$\Delta_e = [\tilde{\mathbf{x}}_2 - \tilde{\mathbf{x}}_1 \quad \tilde{\mathbf{x}}_3 - \tilde{\mathbf{x}}_1 \quad \tilde{\mathbf{x}}_4 - \tilde{\mathbf{x}}_1 \quad \tilde{\mathbf{x}}_3 - \tilde{\mathbf{x}}_2 \quad \tilde{\mathbf{x}}_4 - \tilde{\mathbf{x}}_2 \quad \tilde{\mathbf{x}}_4 - \tilde{\mathbf{x}}_3],$$

and

$$\Xi_e = [\tilde{\mathbf{x}}_1 \times \tilde{\mathbf{x}}_2 \quad \tilde{\mathbf{x}}_1 \times \tilde{\mathbf{x}}_3 \quad \tilde{\mathbf{x}}_1 \times \tilde{\mathbf{x}}_4 \quad \tilde{\mathbf{x}}_2 \times \tilde{\mathbf{x}}_3 \quad \tilde{\mathbf{x}}_2 \times \tilde{\mathbf{x}}_4 \quad \tilde{\mathbf{x}}_3 \times \tilde{\mathbf{x}}_4].$$

Then the representation matrix is

$$L_3 = \begin{bmatrix} \mathbf{1}_4^T & \mathbf{0}_{1 \times 6} \\ \mathbf{0}_{3 \times 4} & \Delta_e \\ -\frac{2}{3}\mathbf{X} & \Xi_e \\ -\frac{2}{3}\mathbf{X} & -\Xi_e \end{bmatrix}.$$

Finally, the desired basis functions are obtained by

$$(E.9) \quad (\tilde{\omega}_1, \tilde{\omega}_2, \tilde{\omega}_3, \tilde{\omega}_4, \tilde{\omega}_{12}, \tilde{\omega}_{13}, \tilde{\omega}_{14}, \tilde{\omega}_{23}, \tilde{\omega}_{24}, \tilde{\omega}_{34}) = (\omega_1, \omega_2, \dots, \omega_{10})L_2^T L_3.$$

APPENDIX F. NUMERICAL RESULTS FOR BOUNDARY-VALUE PROBLEMS

This appendix reports boundary-value experiments for the proposed element, supplementing the eigenvalue tests in Section 6. We consider manufactured solutions on $[0, 1]^2$ and $[0, 1]^3$ and monitor both their mesh-refinement errors in the log–log plots in Figure 15.

F.1. Two-dimensional boundary-value problem. We first consider the two-dimensional boundary-value problem in $H(\text{rot}, \Omega) \cap H_0(\text{div}, \Omega)$. The continuous problem is to find $\omega \in H(\text{rot}, \Omega) \cap H_0(\text{div}, \Omega)$ such that

$$(F.1) \quad (\text{div}\omega, \text{div}\tau) + (\text{rot}\omega, \text{rot}\tau) = (f, \tau), \quad \forall \tau \in H(\text{rot}, \Omega) \cap H_0(\text{div}, \Omega).$$

Here, in two dimensions, rot denotes the scalar rotation of a vector field.

The corresponding discrete problem is to find $\omega_h \in \mathbf{V}_h^{\text{rd}}$ such that

$$(F.2) \quad (\text{div}_h\omega_h, \text{div}_h\tau_h) + (\text{rot}_h\omega_h, \text{rot}_h\tau_h) = (f, \tau_h), \quad \forall \tau_h \in \mathbf{V}_h^{\text{rd}}.$$

Here div_h and rot_h are understood elementwise.

To test the convergence behavior, we take $\Omega = [0, 1]^2$ and prescribe the exact solution

$$\tilde{u} = (\sin(\pi x) \cos(\pi y), \cos(\pi x) \sin(\pi y)),$$

which gives

$$f = 2\pi^2(\sin(\pi x) \cos(\pi y), \cos(\pi x) \sin(\pi y)).$$

F.2. Three-dimensional boundary-value problem. We next consider the three-dimensional boundary-value problem in $H(\text{div}, \Omega) \cap H_0(\text{curl}, \Omega)$. The continuous problem is to find $\omega \in H(\text{div}, \Omega) \cap H_0(\text{curl}, \Omega)$ such that

$$(F.3) \quad (\text{div}\omega, \text{div}\tau) + (\text{curl}\omega, \text{curl}\tau) = (f, \tau), \quad \forall \tau \in H(\text{div}, \Omega) \cap H_0(\text{curl}, \Omega).$$

The corresponding discrete problem is to find $\omega_h \in \mathbf{V}_h^{\text{rd}}$ such that

$$(F.4) \quad (\text{div}_h\omega_h, \text{div}_h\tau_h) + (\text{curl}_h\omega_h, \text{curl}_h\tau_h) = (f, \tau_h), \quad \forall \tau_h \in \mathbf{V}_h^{\text{rd}}.$$

Here div_h and curl_h are understood elementwise.

To test the convergence behavior, we take $\Omega = [0, 1]^3$ and prescribe the exact solution

$$\tilde{u} = (\cos(\pi x) \sin(\pi y) \sin(\pi z), \cos(\pi y) \sin(\pi x) \sin(\pi z), \cos(\pi z) \sin(\pi x) \sin(\pi y)).$$

Accordingly,

$$f = 3\pi^2(\cos(\pi x) \sin(\pi y) \sin(\pi z), \cos(\pi y) \sin(\pi x) \sin(\pi z), \cos(\pi z) \sin(\pi x) \sin(\pi y)).$$

The corresponding log–log convergence plots are shown in Figure 15.



FIGURE 15. Log–log mesh-refinement errors for manufactured boundary-value problems on $[0, 1]^2$ (F.2) (left) and $[0, 1]^3$ (F.4) (right). Solid curves: $\|u_h - \tilde{u}\|_{L^2}$; dashed curves: $|u_h - \tilde{u}|_{H_{\text{div}}} + |u_h - \tilde{u}|_{H_{\text{curl}}}$. Reference slope -1 .

Summary. In both dimensions, the error curves in Figure 15 are parallel to the reference slope -1 , indicating first-order mesh convergence for the manufactured smooth solutions.

INSTITUTE OF COMPUTATIONAL MATHEMATICS AND SCIENTIFIC/ENGINEERING COMPUTING, ACADEMY OF MATHEMATICS AND SYSTEM SCIENCES, CHINESE ACADEMY OF SCIENCES, BEIJING 100190, CHINA

Email address: dongwenyu@lsec.cc.ac.cn

STATE KEY LABORATORY OF MATHEMATICAL SCIENCES (SKLMS) AND STATE KEY LABORATORY OF SCIENTIFIC AND ENGINEERING COMPUTING (LSEC), INSTITUTE OF COMPUTATIONAL MATHEMATICS AND SCIENTIFIC/ENGINEERING COMPUTING, ACADEMY OF MATHEMATICS AND SYSTEMS SCIENCE, CHINESE ACADEMY OF SCIENCES, 100190, BEIJING, CHINA

SCHOOL OF MATHEMATICAL SCIENCES, UNIVERSITY OF CHINESE ACADEMY OF SCIENCES, 100049, BEIJING, CHINA

Email address: szhang@lsec.cc.ac.cn